2007

Genetic and Biochemical Analyses of the Flaviviridae Capsid Proteins

Catherine Lucy Murray

GENETIC AND BIOCHEMICAL ANALYSES OF THE *FLAVIVIRIDAE* CAPSID PROTEINS

A Thesis Presented to the Faculty of

The Rockefeller University

in Partial Fulfillment of the Requirements for

the degree of Doctor of Philosophy

by

Catherine Lucy Murray

June 2007

GENETIC AND BIOCHEMICAL ANALYSES OF THE *FLAVIVIRIDAE* CAPSID PROTEINS

Catherine Lucy Murray, Ph.D.

The Rockefeller University 2007

The small, enveloped viruses of the family *Flaviviridae* are etiological agents of numerous important human and agricultural diseases including hepatitis C, yellow fever, and bovine viral diarrhea. Efficient dissemination of these viruses is dependent on the production of infectious particles, thought to arise by budding of the capsid protein and associated genomic RNA through a host cell-derived lipid membrane outfitted with envelope glycoproteins. The process of virion morphogenesis is not well understood, but the presumed involvement of numerous viral and cellular components makes it an attractive target for novel therapeutic drug design. To investigate the early events of *Flaviviridae* particle assembly, we examined the properties of a major virion structural component, the viral capsid proteins. Biochemical analysis of the *bovine viral diarrhea virus* (BVDV) capsid protein revealed a remarkably flexible molecule, capable of binding RNA with low affinity and low specificity *in vitro*. The ability of BVDV capsid to functionally replace a nonspecific RNA condensing sequence *in vivo* suggests a mechanism for its role in virion assembly. *Hepatitis C virus* (HCV) propagation in tissue culture has very

recently become possible, allowing the role of the capsid (core) protein in the authentic viral life cycle to be studied for the first time. We performed a comprehensive deletion and mutational analysis of the HCV core protein, confirming its importance for infectious virus production and identifying numerous residues essential for this activity. Interestingly, investigation of the virion building blocks converged on a group of nonstructural proteins that may engineer the assembly process. The infectivity of several defective HCV core mutants could be rescued by compensatory mutations in p7, NS2, and NS3, adding to accumulating evidence that these nonstructural proteins are important for virion morphogenesis. The functional determinants of an analogous BVDV protein, uncleaved NS2-3, in infectious virus production were examined. These studies of the *Flaviviridae* capsid proteins provide insights into the mechanisms of viral genome packaging and highlight the importance of nonstructural accessory factors in the initial steps of infectious particle assembly.

To my parents

Acknowledgments

I would first like to thank my advisor, Dr. Charles Rice, for the giving me the opportunity to work under his guidance. Charlie's enthusiasm for science, high standards, and good humor have created a phenomenal work environment with an inspiring and collaborative atmosphere. I have immense respect for Charlie's scientific vision, exceptional knowledge, and for the fact that he was never too busy to answer a question. I am grateful for Charlie's patience, support, and valuable insights during every stage of this work.

I would also like to thank my committee members, Dr. Magda Konarska, Dr. Michael Rout, and Dr. Peter Model. Their enthusiasm, encouragement, and insightful suggestions have been instrumental in making this thesis work possible. I would like to thank Dr. Victor Stollar for taking the time to review my work.

I am extremely grateful to the very talented and very numerous members of the Rice laboratory, who have shared with me their advice, expertise, support, and encouragement throughout my graduate school career. For their help and patience during the early years, I am particularly grateful to Eugene Agapov, Joseph Marcotrigiano, and Arash Grakoui. I would like to thank Shihyun You, Matthew Evans, John Law, Timothy Tellinghuisen, Drew Syder, Erica Machlin, Cristian Cruz, Martina Kopp, Laura McMullan, Ivo Lorenz, Tom Oh, Svetlana Marukian, Edgar Charles, Anesta Webson, Maryline Panis, Jodie Tassello, Annick Gauthier, Glenn Randall,

John-William Carroll, and Matthew Paulson, whose enduring friendship, outgoing personalities, and readiness to help made the laboratory environment enjoyable and productive.

I would like to acknowledge the friendly and hard working Rice laboratory support staff, in particular Patricia Holst, Santa Pecoraro, Lili Zhang, and Merna Torres. I would like to thank Kristen Cullen, Marta Delgado, Sue Ann Chong, and the other members of the Dean's office who make the Rockefeller graduate school experience so pleasant. I am grateful to the many scientists who have shared their expertise with me, especially Margaret MacDonald, Lynn Dustin, Karla Kirkegaard, Santosh Menon, Jennifer Darnell, and Kirk Jensen.

I have been blessed with the support and encouragement of two wonderful individuals, Donna Tscherne and Christopher Jones. Donna's loyal friendship, cheerful nature, and seemingly limitless supply of enthusiasm and support have given me confidence to weather the ups and downs. Chris's ability to keep me laughing, along with his constant encouragement, countless insightful ideas, and gourmet cooking have sustained and inspired me.

I would like to acknowledge my sisters, Ellie and Sarah, who have always been there for me with lively enthusiasm and a sense of perspective. Finally, I would like to thank my parents, who instilled in me a love of science and the natural world and who have unwaveringly supported and believed in me.

Table of Contents

List of Figures

List of Tables

List of Abbreviations

HCV	*hepatitis C virus*
YFV	*yellow fever virus*
WNV	*West Nile virus*
DENV	*dengue virus*
JEV	*Japanese encephalitis virus*
TBEV	*tick-borne encephalitis virus*
BVDV	*bovine viral diarrhea virus*
CSFV	*classical swine fever virus*
BDV	*border disease virus*
kb	kilobase
IRES	internal ribosome entry site
UTR	untranslated region
C	capsid
NS	nonstructural
ER	endoplasmic reticulum
NTPase	nucleoside triphosphatase
E	envelope
prM	precursor to M
cryo-EM	cryo-electronmicroscopy
SPP	signal peptide peptidase

HCVpp	HCV pseudoparticles
HCVcc	HCV cell culture
JFH	Japanese fulminant hepatitis
BHK	baby hamster kidney
Huh	human hepatoma
MDBK	Madin-Darby bovine kidney
nt	nucleotide
bp	base-pair
EMCV	*encephalomyocarditis virus*
Ubi	ubiquitin
FPLC	fast protein liquid chromatography
HPLC	high pressure liquid chromatography
RT	room temperature
cpm	counts per minute
RT-PCR	reverse-transcription-polymerase chain reaction
ELISA	enzyme-linked immunosorbent assay
qRT-PCR	quantitative RT-PCR
mAb	monoclonal antibody
HRP	horseradish peroxidase
TCID50	fifty-percent tissue culture infectious dose

FACS	fluorescence activated cell sorting/flow cytometry
GST	glutathione-S-transferase
PONDR	predictor of natively disordered regions
SELEX	systematic enhancement of ligand binding by exponential enrichment
SEM	standard error of the mean
VLP	virus-like particle
NLP	nucleocapsid-like particle
FMDV	*foot and mouth disease virus*
Jiv	J-domain protein interacting with viral protein
CPE	cytopathic effect
cp	cytopathic
ncp	noncytopathic
NADL	National Animal Disease Laboratories
sg	subgenome
IU	infectious unit
dsRNA	double stranded RNA
dsDNA	double stranded DNA

Chapter 1

Chapter 1: Introduction

Infectious disease continues to be a significant cause of morbidity and mortality for much of the world's population. The burden of these infections falls most heavily on the people of the developing world, where even a vaccine-preventable disease such as yellow fever continues to kill over 30 000 people each year (207). The continuing threat of viral disease has been highlighted in recent years by the HIV pandemic, the spread of *West Nile virus* to new environments, the emergence of severe-acute respiratory syndrome, and by increasing incidences of avian influenza virus transmission to humans. Numerous pathogens of immense human and agricultural impact are encompassed within the family *Flaviviridae*, a group of small, enveloped viruses that is divided into the genera *Hepacivirus*, *Flavivirus*, and *Pestivirus* (116).

Hepatitis C virus (HCV), the sole member of the *Hepacivirus* genus, is a major etiological agent of liver disease, with an estimated 170 million people infected worldwide (222). Although about 20% of individuals exposed to the virus will spontaneously resolve the infection, the majority will become chronic carriers (65). These carriers are at high risk for cirrhosis and hepatocellular carcinoma, as well as extrahepatic manifestations such as immune-complex disease and lymphomas (190). In developed countries, HCV infection is the leading cause of liver transplantation (214). There is no vaccine available to protect against HCV infection and the current therapy, a combination of interferon-α and the nucleoside analog ribavirin, is frequently not effective (116).

Flaviviruses, the insect vector-borne relatives of HCV, are the causative agents of numerous globally significant diseases. *Yellow fever virus* (YFV), the first human virus discovered over a century ago, remains endemic in many parts of the world (207). *West Nile virus* (WNV), *dengue virus* (DENV), and *Japanese encephalitis virus* (JEV) represent pathogens that are resurging and spreading to new environments (127). Other *Flaviviruses*, including *tick-borne encephalitis virus* (TBEV), are highly problematic but less widespread (74). Serious manifestations of *Flavivirus* infections include encephalitis, hemorrhagic fever, and death (127, 74).

Pestiviruses infect wild and agriculturally important animals worldwide. These economically significant pathogens include *bovine viral diarrhea virus* (BVDV), *classical swine fever virus* (CSFV), and *border disease virus* (BDV) (143). *Pestivirus* infection can lead to symptoms ranging from subclinical disease to hemorrhagic syndromes. BVDV has an extremely high prevalence in cattle, with an average of 60-90% of animals infected during their lifetime (143). A major burden of these infections on the livestock industry results from virus-induced infertility, fetal malformations, and stillbirths (143). Complications of BVDV infection include the highly fatal mucosal disease, and the induction of an immunocompromised state, allowing colonization by opportunistic pathogens (143, 28).

Gene expression and replication

The enveloped virions of the *Flaviviridae* contain a positive-sense, single-stranded, RNA genome of approximately 9-12 kilobases (kb). Binding of the virions to their cellular receptors results in endocytosis of the particle and a subsequent low-pH induced fusion event that releases the capsid protein and associated genomic RNA into the cytoplasm (Fig 1-1, ref 209, 39, 111). The genomes, resembling cellular mRNAs, are directly translated on introduction into the cell. For HCV and the *Pestiviruses*, translation is initiated at an internal ribosome entry site (IRES, ref 170, 210); for the *Flaviviruses*, translation is cap-dependent (116). None of the viral genomes are polyadenlyated, but instead have 3' untranslated regions (UTRs) with conserved RNA structural elements (116). Translation yields a polyprotein of approximately 3000 residues, which must be processed by viral and cellular proteases to liberate the individual viral proteins. These proteins are sequentially designated NH_2-C-E1-E2-p7-NS2-NS3-NS4A-NS4B-NS5A-NS5B-COOH for *Hepaciviruses*, NH_2-C-prM-E-NS1-NS2A-NS2B-NS3-NS4A-NS4B-NS5-COOH for *Flaviviruses*, and NH_2-N^{pro}-C-E^{rns}-E1-E2-p7-NS2-NS3-NS4A-NS4B-NS5A-NS5B-COOH for *Pestiviruses* (Fig 1-2). Structural proteins, which make up the physical virion, are found in the amino-terminal region of the polyprotein and are predominantly processed by cellular enzymes such as signal peptidase. They consist of capsid (C), and the envelope proteins. The nonstructural (NS) proteins comprise the remainder of the

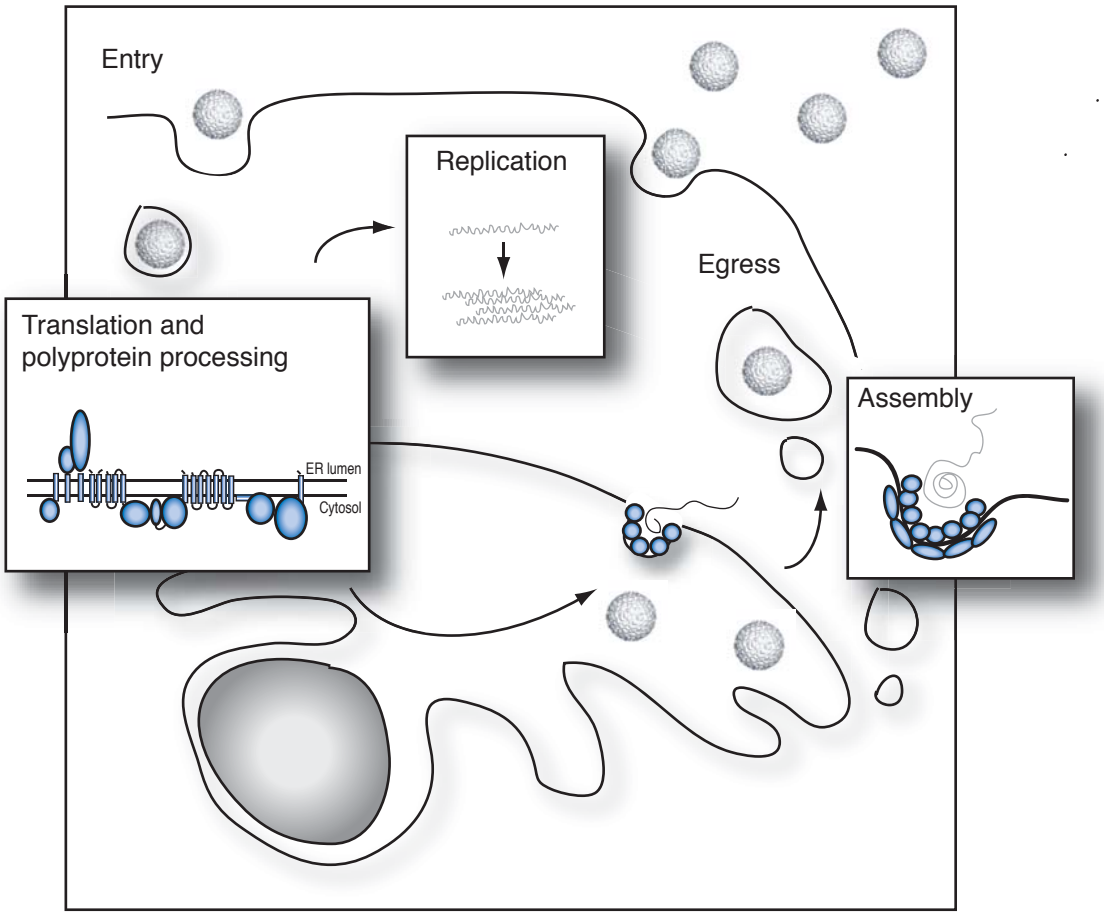

Fig 1-1. Life cycle of the *Flaviviridae*. See text for details.

polyprotein and are liberated primarily by the major viral protease NS3 (10, 224, 34) along with its cofactor NS4A (56, 224) or NS2B (*Flaviviruses* , ref 34).

The nonstructural proteins NS3 to NS5B (NS1 to NS5 in *Flaviviruses*) associate to form the replicase complex. Replication is entirely cytoplasmic and occurs in close association with modified intracellular membranes, likely derived from the endoplasmic reticulum (ER, ref 144). NS5B and NS5 (*Flaviviruses*) constitute the viral RNA-dependent RNA polymerases, which, as part of the replicase complex, catalyze the asymmetric accumulation of genomic, plus-strand, over minus-strand RNA (17, 236, 198). In addition to protease activity, the NS3 proteins possess helicase (217, 218, 131) and nucleoside triphosphatase (NTPase, ref 194, 197, 221) activities essential for RNA replication. HCV and *Pestivirus* NS4B and NS5A proteins, as well as *Flavivirus* NS4A and NS4B proteins, have as yet undefined but essential roles in RNA replication. Accumulating evidence indicates that nonstructural proteins p7 to NS3 (NS2A to NS3 in *Flaviviruses*) are involved in infectious virus production (116).

Infectious virus production

The enveloped virions of the *Flaviviridae* are thought to arise by budding of the capsid and associated genomic RNA into an ER-derived membrane studded with envelope glycoproteins. These virions then egress via the cellular secretory pathway, and are released into the extracellular milieu without lysis

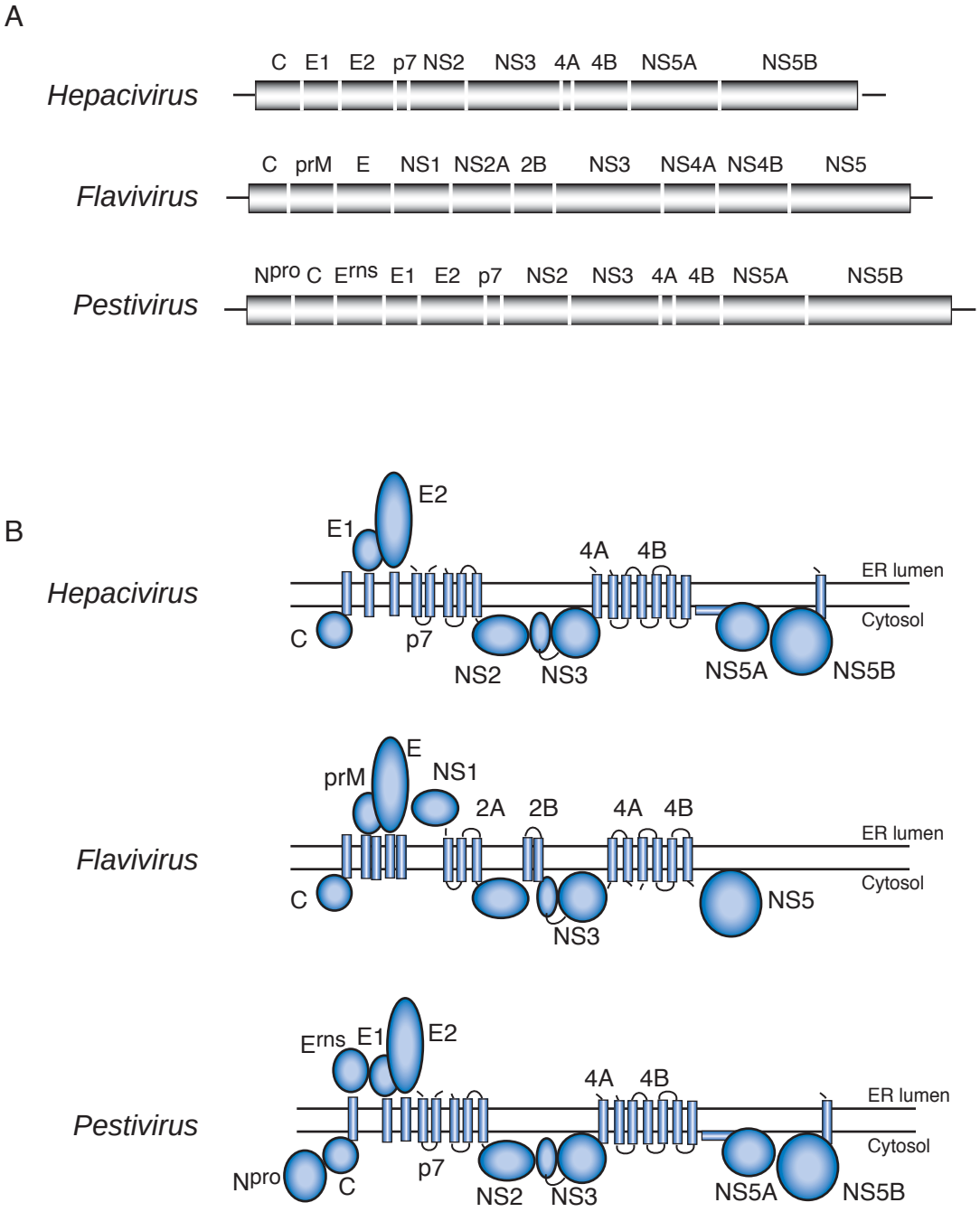

Fig 1-2. Genomes (A) and predicted polyprotein topologies (B) of the *Flaviviridae*. See text for details.

of the host cell. The preponderance of information regarding *Flaviviridae* infectious particle morphogenesis comes from studies of classical *Flaviviruses*. Investigation of HCV assembly has been extremely limited since, until very recently, tissue culture systems that allowed replication of the viral genome did not support infectious particle production.

Flaviviruses

The assembly pathways of the members of the genus *Flavivirus* are the best characterized in the *Flaviviridae* family. In addition to the genomic RNA and a host-derived lipid bilayer, *Flavivirus* virions are composed of the capsid protein, the envelope protein (E), and a fragment of the precursor to M (prM) protein. The capsid protein is the first product encoded by the viral genome, and on translation, targets the nascent polyprotein to the ER membrane via a signal sequence in its carboxy-terminus (129). Processing of capsid from the polyprotein depends on the accumulation of the viral protease NS3 and its NS2B cofactor (NS2B-3). Cleavage of the capsid protein from its membrane anchor by the cytosolic viral protease is a prerequisite for signal peptidase cleavage of the amino-terminus of the first glycoprotein, prM, on the luminal side of the ER membrane (119, 191, 192, 6). After cleavage from its membrane anchor, capsid remains associated with membranes through exposed hydrophobic sequences and dimerizes to form the functional subunit of assembly (124, 97, 89, 50). High-resolution structures of DENV and WNV capsid proteins (124, 50) indicate that

these helix-rich molecules also have numerous surface-exposed basic residues, available for interactions with RNA. Although a specific encapsidation signal in the *Flavivirus* genome has not been identified, capsid may have higher affinity for the 5' and 3' UTRs (96). Interaction of capsid and RNA presumably leads to the formation of a nucleocapsid, although these structures are rarely discernable in infected cells and do not have a defined symmetry in cryo-electronmicroscopy (cryo-EM) image reconstructions of the virus particles (233, 230, 101, 145). Although these results indicate that symmetrically ordered nucleocapsids are not formed during assembly, detergent treatment of TBEV particles releases capsid-RNA complexes (97). It has been suggested that capsid may interact with RNA in a manner resembling histones, instead of forming an ordered shell (50).

Surrounding the capsid-RNA complex is a host-derived lipid membrane outfitted with membrane glycoproteins. These glycoproteins, prM and E, immediately follow capsid in the polyprotein, are ER-associated via transmembrane domains, and heterodimerize soon after synthesis (232, 121). Dimerization allows prM to chaperone the folding of E, which contains the receptor binding and fusion peptide activities (121, 4). prM functions to protect the fusogenic E protein during egress of particles through the low pH compartments of the secretory pathway (79, 126). In the final Golgi compartment, prM is cleaved to pr and M by the host enzyme furin, allowing E to homodimerize (188, 167, 232). The resulting mature, infectious virions are released from vesicles at the cell surface (188). The crystal structures of TBEV,

DENV, and WNV E protein ectodomains have been solved, and show elongated dimers with the fusion peptide of each monomer buried through contacts with the adjacent molecule (167, 234, 91). A structure of the DENV E protein at low pH showed a trimer, with the fusion peptides aligned and exposed at its tip (141).

Budding of the capsid-RNA complex into the ER lumen is driven by lateral associations between the envelope proteins (146). Consistent with this, subviral particles, containing no capsid or RNA, are produced in natural infections and can be induced by overexpression of the glycoproteins alone in cells (5). Cryo-EM image reconstruction has been used to determine the structures of TBEV subviral particles, as well as of immature DENV and YFV particles, and mature DENV and WNV virions (Fig 1-3). Experimentally produced immature DENV and YFV particles retain the prM cap on the E fusion peptide and presumably mimic virions transiting the secretory pathway. The structures of these particles demonstrate prominent spikes emanating from the membrane (Fig 1-3, ref 232). These spikes consist of E protein trimers with their fusion peptides aligned at the surface (141). In the immature particles, prM protects the fusion peptides of the particles that are otherwise primed for fusion (232). In contrast to the conspicuous surface projections of the immature virion, the mature virus particle has a drastically different arrangement of the glycoproteins (Fig 1-3). The E protein was found to lie parallel to the lipid membrane in an unusual herringbone array, completely covering the bilayer in a smooth, proteinaceous coat (101, 234). No contacts were observed between the E and M transmembrane

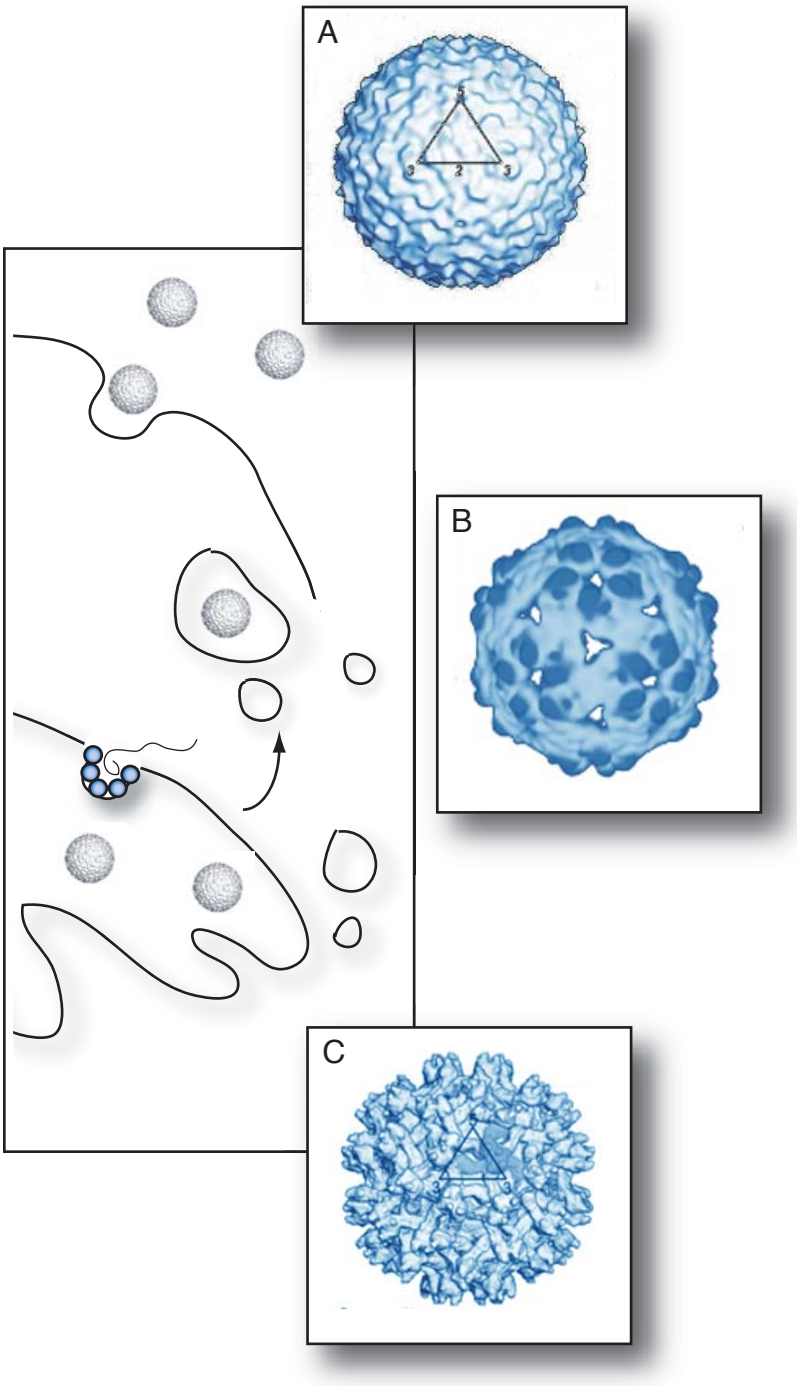

Fig 1-3. Structures of *Flavivirus* particles. (A) Mature DENV virion (101). (B) TBEV subviral particle (58). (C) Immature DENV particle (232).

domains, or between the capsid protein and the envelope proteins. Subviral particles resembled mature particles in the prone conformation of the E protein, but exhibited a classical T=1 symmetry rather than the herringbone array (Fig 1-3, 58). The mechanisms by which prM cleavage in the Golgi leads to the massive glycoprotein rearrangements on the virion surface are not known (232).

Although structural insights have elucidated many aspects of *Flavivirus* maturation and egress, the early events of virion assembly and its regulation are poorly understood. Several nonstructural proteins have been shown to be important for assembly or budding of the nucleocapsid. Mutations in YFV NS2A, a hydrophobic protein of unclear function, were shown to inhibit release of genome-containing, but not subviral particles (103). Compensatory mutations in the NS3 helicase domain overcame this defect, suggesting a functional interaction between NS2A and NS3 might be important for infectivity (103). The nonstructural proteins of the replicase complex may also function in assembly regulation, since it has been observed that only replication-competent genomes are substrates for packaging (95). It is likely that numerous cellular factors are also involved in virion assembly and egress. As well as the host proteases signal peptidase (129) and furin (188), a kinase, c-Yes, has been found to be essential for release of WNV particles, possibly reflecting a role for this protein in vesicular trafficking (80).

Pestiviruses

Pestivirus assembly is not as well understood as *Flavivirus* morphogenesis. The envelope of a *Pestivirus* virion is studded with three glycoproteins, E^{rns} (ribonuclease secreted), E1, and E2 (205). The interior of the particle contains the capsid protein (C) and the genomic RNA (205). Unlike the other *Flaviviridae*, the initial translation product of the *Pestivirus* genome is not structural, but a nonstructural protein, N^{pro}. N^{pro} is an autoprotease that mediates a single cleavage at the amino-terminus of the capsid protein (223, 177). A signal sequence in the carboxy-terminus of capsid targets the nascent polyprotein to the membrane, initiating a dual processing event by host enzymes. Signal peptidase cleaves capsid from E^{rns} in the ER lumen (178), and signal peptide peptidase (SPP) performs an additional processing event within the capsid membrane anchor (78). The highly basic nature of the mature capsid protein indicates that it likely functions to bind and package the RNA genome, although little is known about its role in this respect.

By analogy to the *Flaviviruses*, *Pestivirus* nucleoprotein complexes are presumed to bud into the ER lumen, concurrently acquiring the envelope glycoproteins. Observation of particles within the ER by electron microscopy, as well as the absence of glycoprotein expression on the cell surface, supports this hypothesis (70, 71, 219, 75). The envelope proteins, E^{rns}, E1, and E2, immediately follow capsid in the polyprotein and are targeted to the membrane by signal sequences in capsid and E1 (178). Signal peptidase-mediated cleavages

are thought to create an E^{rns}-E1-E2 precursor, from which E2 is rapidly liberated (178). Cleavage of E^{rns} from E1 is slow and may occur in a post-ER compartment analogous to prM cleavage in *Flaviviruses* (178). After separation from the polyprotein, E1 and E2 rapidly associate with the chaperone calnexin (27). In the virion the envelope proteins assume the form of disulfide-linked E2 homodimers and E1-E2 heterodimers (205). E^{rns} is also a major component of the virion (205). This heavily glycosylated protein does not have a typical transmembrane domain and is thought to incorporate into particles via an unusual membrane anchor of unknown structure (59); it is also secreted in a soluble form from infected cells (178). The most striking feature of the E^{rns} protein is that it possesses ribonuclease activity (181). This enzymatic activity has been shown to be essential for virulence *in vivo*, but not required for growth in cultured cells (139). Although its mechanism of action is not known, it may play a role in immune evasion, either by inducing apoptosis of immune cells (110, 28, 59) or by inhibiting toll-like receptor (TLR-3) activation by degrading its RNA ligand.

Nonstructural proteins have also been shown to function in *Pestivirus* morphogenesis. p7 is a small integral membrane protein that is incompletely processed from E2 by signal peptidase (54). Although neither p7, nor E2-p7 can be detected in virus particles, p7 is absolutely required for infectivity (206, 76). Similarities have been noted between p7 and viroporins, a class of small, hydrophobic, virally encoded proteins that act as ion channels (73). Consistent

with this hypothesis, p7 was found to oligomerize and to form ion-conductive channels when overexpressed in mammalian cells (73). The role of this putative ion channel activity in *Pestivirus* morphogenesis, however, remains controversial. Reminiscent of the proposed functional relationship between *Flavivirus* NS2A and NS3 proteins (103), we have found evidence that *Pestivirus* NS2 and NS3 proteins are essential for virion formation (2).

Hepaciviruses

The sole member of the *Hepacivirus* genus, HCV, has only recently been propagated in tissue culture and studies of its assembly are therefore in their infancy. Analogies with *Flaviviruses* and *Pestiviruses*, as well as characterization of virions isolated from patient sera, have suggested that envelope proteins E1 and E2, along with the capsid protein, genomic RNA, and a host-derived lipid bilayer constitute the infectious particle (68, 227). The capsid protein, termed core, is the first product encoded by the open reading frame. It is liberated from the polyprotein by the host enzymes signal peptidase and SPP in a manner analogous to the *Pestiviruses* (180, 133). Studies of core protein *in vitro* and in overexpression systems have suggested that it interacts homotypically to form dimers and higher order structures, including nucleocapsid-like particles (25, 130, 105, 99). Associations of core with the envelope glycoproteins E1 and E2, as well as with RNA, have also been reported (151, 118, 12, 180, 43, 187). When overexpressed in cells, core is found to localize to cholesterol and triglyceride-

rich storage granules termed lipid droplets (7). Processing of core by SPP is a prerequisite for this association (133). Recent studies of infected cells suggest that lipid droplets and their associated membranes are the only subcellular compartments in which core accumulates, leading to speculation that these fatty deposits may be sites of particle assembly (176). Surprisingly, envelope proteins were not found to colocalize with core in infected cells (176).

In the infectious virion, E1 and E2 are presumably displayed on the particle surface, allowing E2 to mediate interactions with the primary entry receptor, CD81 (160). Transient expression of the structural region has been used to define a putative pathway of HCV glycoprotein maturation. After cotranslational insertion of the polyprotein into the ER membrane, signal peptidase rapidly processes E1 from E2-p7-NS2, the precursor from which E2 is subsequently cleaved (68). E1 and E2 are thought to associate rapidly with the chaperone calnexin (52). E2 folds quickly, attaining its final conformation before it is cleaved from the E2-p7-NS2 precursor (52). E2 then interacts with the slower folding E1 to provide additional chaperone help; in the absence of E2, E1 cannot attain its proper conformation (51). Experimentally produced psuedoparticles (HCVpp), in which E1 and E2 glycoproteins decorate a defective retrovirus core, have been used to study the determinants of envelope protein function (11). Glycosylation of both E1 and E2 ectodomains has been found to be important for folding and heterodimerization of the envelope proteins, and for the assembly and release of HCVpp (116).

As in *Pestiviruses*, nonstructural proteins p7 and NS2 are essential for HCV infectious virus production (179, 90). Both p7 and NS2 appear to act early in assembly and possibly interact with each to accomplish their functions in morphogenesis (90). Similar to BVDV p7, the HCV protein has been found to oligomerize into ion conductive channels *in vitro* (72). The relevance of the *in vitro* ion channel activity to p7 functions in morphogenesis is not yet resolved (90).

HCV infectious system

Almost two decades after the discovery of HCV as the major causative agent of non-A non-B hepatitis (38), the entire infectious cycle of the virus has been recapitulated in tissue culture for the first time (115, 215, 235). HCV cell culture infectious systems (HCVcc) take advantage of a unique genotype 2a patient isolate, Japanese fulminant hepatitis-1 (JFH-1), which both replicates to high levels and supports the release of infectious particles (92, 215, 235).

The efficient replication of JFH-1 has been hypothesized to be central to its singular phenotype (9). Previously, successful replication of HCV genomes in culture required the accumulation of adaptive mutations. These mutations, primarily found in NS3, NS4B and NS5A, were isolated by propagation of genomes containing selectable markers (9, 21, 120). It was speculated that these mutations, as well as increasing replication by unknown mechanisms, might also inhibit infectious virus production, since genomes containing such

changes were not infectious in chimpanzees (29). Interestingly, several of the adaptive mutations altered the phosphorylation state of NS5A, suggesting this nonstructural protein may be important in the regulation of infectivity (55). JFH-1 does not require the accumulation of adaptive mutations in order to replicate in cultured cells (92). The determinants of this robust replication, and of its infectivity, are not known.

JFH-1 infectivity could be enhanced by substitution of its structural proteins with those of another genotype 2a isolate, J6, leading to a chimeric genome termed J6/JFH (115). This chimeric genome was slightly more infectious than JFH-1, reaching titers of approximately 10^5 infectious units/ml (115). The advent of the cell culture infectious system allows the authentic HCV viral life cycle to be studied for the first time, and the long enigmatic process of HCV infectious virion production to begin to be unraveled.

Objectives

The processes of virion assembly and secretion are presumed to require a careful orchestration of numerous viral and cellular interacting factors. The pathways of infectious virion production, therefore, are rich in targets for novel therapeutic drug development. Furthermore, an understanding of virion components and the determinants of virus construction can impact the design of immunogenic particles for vaccines.

The requirements and mechanisms of *Flaviviridae* infectious virus production are the subject of this thesis. In the hopes of understanding the earliest events in assembly, we investigated a particle building block, the viral capsid proteins. Through biochemical analysis, the BVDV capsid protein was determined to be an unusually flexible RNA binding protein, capable of nucleic acid condensation activity *in vivo*. This curiously unconstrained RNA packaging mechanism may be a general feature of the *Flaviviridae*, as discussed in chapter 3. With the advent of the tissue culture infectious system, a study of the HCV core protein in the context of an authentic viral life cycle could be attempted for the first time. As reported in chapter 4, we performed a comprehensive deletion and mutagenesis study of the HCV core protein, identifying numerous residues essential for infectious virus production. Studies of the virion building blocks converged on a group of nonstructural proteins that may represent the assembly architects. In collaboration with Eugene Agapov, a nonstructural precursor, NS2-3, was found to be essential for BVDV infectivity; the determinants of its activity are investigated in chapter 5. Remarkably, studies of HCV core protein uncovered roles for the same nonstructural proteins in *Hepacivirus* morphogenesis; mutations in this region were found to rescue the infectivity of defective core mutants. These new insights into the early events of *Flaviviridae* infectious particle production will hopefully add to the understanding of this important pathway, and lead to its eventual targeting for therapeutic drug design.

Chapter 2

Chapter 2: Materials and Methods

Cell culture. Cells were grown at 37°C in 5% CO_2.

BHK 21 (Baby hamster kidney) cells were propagated in modified Eagle's medium (MEM, Invitrogen, Carlsbad, CA) supplemented with 7.5% fetal bovine serum (FBS, Invitrogen).

Huh-7.5 (Human hepatoma) cells were propagated in Dulbecco's modified Eagle's medium (DMEM, Invitrogen) containing sodium pyruvate, 10 mM nonessential amino acids, and 10% FBS (Invitrogen).

MDBK (Madin-Darby bovine kidney) cells were propagated in DMEM supplemented with sodium pyruvate and 10% horse serum (HS, Invitrogen).

Plasmid constructs. Plasmids were constructed by standard methods. PCR fragments were amplified using Pfu Ultra High Fidelity DNA polymerase (Stratagene, La Jolla, CA) with 30 cycles of denaturing at 95°C for 30 sec, annealing at 55-65°C for 30 sec, and elongation at 72°C for 1 min per kb. Constructs were verified by restriction enzyme digestion and sequencing of PCR amplified segments. Descriptions of the cloning strategies are provided below.

BVDV capsid protein expression constructs

GST-C84. Nucleotides (nt) 890 to 1141 of pBeloBac11/NADL, a bacterial artificial chromosome vector (Invitrogen) encoding the full-length BVDV strain NADL genome (2), were PCR amplified using primers RU-2549 (5'-

CGCGGATCCTCAGACACGAAAGAAGAGGGAG-3') and RU-2550 (5'-CCGCTCGAGTCATTTTTCCAGTTTCTTGCGTGATTC-3'). RU-2549 engineered a *BamH*I site upstream of capsid, keeping it in-frame with GST. RU-2550 engineered a stop codon immediately downstream of capsid amino acid 84 and an *Xho*I site following the stop. The PCR product was digested with *BamH*I/*Xho*I and ligated to the 4757 base-pair (bp) fragment of pGEX-6P-1 (GE Healthcare, Piscataway, NJ) digested with the same enzymes.

GST-C87. Nucleotides 890 to 1150 of pBeloBac11/NADL were PCR amplified using primers RU-2549 (5'-CGCGGATCCTCAGACACGAAAGAAGAGGGAG-3') and RU-4453 (5'-CCGCTCGAGTCACAACAATGCTTTTTCCAGTTTCTTG-3'). RU-4453 engineered a stop codon immediately downstream of capsid amino acid 87 and an *Xho*I site following the stop. The PCR product was digested with *BamH*I/*Xho*I and ligated to the 4757 bp fragment of pGEX-6P-1 (GE Healthcare) digested with the same enzymes.

GST-C90. Nucleotides 890 to 1159 of pBeloBac11/NADL were PCR amplified using RU-2549 (5'-CGCGGATCCTCAGACACGAAAGAAGAGGGAG-3') and RU-4658 (5'-CCGCTCGAGTCATGCCCACGCCAACAATGCTTT-3'). RU-4658 engineered a stop codon immediately downstream of capsid amino acid 90 and an *Xho*I site following the stop. The PCR product was digested with *BamH*I/*Xho*I

and ligated to the 4757 bp fragment of pGEX-6P-1 (GE Healthcare) digested with the same enzymes.

Sindbis plasmid constructs

The Sindbis/luc (pToto1101/luc) backbone encodes a wild-type *Sindbis virus* cDNA with firefly luciferase (1653 nt) inserted within nsP3 (19). Plasmids were propagated in DH5α cells.

Sindbis/luc CΔ2-96. Nucleotides 8471 to 9302 of Sindbis/luc were amplified with RU-8548 (5'-GGATTTTGATGCAATCATAG-3') and RU-8556 (5'-CTCTTTCCGG GTTTGGGTTTCATGGTGGTGGTGTTGTAG-3'). Nucleotides 9588 to 10085 of Sindbis/luc were amplified with RU-8555 (5'-CTACAACACCACCACC ATGAAACCCAAACCCGGAAAGAG-3') and RU-8549 (5'-CTTCTGTCCCTTCC GGGGTC-3'). Primary PCR products were assembled by amplification with flanking primers RU-8548 and RU-8549. PCR products were digested with *Hpa*I/*Aat*II and ligated to the 14211 bp fragment of Sindbis/luc digested with the same enzymes.

Sindbis/luc CΔ50-96. Nucleotides 8471 to 9302 of Sindbis/luc were amplified with RU-8548 and RU-8560 (5'-CTCTTTCCGGGTTTGGGTTTGACGGCTGTGGTCA GTTGC-3'). Nucleotides 9588 to 10085 of Sindbis/luc were amplified with RU-8559 (5'-GCAACTGACCACAGCCGTCAAACCCAAACCCGGAAAGAG-3') and

RU-8549. Primary PCR products were assembled by amplification with flanking primers RU-8548 and RU-8549. PCR products were digested with *Hpa*I/*Aat*II and ligated to the 14211 bp fragment of Sindbis/luc digested with the same enzymes.

Sindbis/luc CΔ72-96. Nucleotides 8471 to 9512 of Sindbis/luc were amplified with RU-8548 and RU-8562 (5'-CTCTTTCCGGGTTTGGGTTTCTGGCGCGGT GGCGGGCGTG-3'). Nucleotides 9588 to 10085 of Sindbis/luc were amplified with RU-8561 (5'-CACGCCCGCCACCGCGCCAGAAACCCAAACCCGGAAA GAG-3') and RU-8549. Primary PCR products were assembled by amplification with flanking primers RU-8548 and RU-8549. PCR products were digested with *Hpa*I/*Aat*II and ligated to the 14211 bp fragment of Sindbis/luc digested with the same enzymes.

Sindbis/luc CΔ2-96/BVDV1-84. Nucleotides 890 to 1141of pBeloBac11/NADL were PCR amplified using primers RU-8727 (5'-TCAGACACGAAAGAAGAGGG-3') and RU-8564 (5'-CTCTTTCCGGGTTTGGGTTTTTTTTCCAGTTTCTTG CGTG-3'). Primer RU-8564 creates the junction between NADL nt 1141 and Sindbis nt 9588. Nucleotides 8471 to 9302 of Sindbis/luc were amplified with RU-8548 and RU-8725 (5'-CCCTCTTCTTTCGTGTCTGACATGGTGGTG GTGTTGTAG-3'). RU-8725 creates the junction between Sindbis/luc nt 9302 and NADL nt 890. Primary PCR products were assembled using RU-8548 and

RU-8564. Nucleotides 9588 to 10229 of Sindbis/luc were amplified with RU-8550 (5'-AAACCCAAACCCGGAAAGAG-3') and RU-8773 (5'-GTAGGCCTCATGGT TCACG-3'). This PCR product was assembled with the secondary PCR product using RU-8748 and RU-8773. Final PCR products were digested with *Hpa*I/*Aat*II and ligated to the 14211 bp fragment of Sindbis/luc digested with the same enzymes.

Sindbis/luc CΔ2-96/BVDV1-90. Nucleotides 890 to 1159 of pBeloBac11/NADL were PCR amplified using primers RU-8727 and RU-8565 (5'-CTCTTTCCGGG TTTGGGTTTTGCCCACGCCAACAATGC-3'). Primer RU-8565 creates the junction between NADL nt 1159 and Sindbis/luc nt 9588. Nucleotides 8471 to 9302 of Sindbis/luc were amplified with RU-8548 and RU-8725. RU-8725 creates the junction between Sindbis/luc nt 9302 and NADL nt 890. Primary PCR products were assembled using RU-8548 and RU-8565. Nucleotides 9588 to 10229 of Sindbis/luc were amplified with RU-8550 and RU-8773. This PCR product was assembled with the secondary PCR product using RU-8748 and RU-8773. Final PCR products were digested with *Hpa*I/*Aat*II and ligated to the 14211 bp fragment of Sindbis/luc digested with the same enzymes.

Sindbis/luc CΔ50-96/BVDV35-83. Nucleotides 992 to 1138 of pBeloBac11/NADL were PCR amplified using primers RU-8728 (5'-AGCAAAACTAAACCTCCGG-3') and RU-8570 (5'-CTCTTTCCGGGTTTGGGTTTTTCCAGTTTCTTGCGTGATTC-

3'). Primer RU-8570 creates the junction between NADL nt 1138 and Sindbis/luc nt 9588. Nucleotides 8471 to 9446 of Sindbis/luc were amplified with RU-8548 and RU-8723 (5'-CCGGAGGTTTAGTTTTGCTGACGGCTGTGGTCAGTTGC-3'). RU-8723 creates the junction between Sindbis/luc nt 9446 and NADL nt 992. Primary PCR products were assembled using RU-8548 and RU-8570. Nucleotides 9588 to 10229 of Sindbis/luc were amplified with RU-8550 and RU-8773. This PCR product was assembled with the secondary PCR product using RU-8748 and RU-8773. Final PCR products were digested with *Hpa*I/*Aat*II and ligated to the 14211 bp fragment of Sindbis/luc digested with the same enzymes.

Sindbis/luc CΔ72-96/BVDV54-83. Nucleotides 1049 to 1138 of pBeloBac11/NADL were PCR amplified using primers RU-8729 (5'-AGGAA GAAGGGAAAAACCAAG-3') and RU-8572 (5'-CTCTTTCCGGGTTTGGGTTTT TCCAGTTTCTTGCGTGATTC-3'). Primer RU-8572 creates the junction between NADL nt 1138 and Sindbis/luc nt 9588. Nucleotides 8471 to 9512 of Sindbis/luc were amplified with RU-8548 and RU-8726 (5'-CTTGGTTTTTCCCTTC TTCCTCTGGCGCGGTGGCGGGCGTG-3'). RU-8726 creates the junction between Sindbis/luc nt 9512 and NADL nt 1049. Primary PCR products were assembled using RU-8548 and RU-8572. Nucleotides 9588 to 10229 of Sindbis/luc were amplified with RU-8550 and RU-8773. This PCR product was assembled with the secondary PCR product using RU-8748 and RU-8773. Final

PCR products were digested with *Hpa*I/*Aat*II and ligated to the 14211 bp fragment of Sindbis/luc digested with the same enzymes.

HCV plasmid constructs

These genomes are based on the J6/JFH chimeric genotype 2a sequence (115), or its derivative J6/JFH(p7Rluc2A), in which a *Renilla* luciferase-2A sequence is inserted between p7 and NS2 (90). ΔE1E2 genomes contain an in-frame deletion of amino acids 217 to 567 (J6/JFH polyprotein numbering), encompassing the majority of the E1 and E2 proteins (90). GND genomes contain a mutation of amino acid D2760 to N (J6/JFH polyprotein numbering), abolishing the conserved RNA-dependent RNA polymerase motif, GDD (90). Plasmids were propagated in DH5α cells.

J6/JFH and J6/JFH(p7Rluc2A) with deletions and substitutions. Deletions or amino acid substitutions were introduced by PCR amplification of the core-coding region of J6/JFH with primers containing the desired changes. Primary PCR products containing the engineered mutations were assembled by amplification with flanking primers RU-6009 (5'-CGACGGCCAGTGAATTCTAATACG-3') and RU-5743 (5'-ATGCCATGCGGTGTCCAG-3'). PCR products were digested with *EcoR*I/*Kpn*I and ligated to the 12073 bp fragment of J6/JFH(p7Rluc2A) or the 11074 bp fragment of J6/JFH digested with the same enzymes.

J6/JFH with p7, NS2, NS3, and core mutations. Isolated compensatory mutations were reengineered into wild-type J6/JFH and the parental core mutants. To facilitate cloning, a wild-type J6/JFH sequence modified to include unique, silent restriction sites at positions 2392 (*Bgl*II) and 2955 (*Not*I) (termed J6/JFH1.1) was used. Compensatory mutations were engineered by PCR amplification of the appropriate J6/JFH1.1 sequences with primers containing the desired changes. Primary PCR products were assembled by amplification with flanking primers RU-6020 (5'-TATGTGGGAG GGGTTGAG-3') and RU-5721 (5'-GCTACCGA GGGGTTAAGCACT-3'). PCR products were digested with *Bgl*II/*Not*I (p7 mutants) or *Not*I/*Spe*I (NS2 and NS3 mutants) and ligated to the 11804 bp *Bgl*II/*Not*I fragment or the 11219 bp *Not*I/*Spe*I fragment of J6/JFH1.1. To engineer the compensatory changes into the parental core mutants, the 11074 bp *EcoR*I/*Kpn*I fragment of the nonstructural protein mutant was ligated to the 1290 bp *EcoR*I/*Kpn*I fragment of the appropriate core protein mutant.

BVDV plasmid constructs

The backbone for the following constructs is the bacterial artificial chromosome vector pBeloBAC11 (Invitrogen). This single copy vector was used since plasmids encoding portions of the BVDV genome are toxic and unstable in bacterial cells. For large-scale plasmid preparation, the smallest colonies were picked from freshly transformed electrocompetent DH10B cells. Overnight cultures were grown from 8 h cultures diluted into 500 ml Terrific Broth with 12.2

μg/ml chloramphenicol. Flasks were covered with two kimwipes, not foil, to allow sufficient aeration. Plasmid was recovered by alkaline lysis followed by single banding on cesium chloride gradient.

N^{pro}-NS2/sg: (Constructed by Eugene Agapov) This genome contains the 5' NTR to NS2 region of the NADL Jiv 90^{-} genome, followed by the *encephalomyocarditis virus* (EMCV) IRES, N^{pro}, NS3 and the remainder of the NADL sequence. A similar strategy as for N^{pro}-E2/sg (2) was used except that nucleotides 4973-5152 of pACNR/NADL were amplified and digested with *Bsp120*I and *Nsi*I. The stop codon is at R1589 (nt 5152, at the end of NS2).

p7-NS2-3-4A/sg: (Constructed by Eugene Agapov) This genome expresses N^{pro} and p7-NS2-3-4A from the BVDV IRES. The cloning strategy left 27 amino acids of C, 7 amino acids of E^{rns}, and 48 amino acids of E2 between N^{pro} and p7, and 37 amino acids of NS4B after NS4A. The downstream cistron, driven by the EMCV IRES, is identical to that of N^{pro}-NS2/sg. The *Xba*I/*Stu*I fragment of N^{pro}-E2/sg (2) was replaced with the *Xba*I/*Dra*I fragment of pNS2 Jiv 90^{-}/sg (2).

Ubi-NS2-3-4A/sg: This genome contains the BVDV IRES and 39 amino acids of N^{pro}, followed by Ubi-NS2-3-4A. The cloning strategy left 37 amino acids of NS4B in the first cistron. The downstream cistron, driven by the EMCV IRES, is identical to that of N^{pro}-NS2/sg. Nucleotides 1147 to 5120 of p7-NS2-3-4A/sg

were amplified by PCR using primers RU-2146 (5'-GTCCCCGCGGTGGCGATTC AGGGGGCCA-3') and RU-2147 (5'-GCCAGTAACGCTCGGTACCC-3'). A *Sac*I site and ubiquitin (Ubi) cleavage consensus sequence (RGG) were engineered immediately upstream of NS2. The PCR product was digested with *Sac*I/*Mlu*I and ligated to the *Sph*I/*Mlu*I fragment of p7-NS2-3-4A/sg and the *Sph*I/*Sac*II (Ubi) fragment of pSph-N^{pro}-Ubi-PAC-EMCV IRES (2).

p7-NS2-3-4A(Δ9-64)/sg: (Constructed by Eugene Agapov) This genome expresses N^{pro} and p7-NS2-3 from the BVDV IRES. The cloning strategy left 27 amino acids of C, 7 amino acids of E^{rns}, and 48 amino acids of E2 between N^{pro} and p7. Eight amino acids of NS4A remained in the first cistron followed by 5 random amino acids and a stop codon. The downstream cistron, driven by the EMCV IRES, is identical to that of N^{pro}-NS2/sg. *Spe*I and *Mlu*I of p7-NS2-3-4A/sg were blunt ended and ligated.

p7-NS2-3/sg: The 4003 bp *Sph*I/*Xma*I fragment of p7-NS2-3-4A/sg, the 524 bp *Xma*I/*Mlu*I fragment of p7-NS2-3(S1842A)/sg, and the 15843 bp *Mlu*I/*Sph*I fragment of p7-NS2-3-4A/sg were ligated together.

p7-NS2-3(S1842A)-4A/sg: (Constructed by Eugene Agapov) This genome is identical to p7-NS2-3-4A/sg except for the S1842A change in NS3 in the first

cistron. The *BsrG*I/*Drd*I fragment of p7-NS2-3-4A/sg was replaced with the corresponding fragment derived from pTM3/BVDV/1598-3035(S1842A) 225.

p7-NS2-3(S1842A)/sg: This genome is identical to p7-NS2-3-(S1842A)-4A/sg except that the first cistron contains a stop codon immediately after NS3. Nucleotides 241 to 2668 and nt 2220 to 4765 of p7-NS2-3(S1842A)-4A/sg were amplified with primers RU-2170 (5'-ACGAGGGCATGCCCAAAGC-3) with RU-2264 (5'-GTTGCCTACCATGAGCA-3'), and RU-2263 (5'-AAGAGGAGAGCAAA GGCT-3') with RU-3286 (5'-CAGTACGCGTTTACCCTACAACCCGGTCACTT GCTTCA-3'), respectively. A stop codon and *Mlu*I site were engineered into RU-3286. The 241-2668 product digested with *Sph*I/*PflM*I and the 2220-4765 fragment digested with *PflM*I/*Mlu*I were then ligated to p7-NS2-3 (S1842A)-4A/sg digested with *Sph*I/*Mlu*I.

Protein purification

Expression and GST-fusion purification

Amino-terminal GST fusion proteins were expressed in *E. coli* K12 UT5600 (NEB, Ipswich, MA) or Rosetta cells (Novagen, San Diego, CA). *E. coli* K12 UT5600 are deficient in the *OmpT* protease, Rosetta cells contain the pRARE plasmid encoding rare tRNAs and a chloramphenicol resistance gene. Expression and solubility were equivalent in either cell type. Cells were grown in Luria-Bertani broth supplemented with appropriate antibiotics at 30°C with

agitation until an OD_{600} of 0.5 was reached. Expression was then induced by addition of a final concentration of 0.5 mM isopropyl-β-D-thiogalactopyranoside (IPTG, Inalco, Milan, Italy). Following induction, cells were grown at 18°C with agitation overnight. Cells were pelleted at 4000 x *g* for 30 min at 4°C and pellets resuspended in 20 ml 0.5 M KCl, 20 mM Hepes [pH 7.4], 10% (v/v) glycerol per liter of bacterial cell culture. Cells were lysed by three passages through a cold French pressure cell (Avestin, Ottawa, Canada) at >10 000 psi. Unlysed and insoluble material were removed by centrifugation at 30 000 x *g* for 45 min at 4°C. Soluble material was loaded on a GSTrap fast protein liquid chromatography (FPLC) column (GE Healthcare, 5ml bed volume) equilibrated with buffer A1 (0.5 M KCl, 20 mM Hepes [pH 7.4]). After washing with buffer B (1 M KCl, 20 mM Hepes [pH 7.4]), fusion protein was eluted with 150 mM KCl, 100 mM Tris [pH 8.0], 15 mM glutathione. GST tag was removed by overnight treatment with Prescission protease (GE Healthcare, 0.5 mg per 1 mg protein) during dialysis against 4 L 100 mM KCl, 20 mM Hepes [pH 7.4] using snakeskin dialysis tubing (3000 molecular weight cut off (MWCO), Pierce, Rockford, IL).

Non-denaturing purification

After removal of GST, BVDV capsid 1-84 (C84) and BVDV capsid 1-87 (C87) were further purified over SP sepharose or heparin FPLC columns (GE Healthcare) equilibrated with buffer A2 (100 mM KCl, 20 mM Hepes [pH 7.4]). A linear salt gradient made from buffer A2 and buffer B (1M KCl, 20 mM Hepes [pH

7.4]) was used to elute the protein, with capsid-containing fractions eluting at approximately 470 mM KCl. BVDV capsid 1-90 (C90) was further purified by binding to a heparin FPLC column (GE Healthcare) equilibrated with buffer A2. A linear salt gradient made from buffer A2 and buffer B was used to elute the protein, with C87-containing fractions eluting at approximately 520 mM KCl.

Denaturing purification

After purification of the GST fusion proteins and cleavage of the GST as above, a final concentration of 1.0% acetonitrile/0.0325% trifluoroacetic acid (TFA) was added to denature the samples. Denatured protein was loaded on a Source 5RPC ST 4.4/150 reverse phase high pressure liquid chromatography (HPLC) column (GE Healthcare, 2.5 ml bed volume) equilibrated with buffer A (2.0% acteonitrile/0.0625% TFA). A (0-50% B) linear acetonitrile gradient made from buffer A and buffer B (80% acetonitrile/ 0.05% TFA) was used to elute the protein, with capsid-containing fractions eluting at approximately 20% (C87) to 24% (C90) acetonitrile. Eluted fractions were lyophilized, resuspended in 6 M guanidine-HCl, 50 mM Hepes [pH 7.5], and refolded by dialysis into 100 mM KCl, 20 mM Hepes [pH 7.4] using Slide-A-Lyzer mini dialysis units (3500 MWCO, Pierce).

Protein was quantified by Abs_{280} using the extinction coefficients (ε) of 2560 $M^{-1}cm^{-1}$ (C87) and 8250 $M^{-1}cm^{-1}$ (C90) and the equation $Abs_{280}/[(\varepsilon)(1cm)]$ =concentration (mol/L). To concentrate protein or exchange buffer, Centricon

centifugal concentrators (3000 MWCO, Millipore, Billerica, MD) were spun 7500 x *g* at 4°C. Concentrated protein was recovered by spinning the inverted Centricon at 2000 x *g* for 5 min. Protein was stored in 100-500 mM KCl, 20 mM Hepes [pH 7.4], 10% (v/v) glycerol or 100 mM KCl, 20 mM Hepes [pH 7.4] without glycerol for circular dichroism applications.

Visualization of Coomasie Brilliant Blue stained SDS-PAGE was used to estimate sample purity at >90%. For amino-terminal sequencing, protein was separated by SDS-PAGE and transferred to Sequiblot PVDF membrane (BioRad, Hercules, CA). Membrane was stained 45 sec in 0.1% (w/v) Coomasie Brilliant Blue, 40% methanol, 10% acetic acid and destained in 50% methanol. Dried membranes were sent to University of Texas Medical Branch protein chemistry core facility (Galveston, TX) for sequencing. For mass spectrometry, liquid samples in 100 mM KCl, 20 mM Hepes [pH 7.5] were analyzed by the Rockefeller University proteomics resource center.

Limited proteolysis assay. 0.2 μg endoprotease GluC (Roche, Mannheim, Germany) was used to digest 2 μg protein in 100 mM KCl, 20 mM Hepes [pH 7.4] at room temperature (RT). After incubation, reactions were stopped by the addition of an equal volume of 2x SDS loading buffer with β-mercaptoethanol (β-ME) and heating to 100°C for 5 min. Samples were resolved by SDS-12% PAGE and visualized by silver staining.

Intrinsic fluorescence spectroscopy. C90 protein (purified under non-denaturing conditions) at 0.03 mg/ml in 100 mM KCl, 20 mM Hepes [pH 7.4] was analyzed using an Olis RSM1000F spectrofluorimeter. For tyrosine spectra, the sample was excited at 280 nm and scanned from 300-430 nm wavelength in 1 nm increments. For tryptophan spectra, the sample was excited at 295 nm and scanned from 310-450 nm. Spectra of buffer alone were subtracted from protein spectra.

Circular dichroism spectroscopy. Protein (purified under non-denaturing conditions) at 0.8-1.0 mg/ml (C87) or 0.3 mg/ml (C90) in 100 mM KCl, 20 mM Hepes [pH 7.4] was analyzed using AVIV 202 circular dichroism (CD) spectrometer. Spectra were read from 250-200 nm wavelengths at 1 nm intervals. Data plotted is the average of 2 scans with the spectrum of buffer alone subtracted. CD readings were converted to molar ellipticity [Θ] using the equation:

$$[\Theta] = (\Theta_{obs} * 100 * MW)/(c * l * n)$$

Where ([Θ]) is in units of deg cm^2/dmole, (Θ_{obs}) is the CD reading in degrees, (MW) is molar mass of the protein in g/mol, (c) is concentration of the protein in g/L, (l) is pathlength in cm, and (n) is the number of residues in the protein

RNA homopolymer labeling and filter-binding assay. RNA homopolymers (Dharmacon, Lafayette, CO) were deprotected according to manufacturers

instructions and resuspended in water. 20 pmol of each RNA homopolymer was end labeled in a 20 μl reaction volume containing 60 μCi ^{32}P γ-ATP, 10 U T4 polynucleotide kinase (PNK, NEB) and a final concentration of 1x PNK buffer (NEB) for 30 min at 37°C. RNA was purified over a P30 spin column (Biorad), and resuspended to 1000 counts per minute (cpm)/ μl in 1x BB (200 mM KOAc, 50 mM TrisOAc [pH 7.7], 5 mM $Mg(OAc)_2$). RNA was heated to 60°C for 5 min and slow cooled to RT immediately before use.

For filter-binding assays, a nine point binding curve of two-fold dilutions of capsid protein was made in 1x BB from 0.05 μM to 5 μM concentration. The final well contained no protein. 10 000 cpm of labeled homopolymer was added to each dilution of capsid protein (50 μl final volume) and incubated for 10 min at RT. Filter-binding was conducted using a twelve well filter-binding apparatus (Millipore) and 0.45 μm nitrocellulose filters (Millipore). 45 μl of each reaction was spotted on a filter with vacuum source applied and immediately washed with 5 ml 1x BB. RNA alone, spotted on a filter without vacuum or washing, was a measure of total counts. Filters were dried, submerged in ReadySafe scintillation cocktail, and counted for 12 sec using a scintillation counter. Curves are fit using Prism graph pad non-linear regression for sigmoidal dose-response (variable slope) modified so that x=concentration of protein rather than log concentration. Dissociation constants were determined from the curve fit.

For competition filter-binding assays, a twelve point binding curve of three-fold dilutions of U oligomer was made in 1x BB from 50 nM to 3 mM of oligo. The

final well contained no competitor. 10 000 cpm of labeled U30 (approximately 5 fmol) was added to each dilution of oligo U. Finally, C90 was added to each well at a final concentration of 0.75 μM. The final reaction volume was 50 μl. Reactions were incubated 10 min at RT, filtered, washed, dried and counted as above. As oligo-Us are of different lengths, competitor is normalized to nucleotide concentration. Curves are fit using one site competition (Prism Graph pad).

Systematic evolution of ligands by exponential enrichment. A DNA template for a 25-mer random RNA library was created by annealing oligonucleotide primers (5 nmol each) RU-4447 (5'-TCCCGCTCGTCGTCT [25N] CCGCATCGTCCTCCCT-3') and RU-4448 (5'-GAAATTAATACGACTCACTATAG GGAGGACGATGCGG-3') (87). The mixed oligos, in a final concentration of 1x EcoPol buffer (NEB), were heated to 95°C for 5 min and cooled prior to the addition of 25 U DNA polymerase I (Klenow fragment, NEB) and 1 mM dNTPs. After 30 min at 37°C, the reaction was stopped by the addition of 25 mM EDTA and 2x RNA loading buffer (Ambion, Austin, TX). The blunt ended template was purified from a 20% native acrylamide gel, run in 1x TBE (90 mM Tris, 90 mM boric acid, 2 mM EDTA). Bands were visualized by UV shadowing, and the excised DNA was eluted from the gel by shearing through a 1 ml syringe, extraction at 37°C for 30 min in elution buffer (1 M NaOAc [pH 5.2], 1 mM EDTA), and subsequent clarification through a 0.22 μm tube filter (Corning, Lowell, MA).

DNA was precipitated with 2 volumes ethanol/isopropanol, centrifuged at 16 000 x *g* for 20 min, and resuspended in 100 μl water; template was quantified by absorbance at 260 nm.

For RNA synthesis, 500 pmol of template was transcribed in a 1 ml reaction containing final concentrations of 1x T7 transcription buffer (Promega), 2 mM NTPs, 10 mM DTT, 2000 U T7 RNA polymerase (Ambion, Austin, TX), 800 U RNAsin (Promega, Madison, WI), and 200 μCi ^{32}P α-UTP. Reactions were incubated at 37°C for 4-6 h, and for an additional 15 min with 60 U DNAse I (Invitrogen). The reaction was stopped by addition of 50 mM EDTA and RNA was precipitated with 200 μg glycogen, 300 mM NaOAc, 5 volumes ethanol, followed by pelleting at 16 000 x *g* for 20 min. RNA was resuspended in 1x urea/EDTA loading buffer (4.5 M urea, 0.5 mM EDTA, 0.025% (w/v) bromophenol blue, 0.025% (w/v) xylene cyanol in 1x TBE) and heated to 95°C for 5 min before loading on a 15% acrylamide/7 M urea denaturing gel. RNA was visualized by autoradiography and the band excised and purified as for the DNA template. The affinity of C87 for the RNA pool was measured by filter-binding assay as described above.

For selection, protein, at a concentration found to bind 5% of the library, was incubated with a 10 to 50-fold molar excess of RNA in 1x BB for 10 min at RT. Unbound RNA was removed by filtering through nitrocellulose (Millipore) and washing with 2 ml 1x BB. Filters were dried and counted without scintillation cocktail using Cherenkov radiation. Background binding of RNA was analyzed in

parallel to ensure nitrocellulose-specific sequences were not evolved. Bound RNA was removed from the filter by extraction in 200 μl 7 M urea, 400 μl phenol, 130 μl chloroform. After incubation at RT for 45 min with shaking, 130 μl water was added, samples were centrifuged at 16 000 x *g* for 5 min, and the aqueous phase was removed and added to 1 M NaOAc, 40 μg glycogen, 7 volumes ethanol/isopropanol. Precipitated RNA was used for reverse transcription (RT) and PCR.

For RT-PCR, extracted RNA was incubated with a final concentration of 0.5 mM dNTPs and 50 pmol RU-4440 (5'-TCCCGCTCGTCGTCTG-3') for 3 min at 70°C. After 2 min on ice final concentrations of 1x first strand buffer (Invitrogen), 10 mM DTT, 20 U RNAsin (Promega), and 100 U SuperScript II reverse transcriptase (Invitrogen) were added and incubated at 42°C for 1.5 h, followed by 72°C for 7 min. 10 U RNaseH (Epicenter, Madison, WI) and 1000 U RNaseT1 (Ambion) were added and incubated at 37°C for 20 min. The RT reaction was then PCR amplified with 1x thermopol buffer (NEB), 0.2 mM dNTPs, 50 pmol RU-4440, 50 pmole RU-4448, and 50 U Taq DNA polymerase (Invitrogen) in a final reaction volume of 500 μl. PCR products were precipitated with 50 μg glycogen, 300 mM NaOAc, 2.5 volumes ethanol, pelleted at 16 000 x *g* for 20 min, resuspended in 100 μl water and used as a template for next round of transcription.

Creation of monoclonal and polyclonal antibodies. The immunogen for both monoclonal and polyclonal antibodies was NADL capsid protein C84 purified under non-denaturing conditions. The GST tag was removed during the purification, as outlined above.

Monoclonal anti-BVDV capsid antibodies

Five mice were immunized five times with 120 μg C84 (monoclonal antibody core facility, Memorial Sloan Kettering, NY). Hybridomas were screened by enzyme-linked immunosorbent assay (ELISA) against recombinant C84. The first mouse selected for fusion did not result in any capsid-specific antibodies. The second mouse fused produced two antibody positive clones, 4F8 and 5E10. These antibodies are both isotype IgG1, κ light chain. Hybridoma supernatants of 4F8 and 5E10 worked in Western blot (1:500), 5E10 in immunoprecipitation, and 5E10 for immunofluorescence (1:500).

Polyclonal anti-BVDV capsid antibodies

Two rabbits (animals 886 and 887) were immunized with 100 μg C84 followed by three boosts with 50 μg protein (Cocalico, Reamstown, PA). Sera were screened in Western blot against NADL-infected cells lysates. Production bleeds from 10-Oct-02 to 22-Jul-03 (886) could be used at 1:5000 to 1:20 000; 26-Nov-02 to 27-May-03 (887) at 1:5000. Sera 10-Dec-02 and 24-Dec-02 (886) could also be used for immunoprecipitation.

RNA transcription.

Sindbis

Plasmids were linearized by digestion with *Xho*I for 3 h at 37°C and templates were purified over Minelute column (Qiagen, Valencia, CA). 0.6 μg was transcribed in a 10 μl reaction using the SP6 mMessage mMachine kit containing cap analog (Ambion). Reactions were incubated for 3 h at 37°C, with subsequent treatment with 3 U DNAseI (Ambion) for 15 min at 37°C. RNA was purified over RNeasy column (Qiagen), quantified by absorbance at 260 nm, and its integrity verified by 0.8% agarose gel electrophoresis.

HCV

Plasmids were linearized by digestion with *Xba*I for 3 h at 37°C, templates were purified over Minelute column (Qiagen) and 1 μg DNA was transcribed in a 10 μl reaction using the T7 Megascript kit (Ambion). Reactions were incubated at 37°C for 3 h followed by 15 min digestion with 3 U DNAseI (Ambion). RNA was cleaned up by RNeasy kit (Qiagen) with an additional on-column DNAse treatment for those samples that would subsequently be analyzed by quantitative reverse transcription-PCR (qRT-PCR). RNA was quantified by absorbance at 260 nm, and its integrity verified by 0.8% agarose gel electrophoresis.

BVDV

Plasmids were linearized by digestion with *Sbf*I for 2 h at 37°C and blunt-ended by addition of 2 U of DNA polymerase I (Klenow fragment, NEB) and 1.2 U of T4 DNA polymerase (NEB), followed by 0.8 μM dNTPs. Templates were purified by extraction once with phenol, twice with chloroform, and precipitated with ethanol and 3 M NaOAc. Transcription of 1 μg template was performed in a 20 μl reaction using the T7 Megascript kit (Ambion). Reactions were incubated for 2 h at 37°C after which RNA was purified using the RNeasy kit (Qiagen). RNA was quantified by absorbance at 260 nm, and its integrity verified by 0.8% agarose gel electrophoresis.

RNA transfection and growth curves.

Sindbis

For electroporation, BHK 21 cells were trypsinized, washed twice with ice-cold RNase-free phosphate-buffered saline (AccuGene PBS; BioWhittaker, Rockland, Maine), and resuspended at 2 x 10^7 cells/ml in PBS. 3 μg of each RNA to be electroporated was mixed with 0.4 ml of cell suspension and immediately pulsed with an ElectroSquare Porator ECM 830 (BTX, Holliston, MA) (960 V, 99 μsec, five pulses). Electroporated cells were diluted in 30 ml MEM/7.5% FBS and plated into 24 well and P100 tissue culture dishes.

At 6 h post-electroporation cells in 24 well plates were washed with Dulbecco's PBS (DPBS) and lysed with cell culture lysis buffer (Promega) for

assay of firefly luciferase activity. At 24 h post-transfection, cell culture supernatants from the P100 dishes were completely removed, clarified with a 0.22 μm filter, aliquoted, and frozen at -80°C for analysis of infectivity; fresh DMEM/10 mM nonessential amino acids/10% FBS was then added to the cells. Infectivity was assayed by infection of approximately 5 x 10^4 cells with 200 μl clarified supernatant and incubation for 1.5 h, after which inoculum was removed and 600 μl fresh medium was added. After a total of 4 h of infection, cells were lysed with cell culture lysis buffer (Promega) and analyzed for luciferase activity. Each infection was done in triplicate.

HCV

Huh-7.5 cells were trypsinized, washed twice with ice-cold RNase-free PBS (AccuGene), and resuspended at 1.5 x 10^7 cells/ml in PBS. 2 μg of each RNA to be electroporated was mixed with 0.4 ml of cell suspension and immediately pulsed with an ElectroSquare Porator ECM 830 (BTX) (820 V, 99 μsec, five pulses). Electroporated cells were diluted in 30 ml of DMEM/10 mM nonessential amino acids/10% FBS and plated into 24 well and P100 tissue culture dishes.

At 8, 24, 48 and 72 h post-electroporation cells in 24 well plates were washed with DPBS and lysed with *Renilla* lysis buffer (Promega) or with RLT buffer (Qiagen) containing 0.14 M β-ME (RLT/β-ME) for assay of replication by luciferase activity or qRT-PCR, respectively. At the same time points, cell culture supernatants from the P100 dishes were completely removed, clarified with a

0.22 μm filter, aliquoted, and frozen at -80°C for analysis of infectivity; fresh DMEM/10 mM nonessential amino acids/10% FBS was then added to the cells. For reporter viruses, infectivity was assayed by infection of naïve cells with 600 μl of clarified supernatant and incubation for 48 h, with subsequent lysis in *Renilla* lysis buffer (Promega) and analysis of luciferase activity. Each infection was done in triplicate.

BVDV

MDBK cells were trypsinized, washed three times with ice cold RNase-free PBS (AccuGene), and resuspended at 2 x 10^7 cells/ml in PBS. 5 μg of each RNA to be electroporated was mixed with 0.4 ml of the cell suspension and immediately pulsed with an ElectroSquare Porator ECM 830 (BTX) (900 V, 99 μs, 5 pulses). Electroporated cells were diluted in 10 ml DMEM/10% HS and plated in 35 mm or P100 tissue culture dishes.

Western blot.

Sindbis

Cells were lysed at 6 h post-electroporation or 4 h post-infection with cell culture lysis buffer (Promega). Lysates were separated on SDS-12% PAGE. After transfer to nitrocellulose membrane, blots were blocked for 1 h with 5% milk/TBST (0.02 M Tris-Cl [pH 7.4], 0.2 M NaCl, 0.1% (v/v) Tween-20). For Sindbis capsid detection, anti-C polyclonal antibody (169), was diluted 1:5000 in

TBST. After overnight incubation at 4°C, and extensive washing with TBST, goat-anti-rabbit immunoglobulin-horseradish peroxidase secondary antibody (Pierce) was added at 1:5000 dilution in 5% milk/TBST for 30 min at RT. After additional washing, blots were developed with SuperSignal West Femto chemiluminescent substrate (Pierce).

HCV

Cells were lysed at 48 h post-electroporation with *Renilla* lysis buffer (Promega). Lysates were separated on SDS-12% PAGE for analysis of core and β-actin, and on SDS-10% PAGE for analysis of NS5A. After transfer to nitrocellulose membrane, blots were blocked for 1 h with 5% milk/TBST. For core detection, monoclonal antibody (mAb) HCM-071-5 (Austral biologicals, San Ramon, CA), which recognizes amino acids 10-53, was diluted 1:750 to 1:1000 in TBST. For NS5A detection mAb 9E10 (115) was diluted 1:100 in TBST. After overnight incubation at 4°C, and extensive washing with TBST, rabbit-anti-mouse immunoglobulin-horseradish peroxidase secondary antibody (Pierce) was added at 1:5000 dilution in 5% milk/TBST for 30 min at RT. After additional washing, blots were developed with SuperSignal West Femto chemiluminescent substrate (Pierce)

BVDV

For detection of NS3, cells were lysed with passive lysis buffer (Promega) at 24 h post-electroporation and clarified by centrifugation at 18 000 x g for 30 seconds. Lysates were separated by SDS-10% PAGE and transferred to a nitrocellulose membrane and blots were blocked for 1 h with 5% milk/TBST. Polyclonal anti-NS3 antiserum (G40) was diluted 1:500 in 3% BSA and incubated for 1 h. After washing with TBST, the secondary antibody (goat-anti-rabbit-horse radish peroxidase (HRP), Pierce) was added at 1:10 000 dilution in 5% milk/TBST and incubated for 30 min at RT. For capsid detection, cells were lysed 6 h post-electroporation or 24 h post-infection with cell culture lysis buffer (Promega) and lysates were separated on SDS-12% PAGE. After transfer to nitrocellulose membrane, blots were blocked for 1 h with 5% milk/TBST, and incubated overnight at 4C with polyclonal anti-capsid antiserum 886 10-Oct-02 diluted 1:5000 in 5% milk/TBST. Goat-anti-rabbit immunoglobulin-horseradish peroxidase secondary antibody (Pierce) was added at 1:5000 dilution in 5% milk/TBST for 30 min at RT. After washing, blots were developed with SuperSignal West Femto chemiluminescent substrate (Pierce).

For detection of β-actin, the primary antibody (mouse-anti-β-actin, Sigma, St Louis, MO) was diluted 1:5000 in 5% milk/TBST and the secondary antibody (rabbit-anti-mouse-HRP, Pierce) was diluted 1:2500 in 5% milk/TBST. After removal of the secondary antibody by washing with TBST, blots were developed with SuperSignal West Pico or WestFemto Chemiluminescent substrate (Pierce).

HCV RNA extraction and qRT-PCR. For analysis of HCV RNA replication, total RNA was extracted from cells lysed with RLT/β-ME (Qiagen) and homogenized by centrifugation through a QiaShredder column (Qiagen) for 2 min at 14 000 x *g*. RNA was isolated by RNeasy kit (Qiagen) and quantified by absorbance at 260 nm. 50 ng of total cellular RNA was used per qRT-PCR. For analysis of released viral genomes, RNA was isolated from 1 ml of cell culture supernatant, harvested at 48 h post-electroporation, using the QiaAmp UltraSens kit (Qiagen). 2 μl of isolated RNA was used per qRT-PCR reaction.

qRT-PCR reactions were performed using the Light Cycler amplification kit (Roche, Basel, Switzerland) with primers directed against the viral 5'UTR. 20 μl reactions were assembled according to the manufacturers instructions. Quantitative RT-PCR amplification and analysis were performed using the LightCycler 480 (Roche) and associated software.

HCV Core ELISA. HCV antigen ELISA (Ortho Clinical Diagnostics, Raritan, NJ) was performed according to the manufacturer's instructions. Briefly, cell culture supernatants harvested at 48 h post-electroporation were diluted 1:10 (wild-type J6/JFH(p7Rluc2A)) or undiluted (mutants) and applied to plates coated with a mixture of anti-core mouse mAbs. Antigen was detected by addition of a second mAb cocktail, conjugated to HRP. Use of multiple mAbs with non-overlapping epitopes ensured detection of all the core mutants. After washing, wells were

developed by addition of substrate and subsequent stop solution; absorbance at 490 nm was measured. Core was quantified using Softmax software and comparison to a standard curve assayed in parallel.

RT-PCR. For analysis of HCV revertants and verification of infectious viruses, total cellular RNA was isolated from cells 48 h post-infection by RNeasy as described above. Approximately 0.2 ng of RNA was converted to first-strand DNA using SuperScript III first-strand synthesis kit (Invitrogen) and primers RU-5716 (5'-CTGCGGAACCGGTGAGTACAC-3'), RU-5927 (5'-CAAGGTCTCCCA CTTTCAG-3'), RU-5999 (5'-GTGTACCTAGTGTGTGCCGCTCTACC-3'), and RU-6000 (5'-ATGCCGCTAATGAAGTTCCAC-3'). After digestion with 1 U of RNaseH for 20 min at 37°C, one quarter of the RT reaction was PCR amplified using appropriate primers. The PCR products were gel purified using GFX columns (GE Healthcare) and used directly for sequencing.

HCV titer by limiting dilution. Clarified cell culture supernatants harvested at various time points post-electroporation were serially diluted and 50 μl of each dilution used to infect approximately 3 x 10^3 cells. At 72 h post-infection, cells were fixed and infected cells detected by immunohistostaining for NS5A. Fifty percent tissue culture infectious dose (TCID50) was calculated as previously reported (115).

HCV intracellular infectivity assay. Cells were collected at 72 h post-electroporation by trypsinization and pelleting at 500 x *g* for 3 min. Pellets were washed and resuspended in 500 μl DMEM/1x non-essential amino acids/10% FBS. Cells were lysed by four freeze-thaw cycles, and debris pelleted by twice centrifuging at 1500 x *g* for 5 min. The supernatant was collected and used for infection of naïve cells in the presence of 10 μg/μl anti-CD81 mAb (JS81, Pharmingen, San Diego, CA) or an isotype control (anti-mouse IgG1, Pharmingen). After 24 h of infection, the media was removed and replaced, and after an additional 24 h, cells were lysed in RLT/β-ME and total cellular RNA harvested for qRT-PCR analysis as above.

Immunohistochemistry. For immunohistochemical detection of HCV NS5A cells were fixed with 100% methanol at 48 h post-electroporation, blocked for 1 h with PBS, 0.2% (w/v) milk, 1% BSA, 0.1% saponin, and subsequently incubated for 5 min with 3% hydrogen peroxide. After washing with PBS and PBSS (PBS with 0.1% saponin), cells were incubated for 1 h at RT with 1:200 dilution of anti-NS5A mAb (9E10, ref 115). The secondary antibody, ImmunPress goat-anti-mouse peroxidase (Vector, Burlingame, CA), was diluted 1:10 and incubated for 30 min at RT. After washing, staining was developed with DAB substrate (Vector) for 5 min. Nuclei were counterstained with Hemotoxylin-2 (Sigma).

Immunofluorescence.

HCV

Approximately $3x10^5$ cells were plated on glass bottom 35 mm dishes (MatTek, Ashland, MA) at 72 h post-electroporation. After 24 h, cells were fixed with 4% paraformaldehyde in PBS for 30 min at RT. Fixed cells were incubated with PBST (PBS, 0.1% Triton X-100) for 30 min RT, followed by washing with PBS. Cells were blocked with PBSF (PBS, 1% FBS) for 1 h RT and stained for core. Primary anti-core mAb HCM-071-5 (Austral biologicals) diluted 1:1000 in PBSF was incubated at 4°C overnight. After washing with PBSF, secondary antibody Alexa 488-goat-anti-mouse IgG (Invitrogen) diluted 1:1000 in PBSF was incubated for 2 h at RT. Following washing with PBSF, cells were stained for lipid droplets. Cells were rinsed with 60% isopropanol in H_2O followed by incubation with 0.6% Oil red O in 60% isopropanol for 2 min at RT. Oil red O (Sigma) was diluted from a stock solution of 1% Oil red O in isopropanol and filtered through a 0.45 μm filter immediately before use. Cells were washed with 60% isopropanol, followed by PBS and H_2O. Cells were overlaid with PBS and viewed on a Zeiss LSM 510 confocal microscope; colocalization was analyzed using the associated software.

BVDV

Cells plated on culture slides (Becton Dickinson, Franklin Lakes, NJ) were washed with DPBS (Invitrogen) and fixed for 20 min with 50% methanol/50%

acetone. After washing twice, anti-NS3 antibody (mAb 184, ref 47) was added at a 1:2000 dilution in PBSG (PBS, 5% goat serum). Cells were incubated for 1 h at RT and then washed twice with PBSG. The secondary antibody (goat-anti-mouse IgG-Alexa 594, Molecular Probes, Eugene, OR) was added at a 1:2000 dilution in PBSG and cells were incubated for 20 min at 4°C. Hoescht 33342 (1 μg/ml) was added and cells were incubated an additional 10 min at 4 °C. Cells were washed 3 times with PBSG and coverslips were mounted. Slides were viewed using a Nikon Eclipse TE 300 microscope.

Heat inactivation of HCV virions. Clarified cell culture supernatants were incubated at 47°C for 30 min to 18 h. 200 μl heat-treated or untreated supernatants was used to infect approximately 1 x 10^5 cells in a 24 well plate. After 2 h, 400 μl media was added to the inoculum and cells were incubated an additional 48 h before lysis with RLT/β-ME and purification of total RNA for qRT-PCR.

Flow cytometry (FACS). Infected or electroporated cells in 35 mm dishes were trypsinized, washed twice with DPBS, and fixed with 0.5% paraformaldehyde in PBS for 20 min at RT. Cells were blocked and permeabilized with PBS, 5% (v/v) GS, 0.1% (w/v) sodium azide, 0.1% (w/v) saponin for 20 minutes at RT. Primary anti-BVDV NS3 antibody (mAb 184) was added at 1:2000 dilution in SB (PBS, 0.5% (w/v) BSA, 0.1% (w/v) sodium azide, 0.1% (w/v) saponin). Cells were

incubated for 1 h at RT and then washed twice with SB. Secondary antibody (goat-anti-mouse IgG Alexa 488, Molecular Probes) was added at 1:1000 dilution in SB and cells were incubated for 30 min at RT. Cells were washed twice with SB and analyzed by flow cytometry on a FACSCalibur (Beckton Dickinson), counting 1 x 10^4 cells for replication assay and 1 x 10^5 cells for infectivity assay. Titers of supernatants were calculated from the average percentage of NS3-positive cells. Infected wells were estimated to contain 1x 10^6 cells; this number was calculated by seeding cells under the same conditions as the assay and counting 24 wells in two independent platings. Since the viruses are incapable of cell-to-cell spread, FACS counts were expected to reflect the number of cells infected by the initial inoculum.

Amino acid alignments. HCV protein alignments were created using the HCV sequence database amino acid alignment tool (http://hcv.lanl.gov/content/hcv-db/index (102).

Chapter 3

Chapter 3: BVDV capsid is a natively unfolded protein that binds RNA

Introduction

All viruses must package a nucleic acid genome into a compact, stable, and dissociable structure for efficient transport to the next host cell. For the enveloped positive-strand RNA viruses, a nucleic acid molecule several thousand bases in length must be packaged into a particle of less than 100 nm in diameter. The viral capsid proteins responsible for this genomic RNA packaging vary in sequence and in structure. Unlike the capsid proteins of DNA and non-enveloped RNA viruses, which commonly adopt a conserved eight-stranded β-barrel motif, enveloped RNA virus capsid proteins are structurally diverse, suggesting distinct evolutionary lineages (48). These proteins resemble folds as disparate as chymotrypsin (*Togavirus*, ref 36, 37), a translation initiation factor domain (*Flavivirus*, ref 124, 50), and the HLA peptide recognition domain (*Arterivirus* and *Coronavirus*, ref 48, 86, 229) (Fig 3-1).

Within the *Flaviviridae* family, capsid protein structures have been determined for DENV and WNV, both members of the *Flavivirus* genus (Fig 3-1, ref 124, 50). These proteins are helix-rich and associated as dimers and tetramers. The anti-parallel helix interface of the WNV capsid protein tetramer has been compared to both an archeal transcription factor and a HEAT repeat domain similar to that found in eIF4G (50). Neither HCV core protein, nor a *Pestivirus* capsid protein has been characterized structurally to atomic resolution.

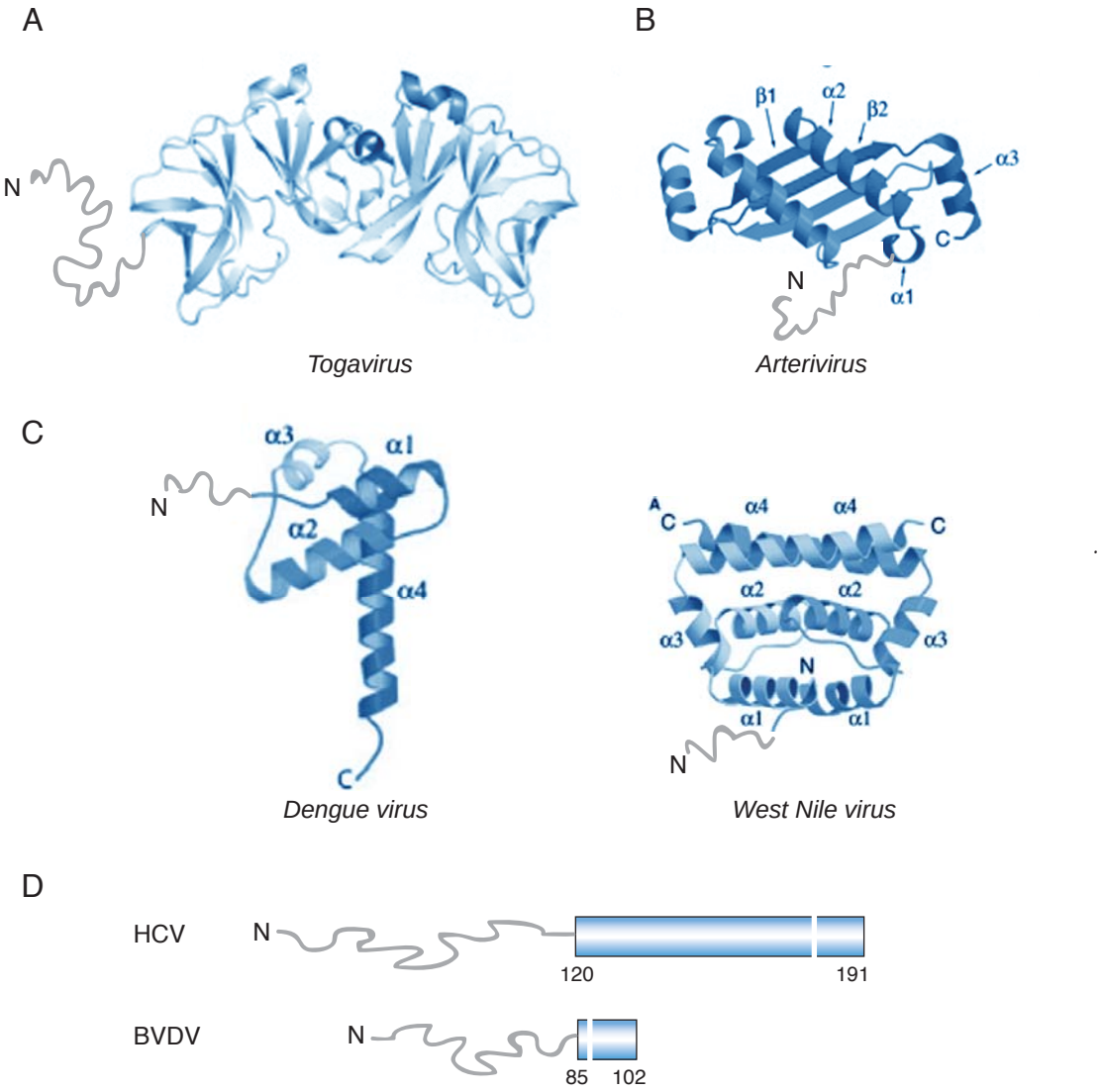

Fig 3-1. Capsid proteins of enveloped positive-strand RNA viruses have disordered regions. Capsid protein structures of (A) *Semliki Forest virus*, a *Togavirus* related to *Sindbis virus* (37, 229), (B) *Porcine respiratory and reproductive syndrome virus*, an *Arterivirus* (48), and (C) *dengue virus* and *West Nile virus*, *Flaviviruses* (50, 124). (D) HCV and BVDV capsid protein structures are not known. Blue bars represent predicted structured domains, white line represents SPP cleavage site. Grey lines indicate unresolved (A-C) or predicted disordered residues (D).

Secondary structure predictions, spectral analyses, and analytical ultracentrifugation have indicated that, similar to the classical *Flaviviruses*, the HCV core protein is dimeric and rich in helices (25, 24). The BVDV capsid protein is similar in size to the classical *Flavivirus* capsids, but, unlike these sequences, is predicted to contain minimal helical content. In fact, its proposed lack of secondary structure and low sequence complexity fit better with the hypothesis that BVDV capsid protein is predominantly disordered.

Unstructured regions are not uncommon in viral capsid proteins. For enveloped positive-sense RNA viruses, disordered sequences containing a high concentration of positively charged residues are ubiquitously found in the capsid protein amino-terminal domains (Fig 3-1). These disordered amino-termini range in length from 19 to 118 amino acids and are not resolved in the crystal structures. Both DENV and WNV capsid proteins contain flexible, basic amino-terminal regions of approximately 20 amino acids (124, 50). HCV core protein has a predicted unstructured domain encompassing the highly basic 117 to 124 amino-terminal residues (Fig 3-1). The flexibility of this region has been supported by circular dichroism and intrinsic fluorescence spectra measurements (25, 106).

The function of the disordered amino-terminal extensions is presumed to be the nonspecific binding and condensation of the RNA genome within the virion. This process is best understood for the *Alphaviruses*, a well-characterized group of enveloped positive-strand RNA viruses in the *Togaviridae* family.

Sindbis virus, the prototype *Alphavirus*, encodes three major structural proteins, capsid (C), and envelope proteins E1 and E2, translated as a NH_2-C-E3-E2-6K-E1-COOH polyprotein from a subgenomic RNA produced subsequent to RNA replication. The *Sindbis virus* capsid protein is 264 amino acids in length, with the carboxy-terminal 150 residues forming a chymotrypsin-like serine protease that mediates a single autoproteolytic cleavage (reviewed in 63). This domain also functions later in assembly, mediating an essential interaction with the cytoplasmic tail of E2 via a hydrophobic pocket located close to the protease active-site. The amino-terminus of the capsid protein is rich in lysine, arginine, and proline residues, which contribute to both specific and nonspecific associations with RNA (64, 117). The amino-terminus also contains sequences required for nucleic acid-dependent dimerization (204), and a putative leucine zipper that has been shown to stabilize these dimers (157, 81). Cryo-EM image reconstructions, combined with fitting of individual protein crystal structures have provided a view of capsid protein architecture within the intact *Alphavirus* particle (231, 147). Beneath the virion envelope, the nucleocapsid is a well-ordered *T*=4 icosahedral shell, with the capsid protease domains forming pentameric and hexameric protrusions from the RNA-containing interior. The flexible amino-terminal residues of the capsid protein extend from the ordered protease domains into the nucleocapsid core, forming a mixed protein-RNA region that does not have a well-resolved structure (35, 231). These studies demonstrated

that the disordered amino-terminus of *Sindbis virus* capsid protein is involved in nonspecifically binding and condensing the genomic RNA.

The *Pestivirus* capsid protein is unique among the enveloped RNA viruses in that it appears to contain only the disordered region and not the prominent structural domain seen in related viral proteins. This predicted paucity of structure is at once distinct to the *Pestivirus* capsid and relevant in understanding important related viruses such as HCV. We therefore investigated how this sequence might function mechanistically.

Results

Expression and purification of recombinant BVDV capsid protein

We cloned and expressed two versions of BVDV capsid protein encompassing the amino-terminal 87 (C87) or 90 (C90) residues fused to glutathione-S-transferase (GST, Fig 3-2A). We hypothesized that deletion of the majority of the capsid hydrophobic tail would facilitate purification and result in proteins related (C87) or identical to (C90) the mature, virion-associated capsid (78). C87 and C90 were initially purified under non-denaturing conditions using a two-step scheme (Fig 3-2B, top). GST-capsid fusion proteins were bound to a GSTrap column in 0.5 M KCl, 20 mM Hepes [pH 7.4]. After washing with high salt to remove nonspecifically bound proteins and nucleic acid, the fusion proteins were eluted with glutathione, and the GST moiety removed by Prescission protease treatment during overnight dialysis into 100 mM KCl, 20

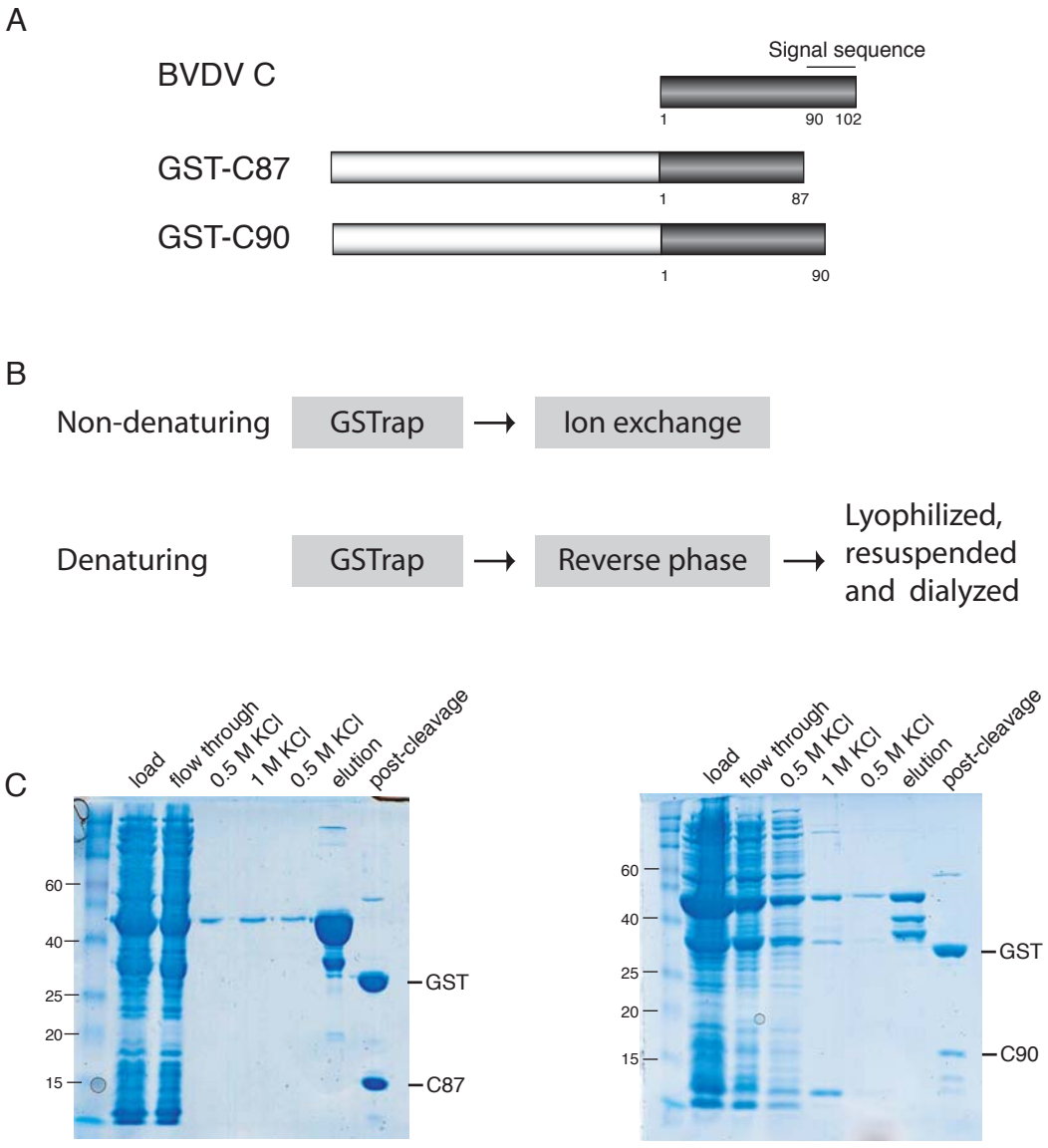

Fig 3-2. Purification of recombinant BVDV capsid protein. (A) Schematics of BVDV capsid protein and GST-fusion proteins. GST, white, BVDV capsid, grey. (B) Non-denaturing and denaturing purification schemes for C87 and C90. Shading indicates use of column. (C) GSTrap purification of GST-C87, left, and GST-C90, right. GST cleaved overnight at 4°C with PreScission protease, final lanes. Samples run on SDS-12%PAGE and stained with Coomasie brilliant blue.

mM Hepes [pH 7.4] (Fig 3-2C). C87 was further purified over an SP sepharose column and eluted within a salt gradient at approximately 470 mM KCl. C90 was further purified by binding to a heparin column, eluting at approximately 520 mM KCl. C87 yields were approximately 3 mg/L bacterial culture whereas C90 yields were between 0.05-0.1 mg/L.

Since C90 could not be purified to satisfactory yields under non-denaturing conditions, a denaturing purification scheme was devised (Fig 3-2B, bottom). After purification of GST-C87 or GST-C90 fusion proteins and removal of GST as above, a final concentration of 1% acetonitrile/0.0325% trifluoroacetic acid (TFA) was added. Denatured protein was loaded on a Source 5RPC ST 4.4/150 reverse phase column and eluted with an acetonitrile gradient. Eluted proteins were lyophilized, resuspended in 6 M guanidine HCl, 50 mM Hepes [pH 7.5], and refolded by dialysis into 100 mM KCl, 20 mM Hepes [pH 7.4]. Yields of C87 purified under denaturing condition were 0.5 mg/L bacterial culture whereas C90 yields were again 0.1 mg/L. The denaturing protocol had the advantage of destroying a co-purifying phosphatase activity, allowing capsid proteins to be assayed for binding to end-labeled nucleic acids without additional purification steps (data not shown). The identities of recombinant proteins produced by denaturing and non-denaturing methods were verified by mass spectrometry and amino-terminal sequencing.

These results showed that recombinant BVDV capsid protein could be expressed in and purified from bacteria. The deletion of three residues in C87

drastically increased yields over C90, possibly because of the hydrophobic nature of these amino acids.

BVDV capsid is a natively unfolded protein

Recently, a growing number of proteins from a wide variety of sources have been found to lack distinct secondary or tertiary structure and have been termed natively unfolded (reviewed in 208, 53, 212). These proteins share similar characteristics including low primary sequence complexity, high susceptibility to proteases, anomalous migration on SDS-PAGE, and lack of secondary structure by spectral methods (208). Since BVDV capsid is a highly basic protein, poor in hydrophobic residues, we decided to test the hypothesis that BVDV capsid possesses other characteristics of a natively unfolded protein. Proteins purified under non-denaturing conditions were tested in various assays for characteristics of intrinsically disordered proteins.

Secondary structure predictions

Secondary structure prediction algorithms were used to estimate the helical nature of the full-length BVDV capsid protein (residues 1-102). Only the carboxy-terminal region was predicted with high confidence to contain helix-forming residues (Fig 3-3A, ref 175). This is in keeping with the function of this region as a signal sequence for E^{rns}. The prediction of natively disordered regions (PONDR) algorithm was used to determine if BVDV capsid was likely to be natively unfolded (113, 174, 173). This prediction takes into account low

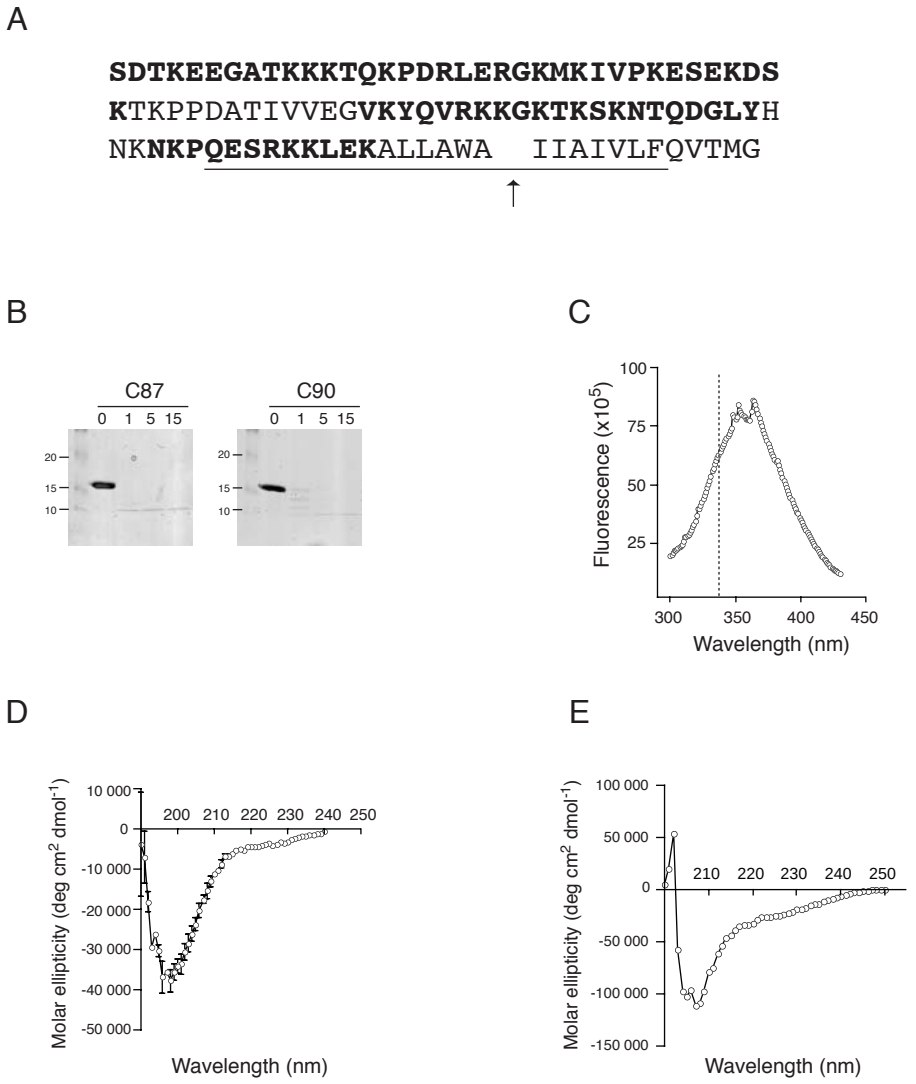

Fig 3-3. BVDV capsid is natively unfolded. (A) BVDV capsid protein sequence and secondary structure predictions. Predicted disordered regions, bold, and proposed helices, underlined. SPP cleavage site designated by an arrow. (B) Limited proteolysis of C87, left, and C90, right, with endoprotease GluC. Incubation times at RT are indicated (min). (C) Tyrosine intrinsic fluorescence spectrum of C90. Dotted line indicates 340 nm. Circular dichroism spectra of C87 (D) and C90 (E).

sequence complexity and paucity of hydrophobic residues as indicators of disorder. Analysis of the BVDV capsid protein indicated a high propensity for an unfolded structure (Fig 3-3A). These results predicted that BVDV capsid consists of a disordered amino-terminal 75 to 84 residues followed by a helical transmembrane domain.

Limited proteolysis

Natively unfolded proteins have a large proportion of solvent-exposed residues and are therefore highly susceptible to proteolysis. Treatment of C87 or C90 with endoprotease GluC resulted in almost completely digestion within one minute when the capsid protein was present in ten-fold excess (Fig 3-3B). Similar results were seen with trypsin and chymotrypsin; for all three enzymes proteolysis of C87 was complete within one hour even when capsid protein was in 300-fold excess (data not shown). These results suggested that the majority of capsid residues are accessible to proteases rather than protected within the hydrophobic core of the protein.

Intrinsic fluorescence spectroscopy

C90 contains two tyrosines, at positions 51 and 69, and one tryptophan, at position 89. Intrinsic fluorescence of these residues can be used to determine their environment since the wavelength of emission correlates with the degree of solvent exposure. Emission maxima for both tyrosine (Fig 3-3C) and tryptophan

spectra (data not shown) were at approximately 360 nm wavelength. Since an emission maximum greater than 340 nm indicates a high degree of solvent exposure, these results suggested that the capsid protein lacked significant globular structure.

Circular dichroism spectroscopy

Far UV circular dichroism (CD) indicates the presence of secondary structural elements in a protein by measuring the interaction of the protein with elliptically polarized light (reviewed in 94). Alpha helices, β-sheets, and disordered random coil sequences produce distinctive spectra, which can be deconvoluted to indicate the proportion of each structural element in the protein. Analysis of C87 by circular dichroism indicated a minimum at approximately 195 nm, indicating a large proportion of random coil (Fig 3-3D). Minima at 208 nm or 222 nm, indicative of α-helical and β-sheet secondary structures, were not observed. C90 produced similar results, although the lower protein concentration made the data less reliable (Fig 3-3E). Taken together, these results suggest the presence of large regions of disorder within the BVDV capsid protein.

BVDV capsid binds RNA with low affinity and low specificity

The extremely basic nature of the BVDV capsid protein, as well as its suspected close proximity to the viral genome within the virion led us to hypothesize that capsid may bind to RNA.

Filter-binding assay

In order to test C87 and C90 for RNA binding activity, we used a quantitative filter-binding assay. Radiolabeled RNA homo-oligomers of adenosine (A), cytidine (C), guanosine (G), and uridine (U) (30 nt in length) were added at constant concentration to a dilution series of protein. Protein purified under denaturing conditions was used in this assay in order to eliminate a bacterial phosphatase that co-purified under native conditions (data not shown). RNA-protein mixtures were applied to nitrocellulose filters under vacuum, washed, and RNA retained on the filter was quantified. Whereas unbound RNA flows through the filter, protein binds the nitrocellulose and will retain any RNA complexed with it. Indeed, in the absence of protein, RNA retention on the filter was generally less than 10% of total counts applied. Using this assay, we determined that C87 and C90 bound RNA equivalently and with approximately 1 μM affinity; a slight preference was seen for G and U homo-oligomers (Fig 3-4C). The low affinity and low specificity of capsid binding to RNA suggested a nonspecific, charge-charge interaction of the highly basic protein and negatively charged phosphate backbone of the nucleic acid.

Systematic enhancement of ligand binding by exponential enrichment

To further investigate the involvement of specificity in capsid-RNA interactions, systematic enhancement of ligand binding by exponential

A

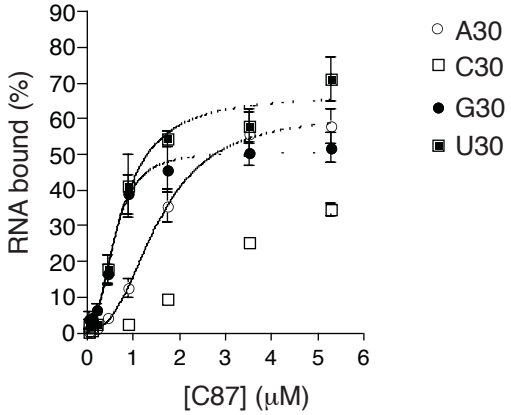

B

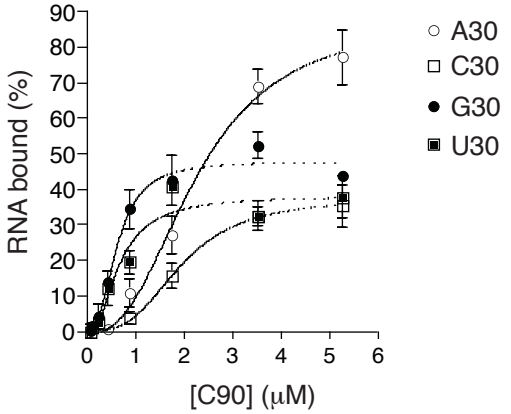

C

	Kd (μM)			
	A	C	G	U
C87	1.6	3.1	0.6	0.7
C90	2.3	2.0	0.6	0.6

Fig 3-4. BVDV capsid binds RNA. Binding of C87 (A) and C90 (B) to RNA homo-oligomers. Means and standard error of the mean (SEM) of at least duplicate binding assays are shown. Curves are fit using sigmoidal variable slope model. (C) Dissociation constants for capsid binding to homo-oligomers.

enrichment (SELEX) was employed. In this approach an RNA library is enriched for sequences with high affinity for the target protein. A random library of 25 nucleotides with flanking T7 promoter and primer binding sites was created from synthesized oligonucleotide primers. RNA transcribed from this library was screened for sequences better able to bind C87, as described in the materials and methods. In the initial rounds of selection, the number of RNA molecules was kept at or above the theoretical complexity of the library (1×10^{15} sequences). At each round of selection, the affinity of the RNA population for C87 was measured and the pool was partitioned by binding to a low concentration of protein. The protein-bound RNA was reverse transcribed (RT), PCR amplified, and used as a template for the synthesis of an enriched RNA pool for the next round of selection. After eight rounds of selection, the RT-PCR amplified RNA pool was cloned and multiple individual colonies were sequenced. Although the affinity of the pool had not significantly increased during the selection, a consensus sequence emerged in all of the 13 clones sequenced (Fig 3-5). This sequence was not detected in 6 clones sequenced from the original library. The consensus sequence, GUGGGA(A/U)NNA, is G-rich, in keeping with the slightly higher affinity for G observed in the homo-oligomer studies. The lack of increased affinity of the pool is also consistent with the similar affinities of the homo-oligomers for capsid and again suggests that capsid binds RNA with little specificity. We cannot rule out the possibility that other selective factors,

A

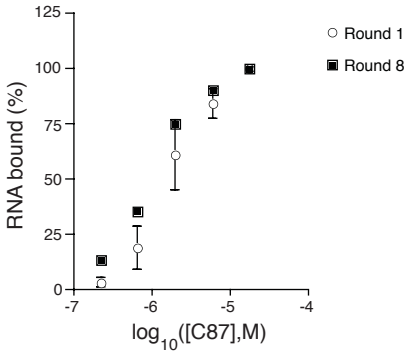

B

Clone	25N sequence
1	GUGGGAUAUAAUAAACAGGUGCGC
2	GUGGGACAAAUGGUAGUUCGAGUC
3	GUGGGAAGGAAAAUACUGUGGUGC
4	GUGGGAUUCAAAUAUAGUUUACCC
5	GUGGGACGUACAUAGAAACGCGGC
6	GGGGGAUAAACUAUAAAUGCGCUA
7	GUGGGACGAAAGAUGACGUUUGUG
8	GUGGGGAGAAGUAUAUGAGCGC--
9	GAGGGAAUAUGACUCGUAGUGAC-
10	GUGGGAUAAGAAAAUUUGUUGCGC
11	GCGGGACGGAGGUUAUGUUUGGG-
12	GUGGGAAUAGAUGUAUAGGUUCCC
13	GUGGGGUAAAGUUGUUAGUCUGGC
Consensus	GUGGGAWNNA

Fig 3-5. Selection of a consensus RNA for C87 binding. (A) Binding of round 1 and round 8 RNA pools to C87. For round 1 binding mean and SEM for triplicate measurements are shown. (B) Sequences of the randomized region of cloned cDNAs from round 8 of selection. Consensus is shown; W, A or U; N, any nucleotide.

such as nuclease resistance, could have also contributed to the emergence of a consensus sequence.

Taken together, these results indicate that BVDV capsid binds RNA, but with low affinity and little specificity. The slight preference for G could indicate a propensity to bind structured RNA molecules.

C90 binds to 14 nucleotides of oligo-U RNA

Capsid protein binding to RNA appeared to be of low affinity and of low specificity. To further investigate the nature of the capsid-RNA interaction, we determined the minimal RNA size that could act as a capsid binding site. We used the filter-binding assay to quantify the ability of oligo-U sequences of different lengths to compete for U30 binding to C90; oligo-G was not chosen because of the possible complication of secondary structures. In this assay the C90 concentration was held constant at approximately the Kd (0.75 μM), radiolabeled U30 concentration was also constant at approximately 100 pM**,** and unlabeled competitor was diluted from 3 mM to 50 nM. While U6 was not able to compete for U30 binding, as the length was increased competition became more efficient (Fig 3-6). From the competition assay, the binding site size for C90 to oligo-U RNA was estimated at 14 nucleotides.

To verify the binding site size, we conducted a direct filter-binding assay of labeled U14 or U30 to C90. As observed previously, the binding affinity of C90 to U30 was approximately 1 μM. The affinity of C90 binding to U14 was lower but

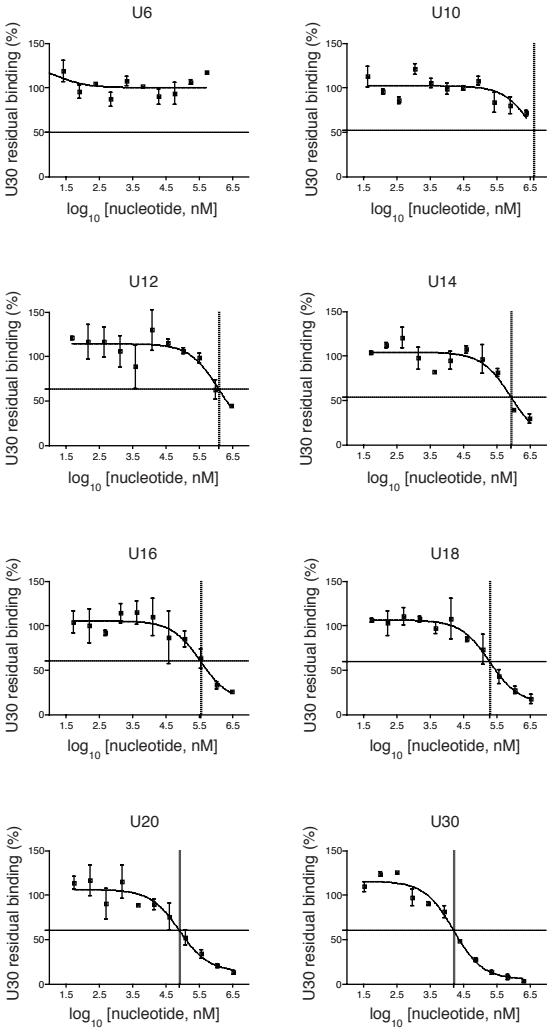

Fig 3-6. C90 minimal RNA binding site size is 14 nucleotides. Competition for C90 binding to U30. Residual U30 binding in the presence of the unlabelled oligomers indicated. Means and SEM of duplicate binding assays are plotted. Curves are fit using one-site competition model.

binding was detectable (Fig 3-7A). Analysis of the cooperativity of binding by Hill plot suggested that two molecules of C90 bind to U30 cooperatively, whereas a single molecule binds to U14 (Fig 3-7B). This analysis is consistent with a minimal C90 binding site size of 14 nucleotides.

BVDV capsid acts as a nonspecific RNA binding protein *in vivo*

Our *in vitro* analyses of BVDV capsid protein suggested a nonspecific, low affinity association with RNA. We hypothesized that BVDV capsid might act as a nonspecific RNA binding protein *in vivo*, and that this type of interaction might allow it to condense and neutralize viral genomic RNA. To test this hypothesis, we investigated whether BVDV capsid protein could functionally replace a known nonspecific RNA condensing sequence. The well-documented RNA packaging activity of *Sindbis virus* capsid protein provided an ideal system for this investigation (Fig 3-8A).

Sindbis genomes were created with in-frame deletions engineered into the amino-terminal domain of the capsid protein (Fig 3-8B). The native sequence from amino acids 97 to 264 was maintained in all constructs, preserving the specific RNA interaction sequence and protease activity (155, 36). In the largest deletion, the methionine start codon was fused directly to amino acid 97. This genome was predicted to be severely impaired in RNA packaging and therefore in infectious virus production (60). To test the ability of the BVDV capsid protein to rescue the deletion mutants, BVDV sequences were inserted in the deleted

A

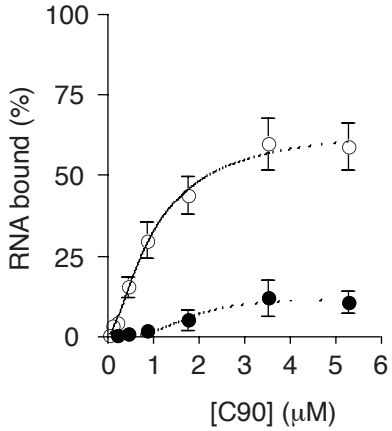

B

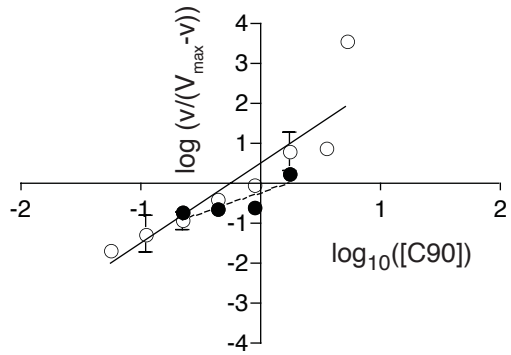

C

	Slope
U14	1.044
U30	1.992

Fig 3-7. C90 binding to U14 and U30. (A) Direct binding of C90 to radio-labelled U14 (black) or U30 (white). Mean and SEM of at least quadruplicate measurements are shown. Curves are fit using sigmoidal variable slope model. (B) Hill plots of C90 binding to U14 (black) or U30 (white). (C) Slopes of Hill plots.

region, while preserving the approximate native length of the Sindbis capsid amino-terminal domain (Fig 3-8C). The parental sequence was a fully infectious *Sindbis virus* genome encoding firefly luciferase as a fusion with the nsP3 protein, facilitating sensitive detection of infectious virus production by reporter gene activity (Sindbis/luc, ref 19).

In vitro generated RNA transcripts of each genome were electroporated into BHK 21 cells. Wild-type Sindbis/luc and Sindbis/luc(Δ*Kpn*I), a replication defective genome with a deletion in nsP4 (19), were electroporated in parallel. Replication was assayed at 6 h post-electroporation by quantification of intracellular luciferase activity. Consistent with the non-essential role of Sindbis capsid in RNA replication, luciferase activities were similar for each of the mutant genomes; Sindbis/luc(Δ*Kpn*I) did not replicate (Fig 3-9A). Intracellular capsid protein expression was also measured at 6 h post-electroporation. Western blot with anti-Sindbis capsid (168) and anti-BVDV capsid polyclonal antibodies (see materials and methods) confirmed the expression of the appropriate sequences (Fig 3-9B). The reduced expression of Sindbis/luc(CΔ2-96) and related chimeras is likely due to the deletion of a translational enhancer present in the capsid coding sequence (61).

At 24 h post-electroporation, cell culture supernatants were harvested, clarified by filtration, and used to infect naïve BHK 21 cells. The infected cells were incubated for 4 h before assay for luciferase activity. Sindbis/luc(CΔ2-96) was severely impaired in infectious virus production, while the less drastic

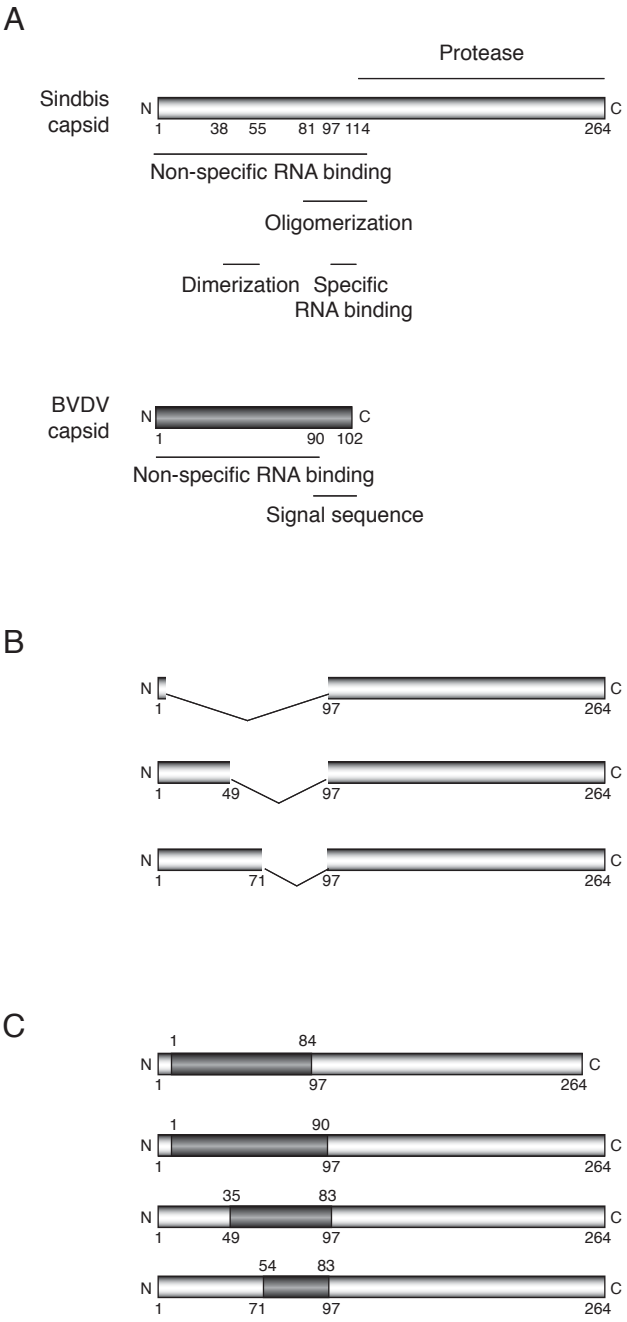

Fig 3-8. Sindbis and BVDV capsid proteins. (A) Schematics of Sindbis, top, and BVDV, bottom, capsid protein functional domains. (B) Deletions in Sindbis capsid protein created in the context of Sind/luc. (C) Chimeras of Sindbis, white, and BVDV, grey, capsid protein sequences in the Sind/luc genome.

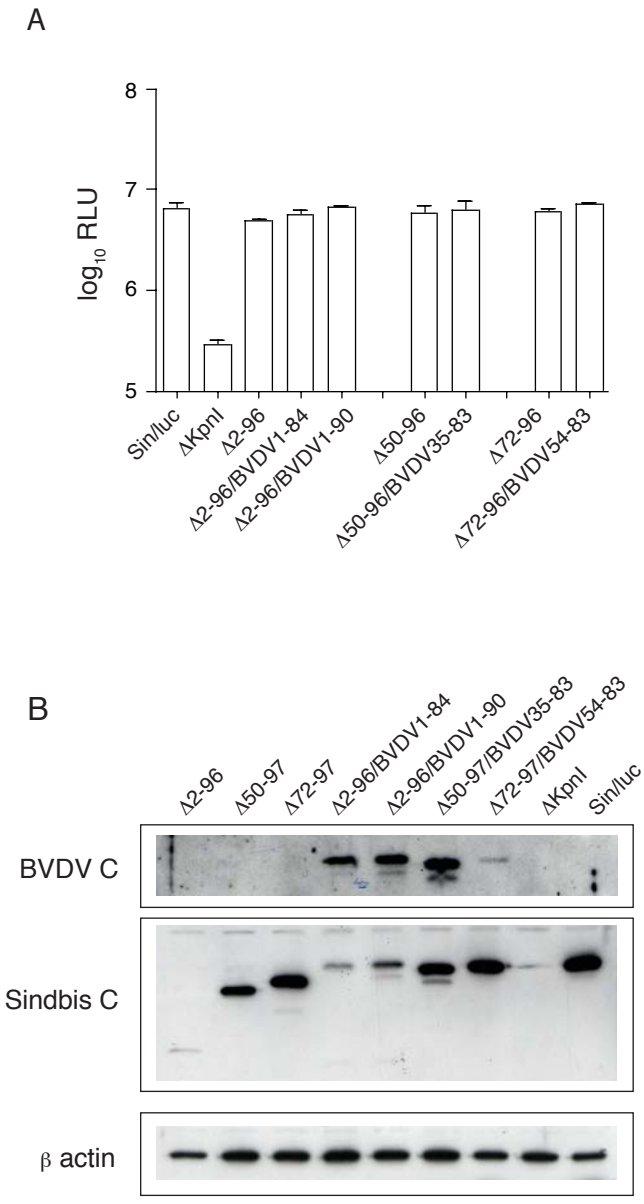

Fig 3-9. Chimeric genomes replicate and express chimeric capsid proteins. (A) Luciferase activity in transfected cells after 6 h. Mean and SEM of duplicate experiments are shown. (B) Protein expression at 6 h post-electroporation. BVDV capsid, top panel, and Sindbis capsid, middle panel, detected using polyclonal antibodies.

deletions, Sindbis/luc(CΔ50-96) and Sindbis/luc(CΔ72-96), showed more moderate reductions in infectivity (Fig 3-10A). In each case, the inclusion of BVDV sequences increased the infectivity of the deletion mutants, indicating that the basic nature of the BVDV residues was sufficient to rescue infectious virion production. In the case of Sindbis/luc(CΔ2-96/BVDV1-90), in which the entire virion associated form of BVDV capsid replaces the basic amino-terminus of Sindbis capsid, the infectivity was only about ten-fold reduced from wild-type Sindbis/luc (Fig 3-10A). This strongly suggested that the BVDV capsid protein could functionally replace the Sindbis capsid amino-terminal domain. Interestingly, infectivity of Sindbis/luc(CΔ2-96/BVDV1-90) was markedly increased over that of Sindbis/luc(CΔ2-96/BVDV1-84) (Fig 3-10A). The requirement for these carboxy-terminal six amino acids, which are actually not basic in nature and have predicted helical character, might point to an additional functional sequence within the BVDV capsid protein.

In order to verify that infectious virus production resulted from the electroporated mutant genomes and not reversions, lysates from infected cells harvested after 4 h (Sindbis capsid blot) or 24 h (BVDV capsid blot) were probed for expression of the viral capsid sequences with polyclonal antibodies. Capsids of the appropriate provenance were detected in each infected cell population, indicating that the infectivities of the mutant genomes were accurately represented (Fig 3-10B).

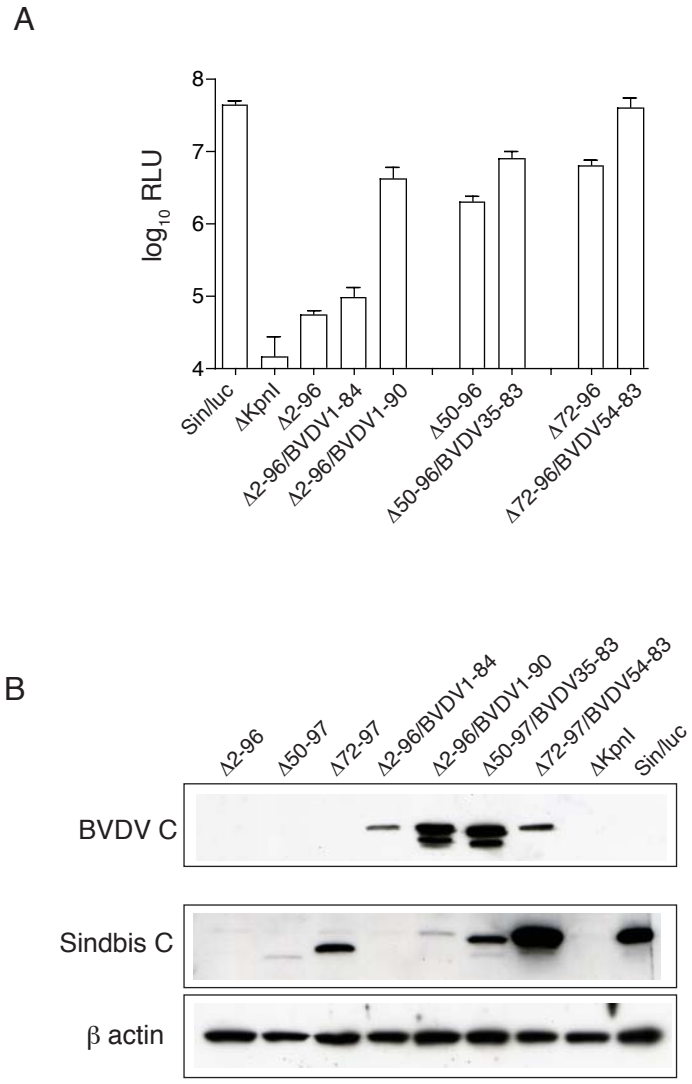

Fig 3-10. Infectivity of chimeric genomes. (A) Luciferase activity in infected cells after 4 h. (B) Protein expression in infected cells. BVDV capsid, top panel, detected at 24 h post-infection. Sindbis capsid, middle panel, and β-actin, lower panel detected at 4 h post-infection.

Taken together, these results suggest that the nonspecific RNA binding properties of BVDV capsid observed *in vitro* are responsible for its ability to functionally replace an RNA condensation sequence *in vivo* and indicate that the BVDV capsid protein likely functions by a similar mechanism in packaging its own genomic RNA.

Discussion

Proteins involved in condensing, protecting, transporting and subsequently releasing a viral genome might be expected to bind RNA with low affinity and to efficiently neutralize its negative charge. We have shown that the highly basic BVDV capsid protein demonstrates this behavior *in vitro* and can functionally replace the nonspecific RNA binding region of another viral capsid protein *in vivo*. The *in vitro* nonspecific RNA binding affinities of BVDV capsid and a portion of the Sindbis capsid amino-terminal region are similar, at approximately 0.5-0.6 μM (117). This relatively low binding affinity likely allows the RNA genome to be released and accessed for translation upon entry into a new host cell. The ability of BVDV capsid to functionally replace the role of the Sindbis capsid amino-terminus in infectious virus production indicates not only a recapitulation of RNA binding and condensation activities, but also of appropriate genome release upon uncoating.

While *Sindbis virus* capsid protein residues 97-106 interact specifically with an encapsidation signal in the genomic RNA (220, 155), BVDV capsid

appears to be far less discerning. Although this could be an artefact of the *in vitro* experimental conditions, the ability of BVDV capsid to readily bind Sindbis RNA *in vivo* favors the hypothesis of largely ionic interactions. This putative inability to discriminate between genomic, antisense, and cellular RNAs may be overcome by local concentration effects caused by intracellular compartmentalization of viral replication and assembly. No evidence for a specific encapsidation signal has been found for any member of the *Flaviviridae*.

While the amino-terminus of *Sindbis virus* capsid protein, and likely of other viral capsid proteins, appear to be functionally homologous to the BVDV capsid, the *Pestivirus* sequence has the unusual lack of a structured carboxy-terminal domain. In the absence of such a domain, it is difficult to envision how the BVDV capsid protein might be able to form a structured casing around the viral RNA. Canonical viral nucleocapsids consist of an ordered array of capsid protein subunits, arranged symmetrically around the nucleic acid interior (88). These nucleocapsids, including those of *Sindbis virus*, can often be assembled *in vitro* from capsid protein and nucleic acid components, and visualized and isolated from infected cells. Interestingly, non-enveloped nucleocapsids are rarely seen in *Flavivirus* or *Pestivirus*-infected cells (116), and limited studies of HCV have also so far failed to detect intracellular nucleocapsids (176). This suggests that *Flaviviridae* cores may not be discrete, stable, proteinaceous coats for the viral genome. Consistent with this, purification and *in vitro* assembly of *Flaviviridae* nucleocapsids have been extremely difficult, and usually result in

structures with pleiomorphic shapes and heterogeneous sizes (97, 105, CLM and CMR unpublished observations).

Further evidence for an absence of defined symmetry in the nucleoprotein core of *Flaviviridae* particles comes from the cryo-EM image reconstructions of DENV and WNV, both members of the *Flavivirus* genus (Fig 3-11, ref 101, 145, 232). In these virion structures no discrete nucleocapsid was detected despite a defined symmetry of the outer envelope protein shell (101, 145, 232, 233). In addition, no transmembrane connections between the envelope proteins and particle inner core were seen, suggesting a symmetry match between the two layers is likely not required (232). The *Flavivirus* capsid protein dimers are predicted to be randomly dispersed within this disordered core, with their overall positive charge neutralizing the genomic RNA (147). Infectious BVDV particles are known to be pleiomorphic in size and shape (70) and can contain genomes varying in size by over 8 kb (13), an extreme flexibility that might be inhibited by the constrained interactions of an icosahedral nucleocapsid. In fact, the icosahedral core may be the exception rather than the rule among enveloped RNA viruses; nucleocapsids of the *Coronaviruses* are reported to be flexible, filamentous structures packed into a spherical virion outer shell (172).

While the BVDV capsid lacks structural features found in other viral capsid proteins, these folded domains may not be necessary in the absence of an ordered nucleocapsid and specific genomic RNA interactions. Interestingly, the predicted short carboxy-terminal helix of the BVDV capsid protein did appear

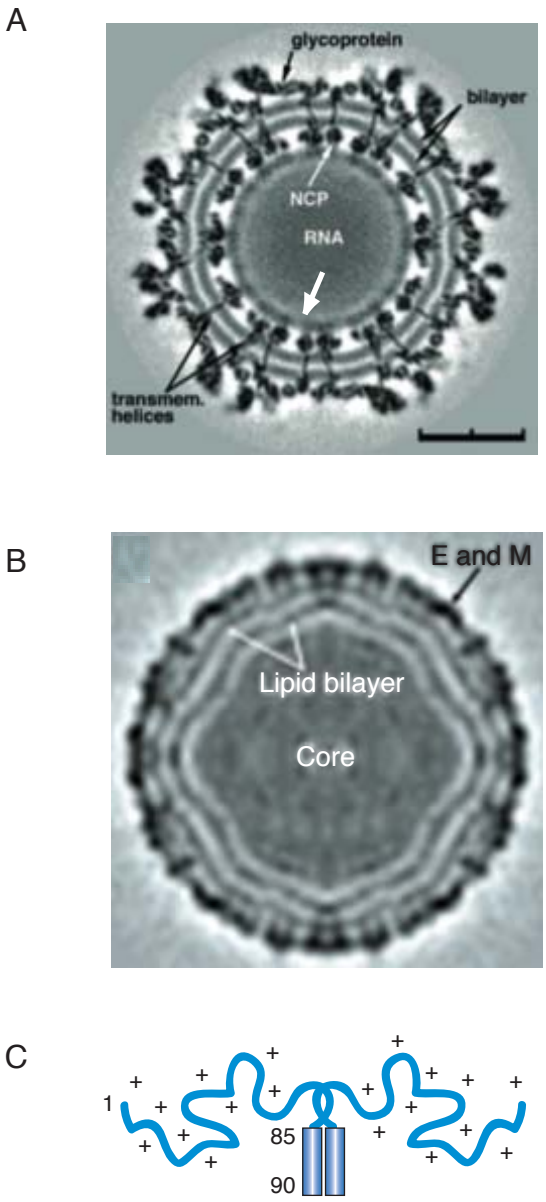

Fig 3-11. Model for BVDV capsid function. (A) Structure of *Sindbis virus* (231) showing ordered nucleocapsid with partially disordered inner layer (arrow). (B) Structure of *West Nile virus* (145) showing unstructured nucleocapsid. (C) Proposed functional domains of BVDV capsid. Residues 1-84 are highly basic, disordered residues available for RNA interactions. Residues 85-90 are hydrophobic residues proposed to mediate interactions between capsid proteins.

to be required for optimal replacement of the *Sindbis virus* capsid amino-terminus function. Since a Sindbis capsid homotypic interaction domain was also deleted in these genomes (157), the possible compensation for this might suggest the presence of at least one other functional region in the BVDV capsid protein. We propose that the hydrophobic resides 85 to 90 are involved in the mediation of capsid-capsid interactions (Fig 3-11). This putative dimer formation is in keeping with our observed cooperativity of RNA binding and reminiscent of the functional dimers formed by other *Flaviviridae* capsid proteins (97, 130, 89, 25).

In conclusion, we found that BVDV capsid is a natively unfolded protein with a large number of basic residues involved in mediating low affinity nonspecific interactions with RNA. We further determined that this *in vitro* behavior likely reflects its *in vivo* mechanism of action as a nonspecific RNA condensing agent.

Chapter 4

Chapter 4: Mutagenesis of the HCV core protein reveals numerous residues essential for infectious virus production in cell culture

Introduction

The HCV capsid protein, termed core, is presumed by analogy to the related *Flaviviruses* and *Pestiviruses* to function primarily as a component of the infectious virion (30). Until very recently propagation of HCV in tissue culture has not been possible, and consequently, this major function of the core protein has not been investigated. Initial sequence analyses of core indicated that this well conserved, 21 kDa, protein has numerous basic residues in its amino-terminal region, followed by a central hydrophobic domain, and a signal sequence for E1 (Fig 4-1, ref 30, 132). The identification of putative nuclear localization signals (30) led to numerous reports that core protein could regulate cellular and heterologous viral promoters (98, 186, 164, 166). Suppression of the *hepatitis B virus* promoter was reported to occur in a phosphorylation dependent manner (185). Since only carboxy-terminally truncated, rather than full-length, core proteins appear to localize to the nucleus, the ability of core to modulate gene expression remains controversial (116).

Processing events required for the production of the mature core protein have been intensively investigated. The carboxy-terminal residue of the virion-associated form of the protein, however, has yet to be unambiguously determined. *In vitro* translation of the structural proteins in the presence of

A

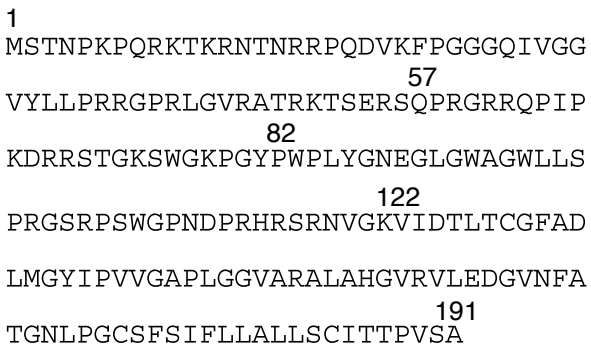

B

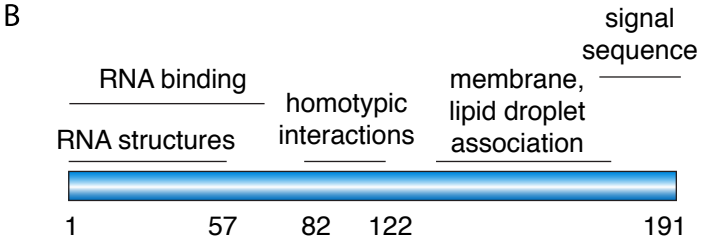

Fig 4-1. HCV core protein seqeunce and features. (A) J6 core amino acid sequence. (B) Previously reported core functional regions (reviewed in reference 132). See text for details.

microsomal membranes implicated signal peptidase and another host enzyme (180), later identified as SPP, as important for core processing (133). Attempts to identify the SPP processing site by mutation of the core protein have led to disparate conclusions. This is likely because cleavage form resolution depends on the gel system chosen (82), and since purified core protein size standards containing the appropriate mutations have not been employed. Cleavage of core by SPP has been shown to regulate the intracellular localization of the protein, liberating it from the ER membrane and allowing it to traffic to lipid droplets (133). Although overexpression systems have suggested the targeting of core to various compartments including the nucleus (186, 195) and mitochondria (182, 195), recent studies of infected cells suggests the protein accumulates solely at lipid droplets and their associated membranes (176).

In the absence of a full infectious system for HCV, production of virus like particles (VLPs) has been used to investigate assembly requirements. Budding of enveloped particles containing short fragments of RNA could be induced by overexpression of core, E1, and E2 in insect and mammalian cells (12, 20). Electron microscopy revealed nucleocapsids in the process of budding through the membranes of ER-derived tubules, but the absence of particles in the supernatant indicated that this process was abortive (20). Association of capsid and RNA into nucleocapsid like particles (NLPs) has been seen by core overexpression in yeast, in an *in vitro* translation-assembly system, and using recombinant protein (105, 99, 1). These systems have been used to

demonstrate core interactions with itself and with RNA (25, 105, 99), and to suggest associations with the envelope glycoproteins (12).

In addition to a high degree of amino acid conservation, the core coding sequence is well preserved among HCV isolates (30). This conservation, originally speculated to maintain the expression of an alternate reading frame protein (216, 23), has now been shown to preserve RNA structures important for replication efficiency and infectivity in chimpanzees (134). Additional RNA structures in the core coding region have been predicted, but not confirmed to be essential (211).

The advent of the cell culture infectious systems allows role of core in virus life cycle to be studied for the first time. Here we have performed a comprehensive deletion and alanine-scanning mutagenesis study of the core protein in the context of an infectious J6/JFH reporter virus. We have confirmed that core protein is essential for infectious virion production, and have identified numerous residues critical for this activity. Passage of assembly-defective core mutant genomes identified compensatory mutations in nonstructural proteins p7, NS2, and NS3. The detection of genetic interactions between core and these proteins adds to accumulating evidence that nonstructural factors play important roles in *Flaviviridae* virion morphogenesis.

Results

Characterization of a J6/JFH reporter virus

To facilitate the analysis of core protein mutations, we utilized a recently developed J6/JFH reporter virus, J6/JFH(p7Rluc2A) (90). This genome encodes *Renilla* luciferase followed by the *foot and mouth disease virus* (FMDV) 2A autoproteolytic peptide between p7 and NS2 (Fig 4-2A). Since this virus was uncharacterized, we determined the validity of the reporter activity as an assay for replication and infectious virus quantification. *In vitro* generated RNA transcripts were electroporated into Huh-7.5 cells and viral RNA replication was measured after 8, 24, 48 and 72 h by both luciferase assay (Fig 4-2B, left panel) and by quantitative RT-PCR (qRT-PCR) using a probe directed against the 5'UTR of the viral genome (Fig 4-1B, right panel). Whereas J6/JFH(p7Rluc2A) and a genome with a large in-frame deletion of the envelope proteins, J6/JFH(p7Rluc2A)/ΔE1E2, replicated similarly, a genome with a lethal mutation of the essential NS5A RNA-dependent RNA polymerase motif GDD to GND, J6/JFH(p7Rluc2A)/GND, did not replicate. Luciferase activity closely reflected viral RNA accumulation, indicating the validity of the reporter for analysis of RNA replication.

Infectious particle production was assayed at 8, 24, 48, and 72 h post-electroporation by inoculation of naïve Huh-7.5 cells with filtered cell culture supernatants. Infectivity was quantified by luciferase assay of the infected cell lysates after 48 h, and by limiting dilution assay to determine a fifty-percent tissue

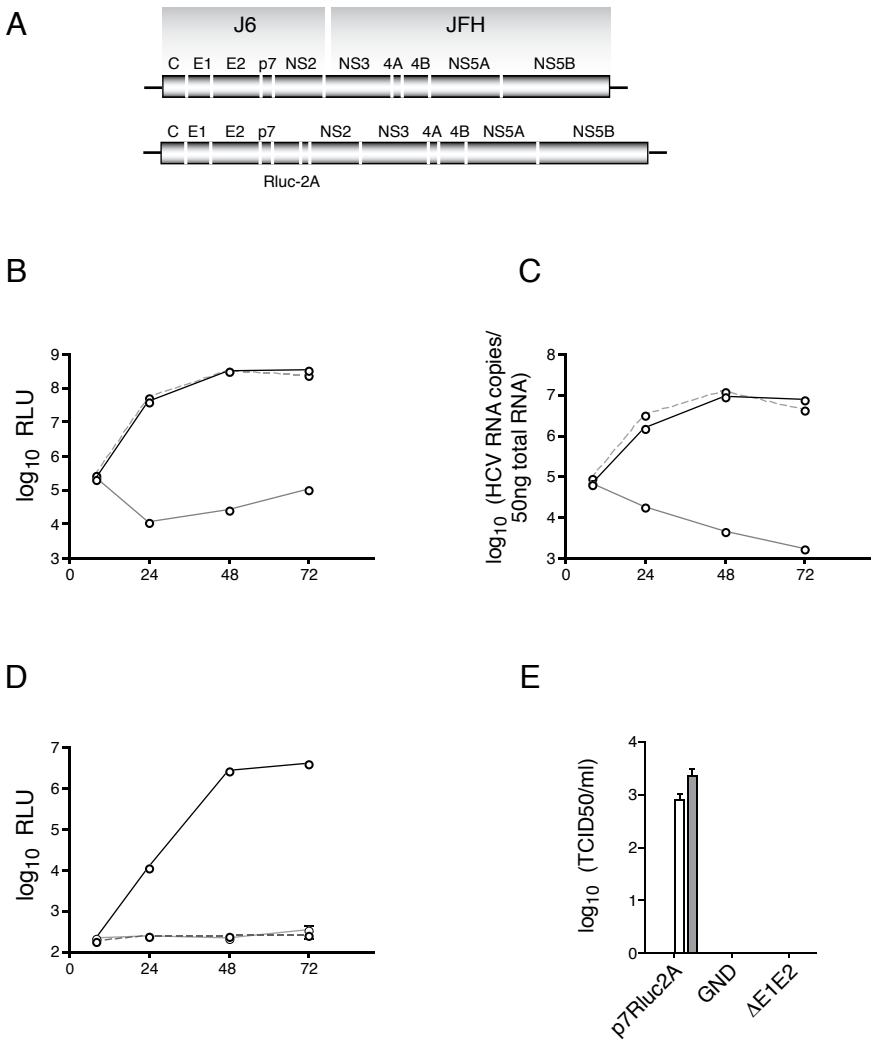

Fig 4-2. Characterization of the J6/JFH(p7Rluc2A) reporter virus. (A) A schematic representation of the full-length J6/JFH genome, top, and the J6/JFH(p7Rluc2A) reporter virus, bottom. The J6/JFH(p7Rluc2A) genome has an insertion of *Renilla* luciferase and the *foot and mouth disease virus* 2A peptide between p7 and NS2. (B) Replication of J6/JFH(p7Rluc2A) (—○—), J6/JFH(p7Rluc2A)/ΔE1E2 (···○···) and J6/JFH(p7Rluc2A)/GND (—○—) measured by luciferase activity. (C) Replication measured by qRT-PCR analysis of RNA accumulation. (D) Infectious virus production measured by luciferase assay of infected cells. (E) Infectious virus production measured by limiting dilution assay (TCID50) at 8 (<30 TCID50/ml), 24 (<30 TCID50/ml), 48 (white), and 72 h (grey) post-electroporation. Means and SEM of triplicate experiments are shown.

culture infectious dose (TCID50). Whereas no virus was detected in culture supernatants of cells harboring J6/JFH(p7Rluc2A)/ΔE1E2 or J6/JFH(p7Rluc2A)/GND, J6/JFH(p7Rluc2A) produced robust levels of infectious virus as assayed by either method (Fig 4-1C). These results indicate that luciferase activity is an appropriate reporter for both replication and infectious virus production of J6/JFH(p7Rluc2A).

Core protein is essential for infectious virus production in HCVcc

Core protein is thought to be an integral part of the HCV virion. The extent to which deletions in core affect infectious virus production in the HCVcc system, however, is not known. To determine the contributions of various regions of the core protein to infectious virus production, we engineered in-frame deletions of core between amino acids 57 and 160 into the J6/JFH(p7Rluc2A) genome. Residues before amino acid 57 were not included in the deletion analysis because of conserved RNA structures within this region important for replication (211, 134). Similarly, amino acids 161-191 were left intact to ensure proper membrane targeting of E1 (180). *In vitro* generated RNA transcripts of each genome were electroporated into Huh-7.5 cells. Viral RNA replication was measured by assay of cell lysates for luciferase activity after 8 h and 48 h. None of the seven partial deletions of core significantly affected RNA replication as compared to wild-type J6/JFH(p7Rluc2A); J6/JFH(p7Rluc2A)/GND did not replicate (Fig 4-3A).

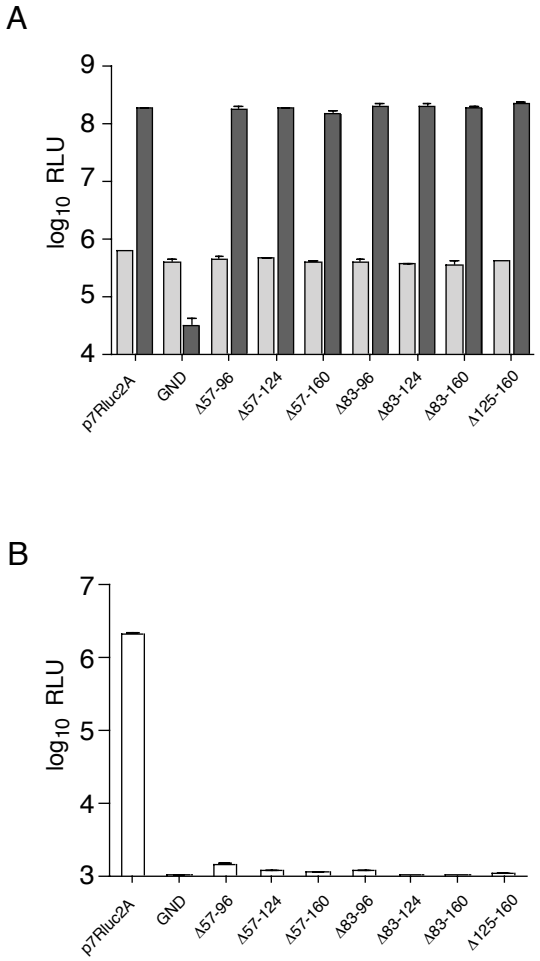

Fig 4-3. Deletions in core abolish infectious virus production. (A) Replication of J6/JFH(p7Rluc2A) genomes with deletions in core. Replication was assayed by luciferase activity at 8 h, grey, and 48 h, black, post-electroporation. (B) Infectious virus production at 48 h post-electroporation. Means and SEM of duplicate electroporations are shown.

Infectious particle production was assayed at 48 h post-electroporation by inoculation of naïve Huh-7.5 cells with filtered cell culture supernatants and luciferase assay of the infected cell lysates after 48 h. In contrast to the robust infectious virus production of wild-type J6/JFH(p7Rluc2A), none of the genomes containing deletions in core produced detectable levels of infectious virus (Fig 4-3B). These data indicated that core protein is essential for infectious virus production and that this function is intolerant to deletions within the central region of the protein.

Mutagenesis of conserved features of core

Sequence analysis of core, as well as data from overexpression systems, have suggested the importance of various conserved residues. With the advent of the HCV tissue culture infectious system, the importance of these sequences in the viral life cycle can be investigated for the first time.

Mutagenesis of putative phospho-serines

Initial analyses of the core amino acid sequence indicated the presence of a conserved phosphorylation motif at serine 99 (30). Subsequent studies of core overexpression in insect and mammalian cells suggested phosphorylation of serines 53, 99, and 116 (185, 123). The exact residues and kinases involved, however, as well as functional significance of the putative phosphorylation events remain controversial.

To investigate the importance of serines 53, 99, and 116 for HCVcc infectivity, we individually mutated these residues to alanine in the context of the J6/JFH(p7Rluc2A) reporter virus. Whereas mutation of these amino acids did not affect RNA replication (Fig 4-4A), mutation of serine 99 to alanine (S99A) severely impaired infectious virus production (Fig 4-4B). S53A and S116A mutations less significantly impacted infectivity (Fig 4-4B). Mutation of each combination of two serines to alanine confirmed that serine 99 was the only residue absolutely required for infectious virus production (Table 1). Mutation of each serine to aspartic acid, to mimic constitutive phosphorylation, abolished infectivity in all three cases (Table 1). Mutation to another serine codon did not impact infectivity, suggesting that the defect caused by the S99A mutation was at the amino acid, and not RNA, level (Table 1).

These results suggest that serine 99 plays an essential role in HCV infectivity, and that phosphorylation, if it occurs, must be regulated rather than constitutive. While the effect of the S99A mutation on core protein stability was not assayed directly, analysis of this mutation in the context of neighboring alanine-substitutions suggested the change did not impair core expression (see below). Attempts to immunoprecipitate radiolabeled core protein from transfected cells were not successful, leaving the relevance of serine 99 phosphorylation still to be investigated.

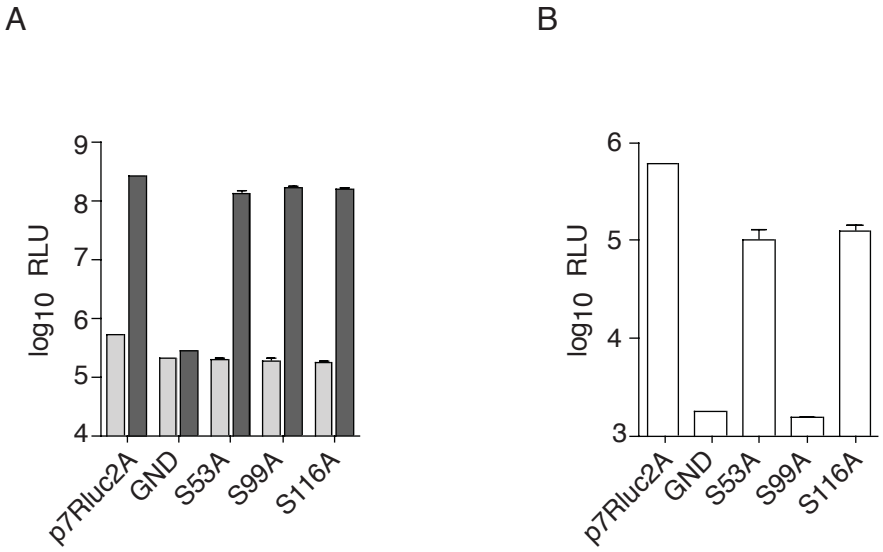

Fig 4-4. Serine 99 is essential for infectious virus production. (A) Replication of J6/JFH(p7Rluc2A) genomes with serine to alanine substitutions in core at 8 h, grey, and 48 h, black, post-electroporation. (B) Infectious virus production at 48 h post-electroporation. Means and SEM are shown for serine mutants, wild type and polymerase defective controls represent single electroporations.

Table 1. Core serine mutagenesis.

	RNA replication[a]	Infectious virus production[a]
Alanine		
53[b]	+	+
99	+	-
116	+	+
53/99	+	-
53/116	+	+
99/116	+	-
Aspartic acid		
53	+	-
99	+	-
116	+	-
Serine[c]		
53	+	+
99	+	+
116	+	+

[a] Assayed by immunohistochemical staining for NS5A
[b] Core serine mutated (J6/JFH polyprotein numbering)
[c] Codon changed

Mutagenesis of core amino acids 172 and 173

While the J6/JFH chimeric virus used in our studies has been found to be more infectious than JFH-1 alone (115, 235), the determinants of this enhanced infectivity are not known. Comparison of J6 and JFH-1 core sequences identified an unusual mutation of a highly conserved C/S sequence to F/P at residues 172/173 of the JFH-1 protein (93). The identification of a second genome encoding the S173P change (JFH-2) led to speculation that mutations in this region might correlate with the fact that both these isolates came from patients with fulminant hepatitis, a rare acute clinical presentation with unknown relevance to the tissue culture infectious phenotype (93). Since the J6 protein contains the canonical C/S sequence at amino acids 172/173, we hypothesized this core sequence might be a determinant of enhanced J6/JFH infectivity. Interestingly, the C/S motif had been previously recognized to resemble an NS3 protease cleavage site (180, 2). The presence of similar cleavage sites in related viral capsid proteins led to the speculation that, while host enzymes rather than NS3 are responsible for processing of HCV core, binding of the viral protease might play a role in infectivity.

To investigate the functional relevance of the C/S motif, we undertook a mutational analysis of these residues in the context of the J6/JFH(p7Rluc2A) reporter virus**.** RNA replication, measured at 8 h and 48 h post-electroporation of Huh-7.5 cells with *in vitro* transcribed RNA, was not significantly affected by the presence of substitutions at amino acids 172 or 173 (Fig 4-5A). In contrast,

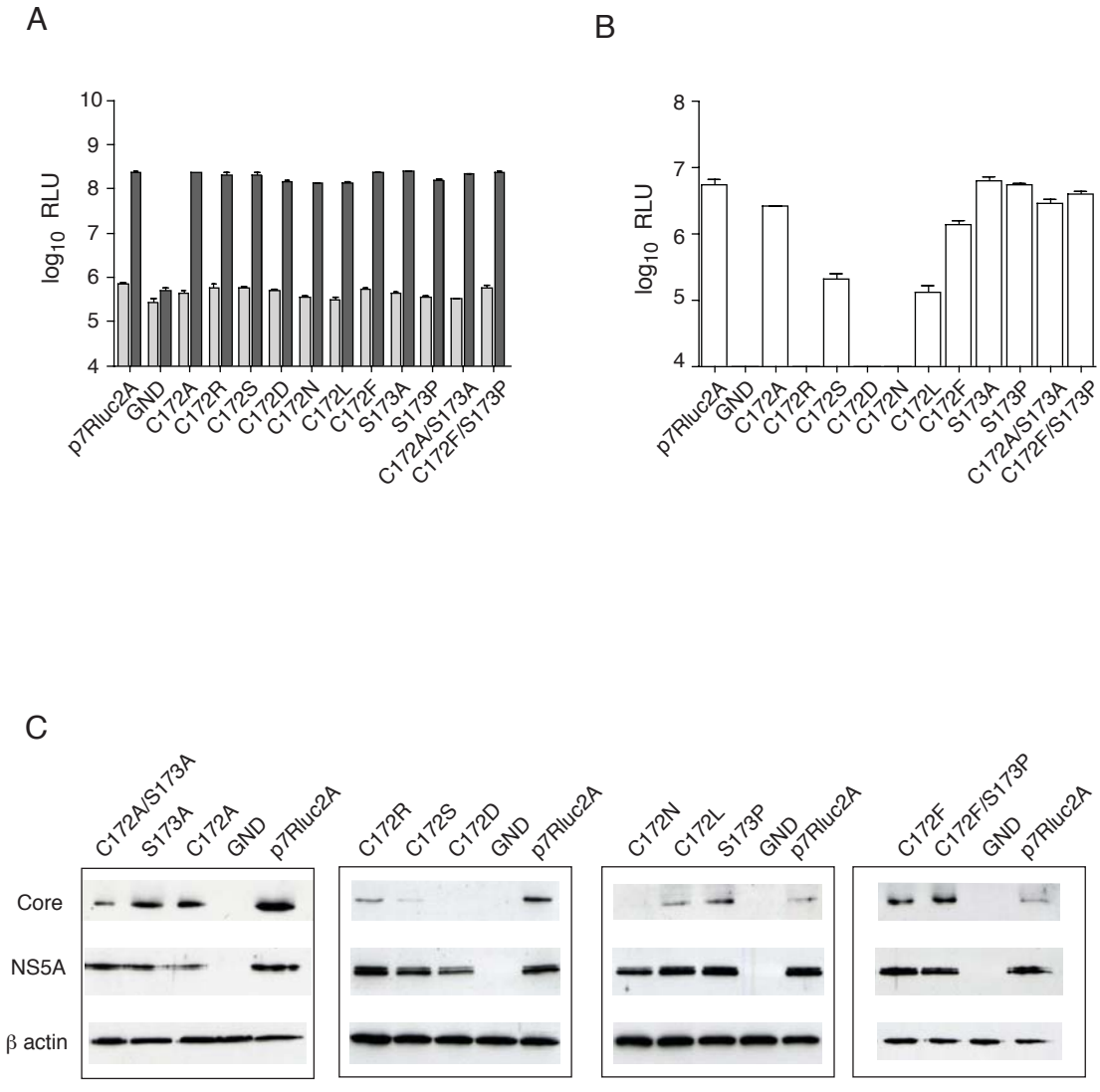

Fig 4-5. Mutations of core C172/S173. (A) Replication of J6/JFH(p7Rluc2A) genomes with substitutions of core C172/S173 at 8 h, grey, and 48 h, black, post-electroporation. (B) Infectious virus production at 48 h post-electroporation. Mutated residues are identified. Means and SEM of at least duplicate electroporations are shown. (C) Western blot analysis of lysates harvested at 48 h post-electroporation. Core, top panels, NS5A, middle panels, and β-actin, lower panels are shown. Blots are representative of at least duplicate analyses from independent electroporations.

infectious virus production was abolished by mutation of C172 to R, D, or N, and impaired by mutation of C172 to S, L, or F (Fig 4-5B). Mutation of C172 or S173 to alanine alone or in combination did not drastically affect infectivity. Mutation of S173 to P, as in JFH-2, resulted in robust infectious virus production, as did mutation of C172/S173 to F/P, the JFH-1 sequence (Fig 4-5B). Analysis of mutant core protein stability in transfected cell lysates harvested 48 h post-electroporation indicated that the abolished infectivities of J6/JFH(p7Rluc2A)/C172D and J6/JFH(p7Rluc2A)/C172N were likely due to the absence of stable core expression (Fig 4-5C). Other mutants, such as J6/JFH(p7Rluc2A)/C172R, were impaired in infectious virus despite near wild-type core expression.

These results suggested that the JFH-1 (C172F/S173P) and JFH-2 (S173P) changes at residues 172/173 do not drastically impair infectivity of a J6/JFH genome, indicating that the identity of these residues is likely not a major determinant of enhanced J6/JFH infectivity. Since the S173P change is predicted to be severely inhibitory to NS3-catalyzed proteolysis (100) and presumably binding (77), the finding that this change does not impact infectivity does not support the hypothesis of an essential role for NS3 binding to this region of core.

Alanine-scanning of core amino acids 57 to 191 reveals numerous residues critical for infectious virus production

To more extensively investigate regions of core essential for infectious virus production, we performed a comprehensive mutagenesis of amino acids 57 to 191 to alanine. Residues were mutated in blocks of four amino acids in the context of the J6/JFH(p7Rluc2A) genome, and Huh-7.5 cells were electroporated with *in vitro* transcribed RNA generated from each construct. RNA replication was measured at various time points post-electroporation by quantification of luciferase activity in the cell lysates; replication at 8 h and 48 h are shown (Fig 4-6A). In accordance with the results of the deletion analysis, none of the alanine mutations significantly affected RNA replication as compared to wild-type J6/JFH(p7Rluc2A), while J6/JFH(p7Rluc2A)/GND did not replicate (Fig 4-6A).

To assay infectious virus production, naïve Huh-7.5 cells were inoculated with filtered supernatants harvested at 48 h post-electroporation and cell-associated luciferase activity was measured at 48 h post-infection. Despite near wild-type levels of replication, the majority of the mutants were significantly impaired in infectious virus production, producing titers of less than 1% wild-type J6/JFH(p7Rluc2A) (Fig 4-6B). Exceptions were J6/JFH(p7Rluc2A)/C181-184A, J6/JFH(p7Rluc2A)/C185-188A, and J6/JFH(p7Rluc2A)/C189-191A which produced close to wild-type levels of infectious virus. RT-PCR and sequencing of viral RNA isolated from cells infected with these viruses verified the presence of the engineered mutations in these genomes. These results indicated that

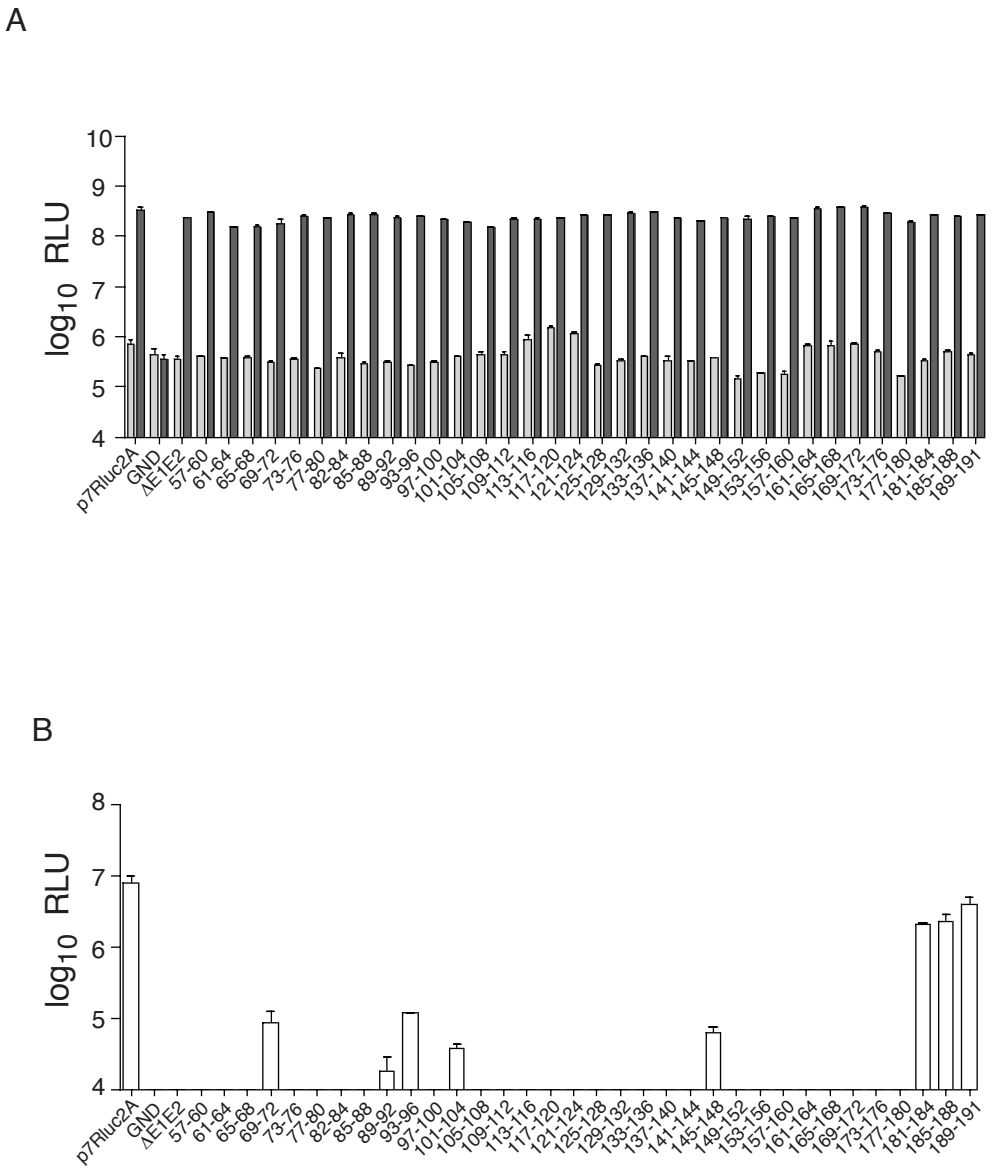

Fig 4-6. Alanine-scanning mutagenesis of core. (A) Replication of J6/JFH(p7Rluc2A) genomes with quadruple alanine substitutions in core at 8 h, grey, and 48 h, black, post-electroporation. (B) Infectious virus production at 48 h post-electroporation. Residues mutated to alanine are identified. Means and SEM of at least duplicate electroporations are shown.

numerous residues within the carboxy-terminal two-thirds for the core protein are dispensable for RNA replication but essential for robust infectious virus production.

Some alanine mutations disrupt core stability

We hypothesized that certain alanine substitutions may have destabilized the core protein, leading to the observed defects in infectious virus production. Cell lysates were analyzed at 48 h post-electroporation for the presence of core and NS5A by Western blot (Fig 4-7). Core was detected using mAb HCM-071-5, which recognizes an epitope outside the region of mutagenesis. NS5A was detected using mAb 9E10 (115). While all replicating constructs expressed similar levels of NS5A, the stability of core protein varied among the alanine-scanning mutants. In those mutants that stably expressed core, levels of the protein were much the same as wild-type. Exceptions were constructs J6/JFH(p7Rluc2A)/C161-164A and J6/JFH(p7Rluc2A)/C169-172A, in which core could be detected, but was significantly decreased compared to J6/JFH(p7Rluc2A) (Fig 4-7, lower panel). With the exception of a possible uncleaved form visible on overexposure of the J6/JFH(p7Rluc2A)/C169-172A blot (Fig 4-7, lower panel), no differences in core processing were detected, although the ability of our gel system to resolve the cleavage products has not been established. None of the mutants with undetectable core protein were among those that produced low levels of infectious virus (Fig 4-6B), consistent

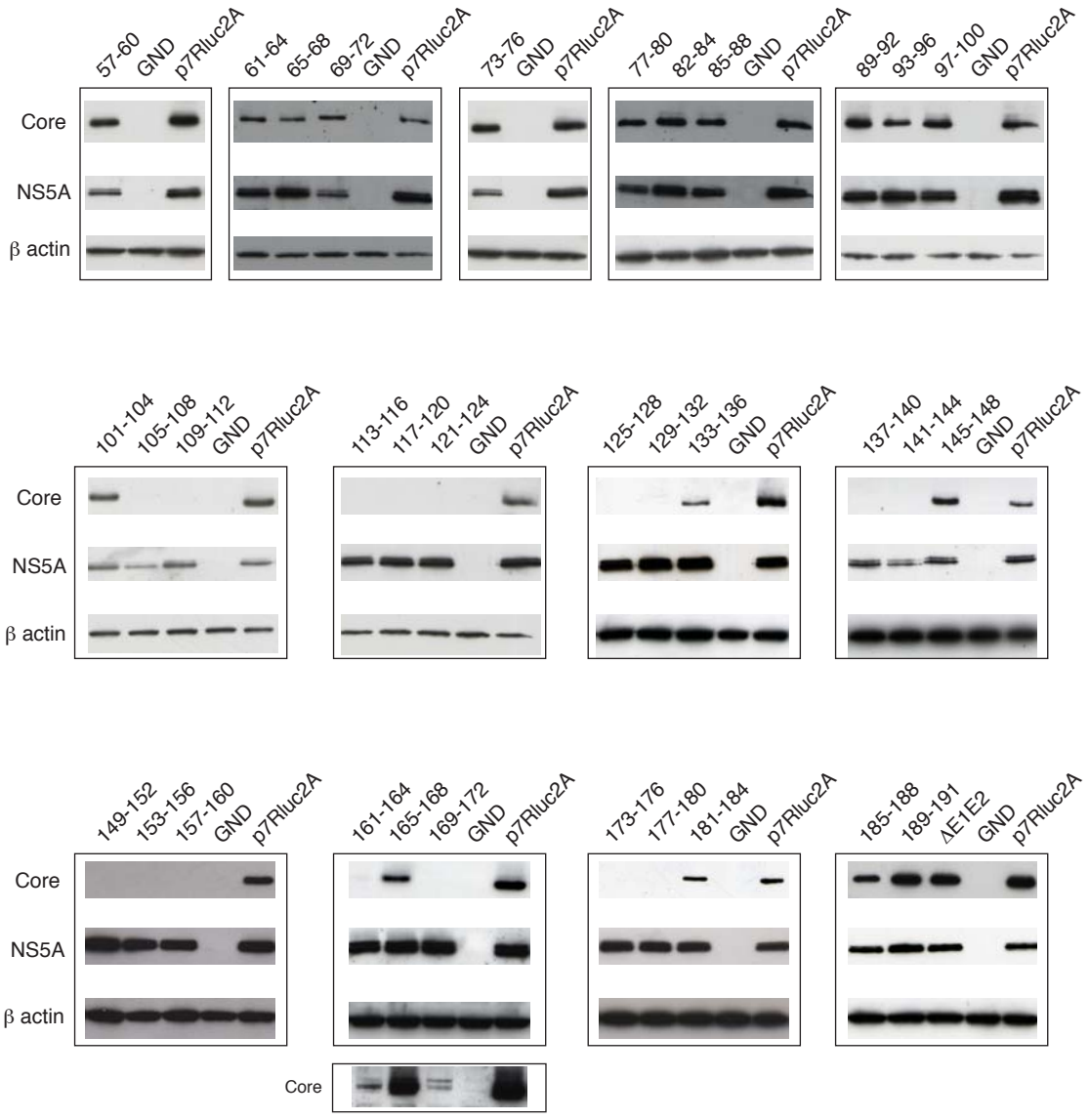

Fig 4-7. Stability of mutant core proteins. Western blot analysis of lysates harvested at 48 h post-electroporation. Core, top panels, NS5A, middle panels, and β-actin, lower panels are shown. Residues mutated to alanine are identified. Blot 11 lowest panel is an over exposure of the core blot demonstrating low levels of protein expression. Blots are representitive of at least duplicate analyses from independent electroporations.

with the finding that core expression is essential for infectious virus production. These data indicated that, while about half of the alanine-substitution mutants were blocked at the level of stable core expression, many were severely impaired in infectious virus production despite wild-type levels of core protein.

Alanine mutants do not produce noninfectious particles

It was possible that mutations in core might lead to defects in entry, such as particle disassembly. Those mutants that stably expressed intracellular core were further analyzed to determine whether they produced noninfectious virions. To assay for the release of noninfectious particles, RNA and core protein levels in the supernatant were determined. To assess HCV RNA release, total RNA purified from cell culture supernatants 48 h post-electroporation was analyzed by qRT-PCR (Fig 4-8A). Although limited amounts of RNA were detected in the supernatants of cells harboring the mutant genomes, the levels of RNA released were not significantly higher than those secreted by J6/JFH(p7Rluc2A)/ΔE1E2. This release of RNA by replication-competent genomes in the absence of infectious virus production has been reported previously (215).

These data indicated that the core alanine-substitution mutants do not release substantial quantities of RNA-containing noninfectious particles. To investigate whether particles lacking RNA were produced, core secretion was quantified. Cell culture supernatants harvested at 48 h post-electroporation were assayed for core by enzyme-linked immunosorbent assay (ELISA, Fig 4-8B).

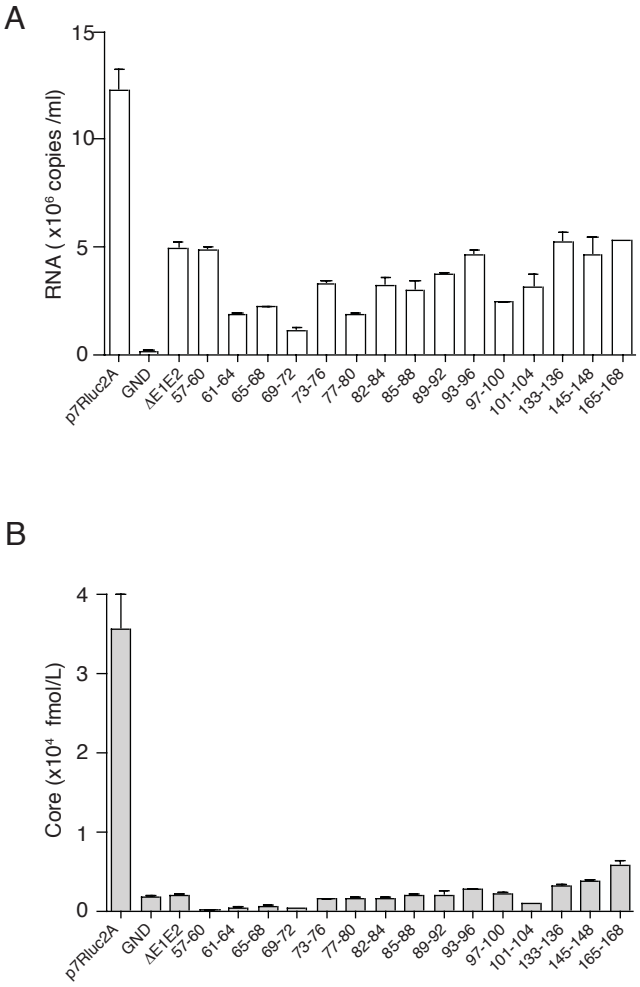

Fig 4-8. Noninfectious particles are not released by core alanine-substitution mutants. (A) Total viral RNA release and (B) total core protein release at 48 h post-electroporation. Only mutants with stable intracellular core protein were tested, residues mutated to alanine are designated. Means and SEM of at least duplicate electroporations are shown.

None of the core alanine-substitution mutants produced drastically higher levels of secreted core than J6/JFH(p7Rluc2A)/ΔE1E2, suggesting that RNA-deficient noninfectious particles were not produced.

Taken together these data indicate that the majority of the core alanine-substitution mutants are defective at a step after the accumulation of core protein and before the release of infectious or noninfectious particles.

Isolation of compensatory mutations in the nonstructural proteins

In an attempt to identify second-site changes that could compensate for the defective core proteins, cells harboring the mutant genomes were serially passaged. Genomes encompassing alanine-substitutions between amino acids 57 and 104 were selected for this analysis, as they appeared to be in a region of core in which protein stability was not compromised by the mutations (Fig 4-7). In order to avoid the emergence of second-site mutations related to the presence of the luciferase reporter gene, each of these quadruple alanine mutations was cloned into the non-reporter J6/JFH genome. For each construct the passaging experiment was conducted in duplicate.

Because initial levels of virus production from these genomes were very low or undetectable, electroporated cells, rather than culture supernatants, were serially passaged (134). Replication at each passage was monitored by immunohistostaining for NS5A. While J6/JFH electroporated cells maintained a high proportion of NS5A-positive cells, those harboring genomes that could

replicate but not produce infectious virus had diminishing quantities of NS5A-positive cells over time (data not shown). For several of the genomes (J6/JFH/C65-68A, J6/JFH/C69-72A, and J6/JFH/C93-96A) the number of NS5A positive cells either did not diminish as rapidly or markedly increased during passage, indicating that infectious virus may have emerged. Subsequently, cell free supernatants from these populations were passaged three times on naïve cells. RNA harvested from the infected cells was then RT-PCR amplified and sequenced over the core to NS5A region. For each of the mutants, the originally engineered alanine substitutions were maintained and a number of additional mutations were present; those that conveyed an infectious phenotype when individually reengineered into the parental alanine mutant are shown (Fig 4-9A and Table 2).

For J6/JFH/C65-68A, second-site mutations emerged at nucleotides T2666C (J6/JFH amino acid F776L, p7 F26L) and A3965G (J6/JFH amino acid T1209A, NS3 T178A). The presence of the F776L mutation significantly increased infectious virus production of J6/JFH/C65-68A from undetectable levels. The NS3 change, T1209A, while allowing detectable infectivity, very weakly rescued the core mutant (Fig 4-9B). The J6/JFH/C69-72A genome produced very low titers of infectious virus in the context of J6/JFH(p7Rluc2A) (Fig 4-9B). These titers were drastically increased by the presence of either of two emergent mutations, T2667C (J6/JFH amino acid F776S, p7 F26S) or G2978C (J6/JFH amino acid A880P, NS2 A67P). Unlike the other core mutants,

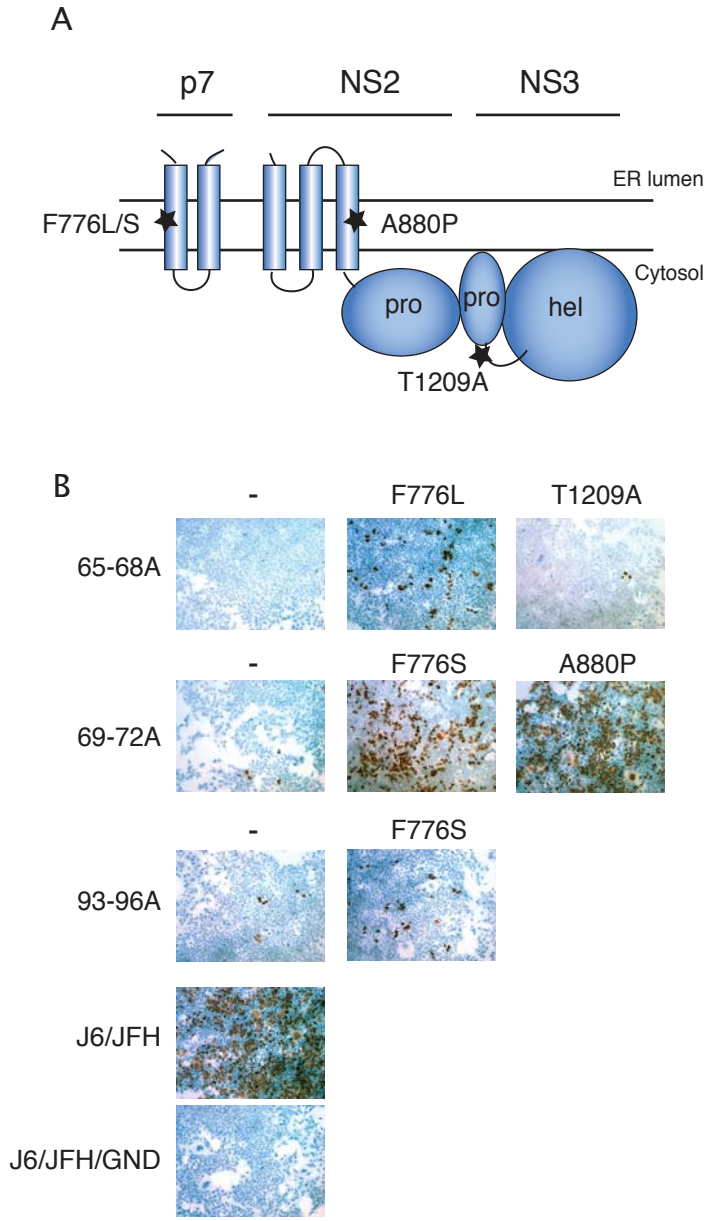

Fig 4-9. Compensatory mutations in nonstructural proteins are isolated by passaging. (A) Putative topology diagram of the p7 to NS3 region of the HCV polyprotein. Positions of isolated mutations are designated. (B) Infectious virus production at 48 h post-electroporation of core alanine-substitution mutants with or without compensatory mutations. Infectious virus is detected by immuno-histostaining for NS5A at 48 h post-inoculation of naïve cells. Nuclei are counter-stained with hemotoxylin-2. Core mutations are designated on the left, additional mutations described above. All mutations are J6/JFH polyprotein numbering.

Table 2. Isolated compensatory mutations.

	J6/JFH[a]		H77[b]	
location	aa[c]	nt	aa	nt
p7	F776S	T2666C	F772	T2655
p7	F776L	T2667C	F772	T2656
NS2	A880P	G2978C	L876	C2967
NS3	T1209A	A3965G	M1205	A3954

[a] J6/JFH changes isolated
[b] Equivalent numbering in H77 genotype 1a consensus sequence
[c] Polyprotein numbering (amino acid, aa); genome numbering (nucleotide, nt)

J6/JFH/C69-72A was the only genome in which both replicate experiments produced revertant viruses, with F776S isolated from one population and A880P from the other. This genome also reverted the most quickly, in three passages as opposed to six. The J6/JFH/C93-96A genome also produced very low titers in the J6/JFH(p7Rluc2A) background (Fig 4-9B). Infectious virus production was slightly increased by the emergence of the T2667C (J6/JFH amino acid F776S, p7 F26S) mutation (Fig 4-9B).

These data suggest that mutations in the nonstructural proteins are capable of overcoming severely inhibitory mutations in the core protein. It is interesting to note that a mutation of p7 (F776) emerged independently in each of the passaged genomes. This mutation maps to within the first transmembrane domain of p7; the NS2 mutation also maps to a putative transmembrane region (Fig 4-9A).

Compensatory changes in p7 and NS2 overcome an infectious particle assembly defect of the parental core mutants

We next quantitatively analyzed the effects of the nonstructural protein changes on the parental core mutants. Replication was monitored by qRT-PCR analysis of total cellular RNA at various time points after electroporation (Fig 4-10A). No significant differences in RNA replication were seen for the core alanine-substitution mutants, in the presence or absence of the compensatory

Fig 4-10. Compensatory mutations rescue core alanine-substitution mutants. (A) Replication of J6/JFH genomes with core alanine substitutions and the presence or absence of compensatory mutations at 8, 24, 48 and 72 h post-electroporation (light grey to black, respectively). Replication was measured by qRT-PCR analysis of RNA accumulation. (B) Infectious virus production at 48 h post-electroporation measured by limiting dilution assay (TCID50). (C) RNA secreted into the supernatant at 72 h post-electroporation as measured by qRT-PCR. (D) Intracellular infectious virus accumulation at 72 h post-electroporation as measured by quantification of RNA replication in infected cells by qRT-PCR at 48 h post-inoculation. Means and SEM of duplicate experiments are shown.

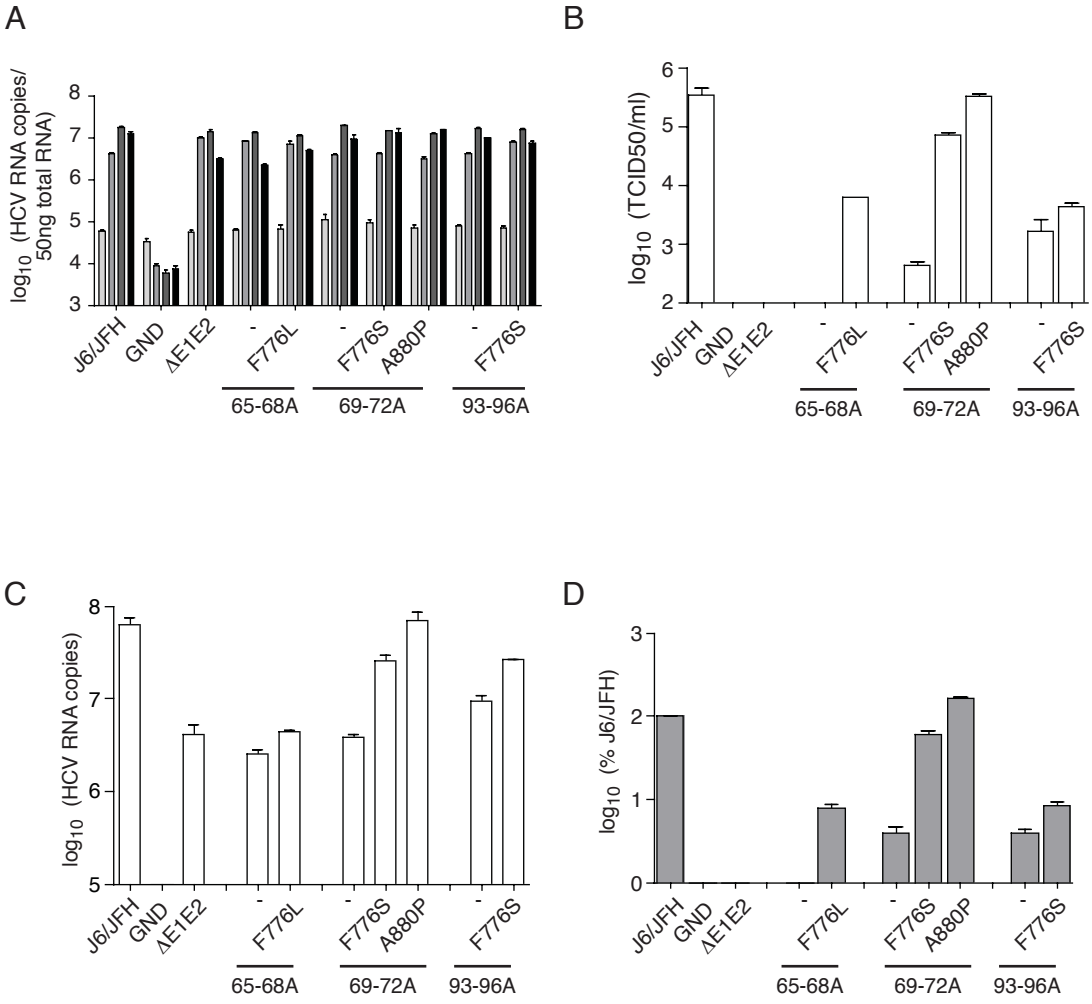
A
log10 (HCV RNA copies/ 50ng total RNA)
8
7
6
5
4
3
J6/JFH
GND
ΔE1E2
-
F776L
-
F776S
A880P
-
F776S
65-68A
69-72A
93-96A
B
log10 (TCID50/ml)
6
5
4
3
2
J6/JFH
GND
ΔE1E2
-
F776L
-
F776S
A880P
-
F776S
65-68A
69-72A
93-96A
C
log10 (HCV RNA copies)
8
7
6
5
J6/JFH
GND
ΔE1E2
-
F776L
-
F776S
A880P
-
F776S
65-68A
69-72A
93-96A
D
log10 (% J6/JFH)
3
2
1
0
J6/JFH
GND
ΔE1E2
-
F776L
-
F776S
A880P
-
F776S
65-68A
69-72A
93-96A

mutations, as compared to wild-type J6/JFH. These data suggested that the nonstructural mutations did not act at the level of RNA replication.

Infectious titers of the core alanine-substitution mutants, with or without the compensatory mutations, were quantified by limiting dilution assay. As seen in the context of J6/JFH(p7Rluc2A), the core mutants produced less than 1% of wild-type titers. J6/JFH/C65-68A was especially impaired, with no detectable infectious virus produced (Fig 4-10B). The presence of the second-site changes drastically increased the titers of J6/JFH/C65-68A and J6/JFH/C69-72A, with J6/JFH/C69-72A/A880P titers reaching almost wild-type levels. J6/JFH/C93-96A was not as efficiently rescued by the presence of the F776S change, indicating that the same p7 mutation had disparate effects on two different core mutations. RNA release correlated with infectious virus titers, suggesting that increased secretion of total, including noninfectious, particles did not account for rescue of the core defects (Fig 4-10C).

Although the core alanine-substitution mutants were defective in the release of infectious particles, it was possible that they supported assembly of intracellular infectious particles but were defective in egress. To determine if the compensatory mutations acted at the level of secretion, cells were washed and lysed by multiple freeze thaw cycles at 72 h post-electroporation. Cleared lysate was used to infect naïve cells and infectivity was quantified by analysis of RNA levels in the infected cells after 48 h. Core mutants J6/JFH/C65-68A, J6/JFH/C69-72A, and J6/JFH/C93-96A did not produce significant levels of

intracellular infectivity, indicating that these mutants were impaired before infectious particle assembly (Fig 4-10D). The presence of the compensatory mutations increased intracellular infectious virus production in proportion to the increased extracellular titers. These data suggest that the core mutants are blocked at an early step of infectious virion production and that the p7 and NS2 second-site changes can overcome this defect. The more drastic effects of the F776L/S mutations on J6/JFH/C65-68A and J6/JFH/C69-72A as compared to the slight enhancement of J6/JFH/C93-96A infectivity suggests that a core-specific mechanism may account for this rescue of infectivity.

Characterization of p7 and NS2 mutations in wild-type virus

It was possible that the nonstructural protein changes might increase the fitness of wild-type virus, and that this enhancement could result in the suppression of core defects. To test this hypothesis we engineered the F776L, F776S, and A880P mutations into the wild-type J6/JFH genome and analyzed replication at various times post-electroporation by qRT-PCR (Fig 4-11A). None of the nonstructural protein mutants differed significantly in replication kinetics from J6/JFH. This again indicated that the compensatory mutations did not act by increasing RNA replication.

Infectious virus titers were determined by limiting dilution assay of cell culture supernatants harvested at 72 h post-electroporation. J6/JFH/F776L, J6/JFH/F776S had titers nearly identical to wild-type virus, while J6/JFH/A880P

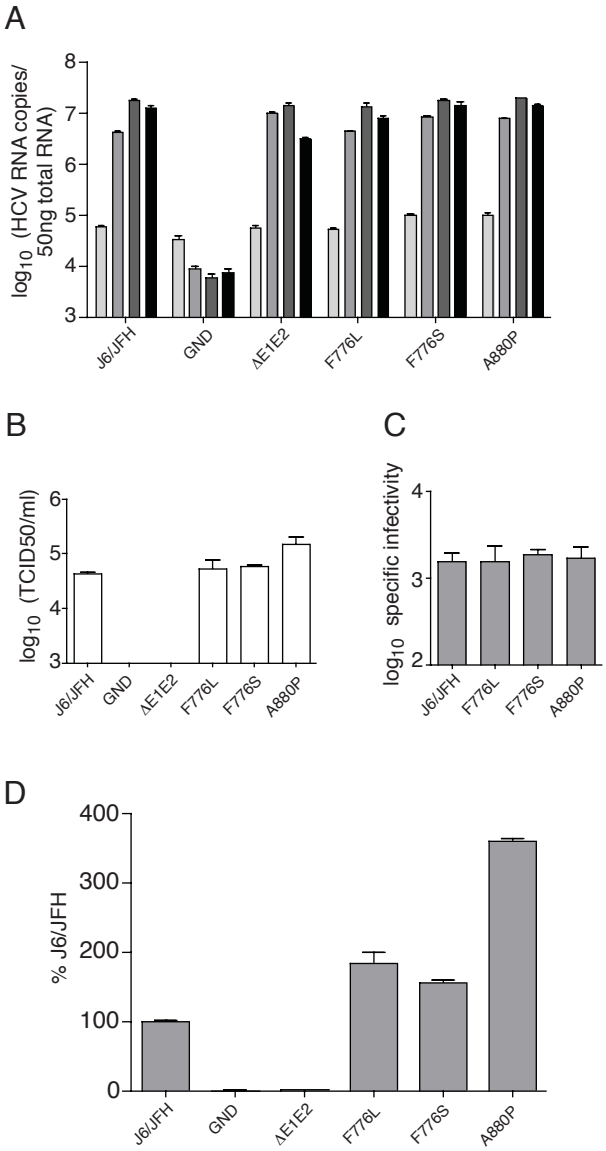

Fig 4-11. Analysis of compensatory mutations in wild-type J6/JFH. (A) Replication of J6/JFH genomes with nonstructural protein mutations at 8, 24, 48 and 72 h post-electroporation, light grey to black, respectively. Replication was measured by qRT-PCR analysis of RNA accumulation. (B) Infectious virus production at 72 h post-electroporation measured by limiting dilution assay (TCID50). (C) Specific infectivity of particles released 72 h post-electroporation. Measured by division of released RNA copies/ml by TCID50/ml. (D) Intracellular infectious virus accumulation at 72 h post-electroporation as measured by quantification of RNA replication in infected cells by qRT-PCR at 48 h post-inoculation. Means and SEM of duplicate electroporations are shown.

produced titers approximately three-fold higher than J6/JFH (Fig 4-11B). The specific infectivity of the particles was determined by relating released RNA copies/ml to the infectious titer. The specific infectivity of wild-type J6/JFH was similar to that previously reported (115) and did not differ significantly from genomes containing the nonstructural protein changes (Fig 4-11C). These data indicated that the presence of the p7 and NS2 mutations led to minimal enhancements of wild-type virus infectivity.

We next tested whether the presence of the nonstructural protein changes affected the accumulation of intracellular infectious virus. At 72 h post-electroporation, cells were lysed by multiple freeze thaw cycles and the clarified lysates used to infect naïve cells. Infectivity was measured by qRT-PCR analysis of the infected cells after 48 h. The presence of the p7 or NS2 mutations resulted in slight increases in intracellular infectivity as compared to J6/JFH, with J6/JFH/A880P producing almost four-fold wild-type levels (Fig 4-11D). The levels of intracellular infectivity correlated well with extracellular infectious titers.

The minimal enhancement of J6/JFH fitness in the presence of the F776S or F776L changes again suggests that these mutations may specifically compensate for defects in core amino acids 65-72, and to a lesser extent core residues 93-96. The A880P mutation, while capable of more significant enhancement of wild-type infectivity, may also be involved in a specific genetic interaction with core protein, as the effect of this mutation on J6/JFH/C69-72A is drastically greater than on J6/JFH.

Characterization of the NS3 compensatory mutation in core mutant and wild-type virus

A T1209A change in NS3 was isolated by passage of J6/JFH/C65-68A. Whereas J6/JFH/C65-68A was highly defective in infectious virus production, the presence of the reengineered NS3 compensatory mutation resulted in infectious virus production reproducibly detectable by immunohistochemical staining for NS5A (Fig 4-9B). Attempts to quantify the rescued virus by limiting dilution assay, however, resulted in titers below the limit of detection (30 TCID50/ml, Fig 4-12B). To investigate how the T1209A change might render J6/JFH/C65-68A infectious, however inefficiently, we analyzed the RNA replication of wild-type and core mutant genomes in the presence or absence of the T1209A change. Similar replication efficiencies were seen for genomes with or without the NS3 mutation, suggesting this change did not act at the level of RNA accumulation (Fig 4-12A). We next tested whether the T1209A substitution increased infectious virus production in a wild-type genome. Titers of J6/JFH/T1209A were slightly higher than those of J6/JFH at 48 h post-electroporation, while at 72 h post-electroporation infectious virus release was similar for the two genomes. These results suggested that the T1209A change was likely acting as a weak general enhancer of J6/JFH infectious virus production.

To determine if the T1209A mutation might also increase the infectivity of the released particles, the specific infectivity of virions released at 72 h post-

Fig 4-12. Analysis of the NS3 compensatory mutation in core mutant and wild-type virus. (A) Replication of J6/JFH genomes with nonstructural protein mutations at 8, 24, 48 and 72 h post-electroporation, light grey to black, respectively. Replication was measured by qRT-PCR analysis of RNA accumulation. (B) Infectious virus production at 48 h (white) and 72 h (grey) post-electroporation measured by limiting dilution assay (TCID50). For genomes not producing infectious virus, only titers at 48 h were measured. (C) Specific infectivity of particles released 72 h post-electroporation, as measured by division of released RNA copies/ml by TCID50/ml. (D) Intracellular infectious virus accumulation at 72 h post-electroporation as measured by quantification of RNA replication in infected cells by qRT-PCR at 48 h post-inoculation. Means and SEM of duplicate electroporations are shown.

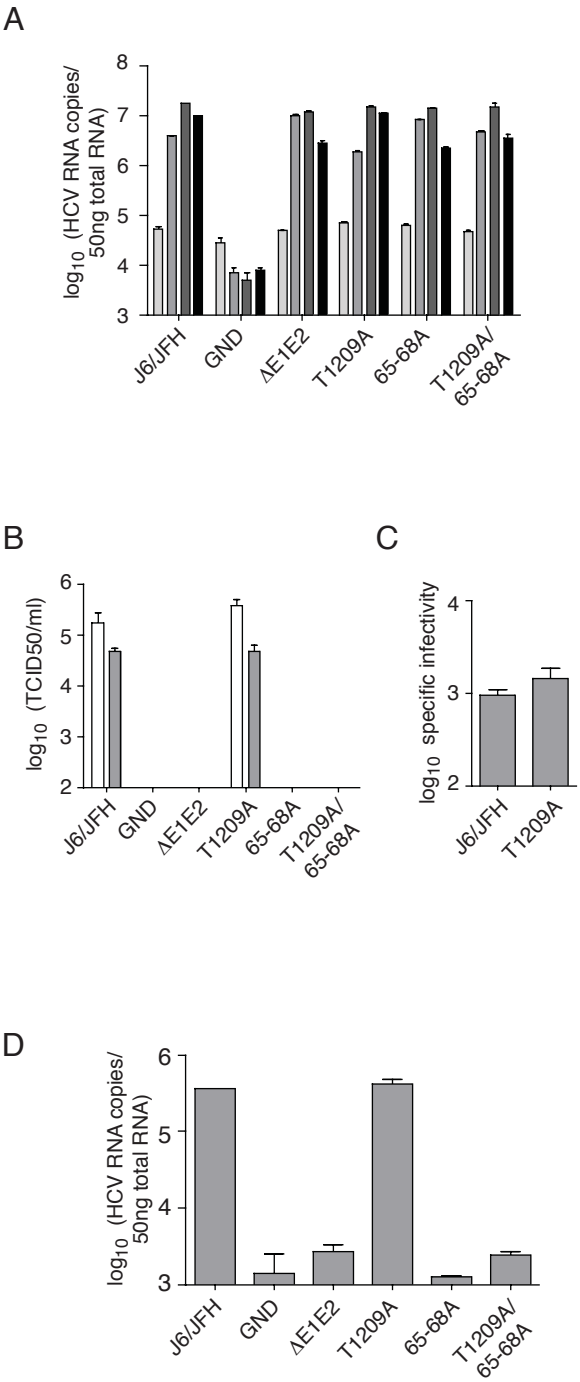
A
log10 (HCV RNA copies/ 50ng total RNA)
8
7
6
5
4
3
J6/JFH
GND
ΔE1E2
T1209A
65-68A
T1209A/ 65-68A
B
log10 (TCID50/ml)
6
5
4
3
2
J6/JFH
GND
ΔE1E2
T1209A
65-68A
T1209A/ 65-68A
C
log10 specific infectivity
4
3
2
J6/JFH
T1209A
D
log10 (HCV RNA copies/ 50ng total RNA)
6
5
4
3
J6/JFH
GND
ΔE1E2
T1209A
65-68A
T1209A/ 65-68A

electroporation was calculated. Rather than rendering wild-type J6/JFH more infectious, J6/JFH/T1209A actually slightly increased the number of viral genomes per infectious unit (Fig 4-12C), suggesting it did not act at the level of particle infectivity. We next tested whether T1209A increased the accumulation of infectious intracellular virus by lysis of cells by freeze-thaw at 72 h post-electroporation. J6/JFH and J6/JFH/T1209A showed similar levels of intracellular infectious virus (Fig 4-12D). In the J6/JFH/C65-68A background, the T1209A change slightly increased intracellular infectivity of the core mutant, but not significantly above J6/JFHΔE1E2 background levels. Taken together, these results suggest that T1209A might weakly increase J6/JFH infectious virus production, and that this slight enhancement could lead to the augmentation of J6/JFH/C65-68A infectivity.

Additional characterization of the block of alanine-substitution mutants

To investigate how changes in the nonstructural proteins might compensate for mutations in core, we attempted to further define the stage of virion morphogenesis at which mutants J6/JFH/C65-68A, J6/JFH/C69-72A, and J6/JFH/C93-96A were impaired.

Core mutants localize to lipid droplets

Wild-type core protein has been reported to localize to lipid droplets within an infected cell (7). To determine whether J6/JFH(p7Rluc2A)/C65-68A,

J6/JFH(p7Rluc2A)/C69-72A, and J6/JFH(p7Rluc2A)/C93-96A core proteins were also localized to these structures, cells transfected with each of these genomes were analyzed by immunofluorescent staining. Core protein was detected using mAb HCM-071-5, previously shown by Western blot to efficiently recognize each of these mutant proteins (Fig 4-7). Lipid droplets were stained with Oil red O (84). Visualization of stained cells by confocal microscopy indicated that core could colocalize with lipid droplets similarly in the presence or absence of the engineered mutations (Fig 4-13). These results were consistent with previous reports that sequences carboxy-terminal to amino acid 122 mediate lipid droplet localization (84, 24). Core mutants J6/JFH(p7Rluc2A)/C65-68A, J6/JFH(p7Rluc2A)/C69-72A, and J6/JFH(p7Rluc2A)/C93-96A, therefore, appeared to correctly localize to putative sites of assembly in the absence of compensatory mutations.

Core mutations do not allow for temperature-dependent infectivity

If the alanine-substitutions in core impaired interactions of the protein with other components of the assembly pathway, lowering the temperature, and thereby increasing the stability of those associations, might allow infectious virus to be produced. Cells electroporated with J6/JFH(p7Rluc2A)/C65-68A, J6/JFH(p7Rluc2A)/C69-72A, or J6/JFH(p7Rluc2A)/C93-96A genomes were grown at 28°C or 37°C for 4 days. Replication, quantified by luciferase assay of transfected cell lysates, was again found to be similar between wild-type

Fig 4-13. Core localizes to lipid droplets. Cells fixed at 4 days post-electroporation were stained for core with mAb HCM-071-5, left panels, and for lipid droplets with Oil red O, middle panels. Samples were analyzed using Zeiss LSM 510 confocal microscope and associated software. Histograms, right panel, show signal intensities in the region indicated by an arrow in the merged image.

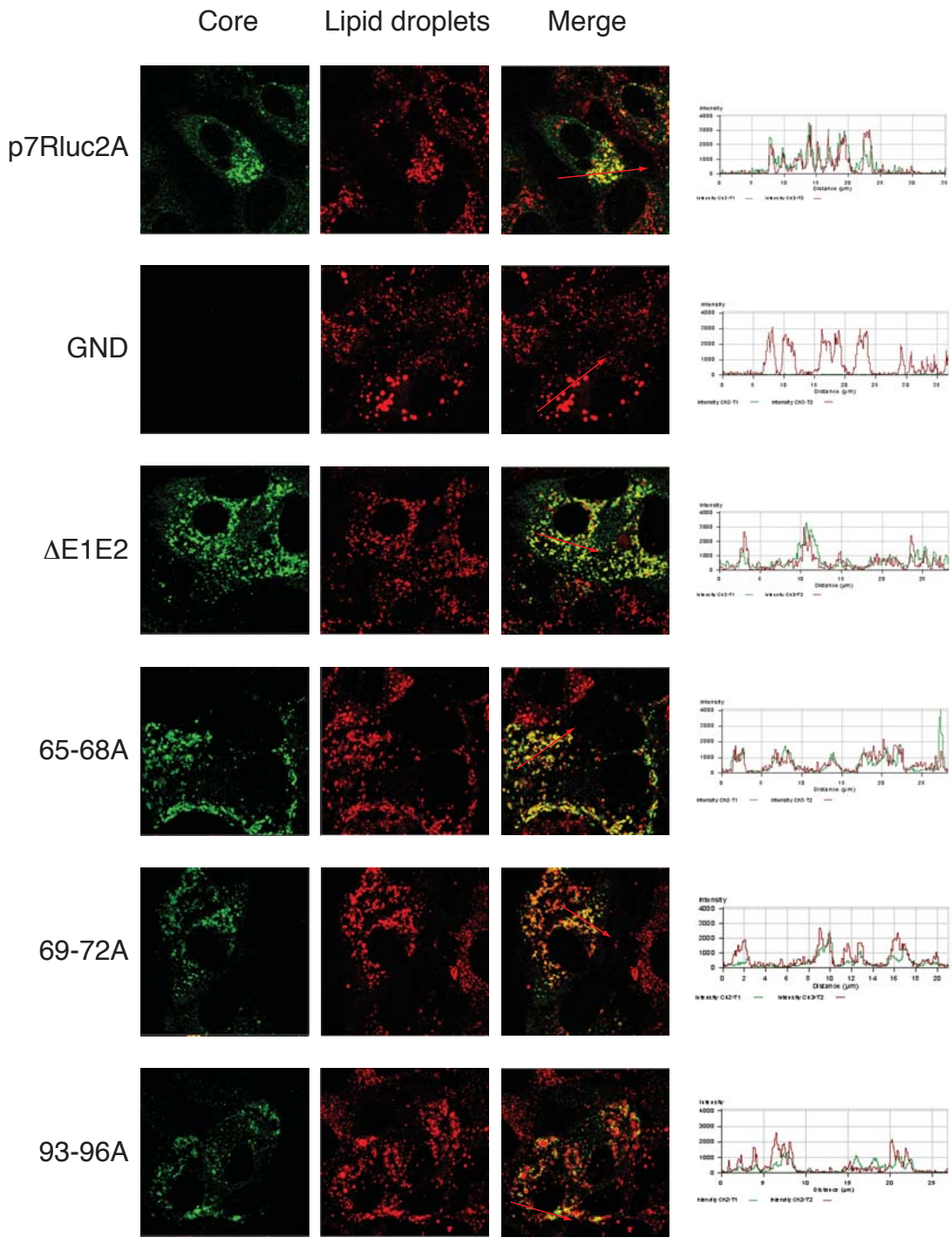
Core
Lipid droplets
Merge
p7Rluc2A
GND
ΔE1E2
65-68A
69-72A
93-96A

J6/JFH(p7Rluc2A) and the core mutants at 37°C (Fig 4-14A). Although all genomes, with the exception of J6/JFH(p7Rluc2A)/GND, replicated at 28°C, greater variability was seen at the low temperature, possibly because of extremely slow cell growth (Fig 4-14A).

Infectious virus production was quantified 4 days post-electroporation by inoculating naïve cells with filtered supernatants and culturing at 37°C for 48 h. Similar to previous results, J6/JFH(p7Rluc2A)/C69-72A and J6/JFH(p7Rluc2A)/C93-96A produced infectious titers of less than 1% of wild-type, and no infectious virus was detected for J6/JFH(p7Rluc2A)/C65-68A. Infectious virus production at 28°C was not enhanced in any of the mutant genomes, although J6/JFH(p7Rluc2A)/C93-96A was able to produce titers similar to the reduced wild-type levels at this temperature. These results suggested that nonspecific enhancement of interactions by reduced temperature was not able to induce robust infectivity of the core mutant genomes. The caveat of significant impairment of cell growth at 28°C, however, suggested that further optimization might yield a permissive temperature.

Amino acids 65-72 are not amenable to the insertion of epitope tags

We were able to isolate compensatory mutations capable of rescuing neighboring core sequences 65-68A and 69-72A. This suggested that this region of the protein might have a general flexibility amenable to the insertion of epitope tags. We therefore created J6/JFH genomes in which HSV glycoprotein, Flag, or

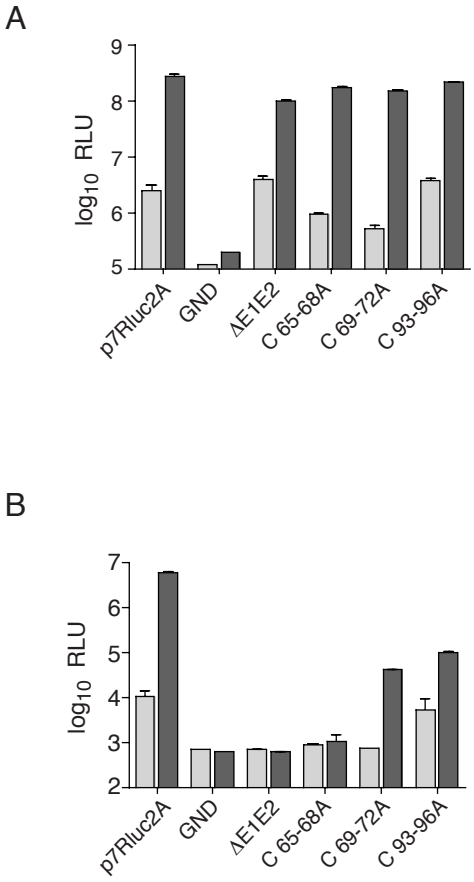

Fig 4-14. Core mutants are not temperature sensitive.

(A) RNA replication at 28°C, grey, and 37°C, black, at 4 days post-electroporation. (B) Infectious virus production from cells grown at 28°C, grey, or 37°C, black, at 4 days post-electroporation. Infections were performed at 37°C in each case. Means and SEM of duplicate experiments are shown.

HA epitope tags replaced amino acids 65 to 72 or 73 of core (Fig 4-15). Immunohistostaining for NS5A expression indicated that the presence of the epitope tags did not affect RNA replication, but that infectious virus production was reduced to below the limit of detection (Fig 4-15). Since alanine mutations in this region of core had also been deleterious to infectivity in the absence of compensatory mutations, we passaged cells harboring tagged genomes with the hopes of selecting for similar second-site mutations but without success (data not shown). These results indicated that amino acids 65-72 of core are not amenable to extensive mutation and that the ability to select for compensatory mutations may depend on more subtle changes in this region.

Core mutations do not affect particle stability

Mutations in core might be envisioned to impair interactions of the protein with components of the virion itself. The residues mutated in J6/JFH(p7Rluc2A)/C93-96A lie within a proposed homotypic interaction domain (154), and all three groups of mutations are in close proximity to a putative glycoprotein association region (151), and RNA binding sequences (180). To test whether incorporation of mutant core proteins led to virions of reduced stability, J6/JFH/C65-68A, J6/JFH/C69-72A, and J6/JFH/C93-96A viruses, produced in the presence of their isolated compensatory mutations, were incubated at elevated temperature (47°C) for various amounts of time. The proportion of residual infectivity was quantified by qRT-PCR analysis of

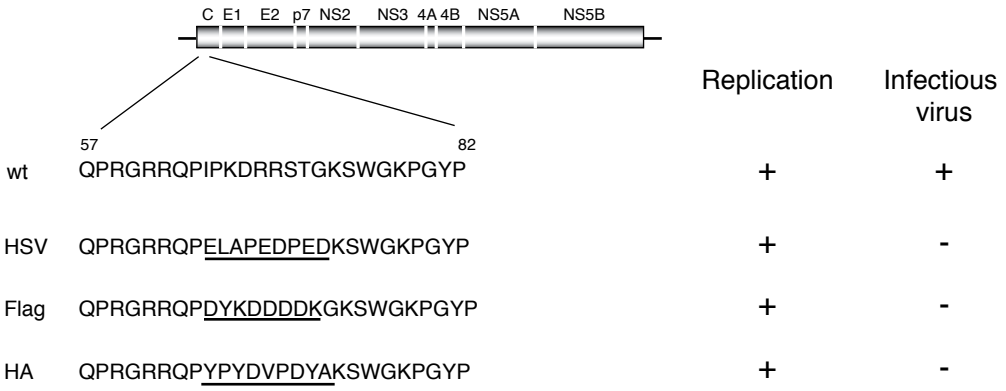

Fig 4-15. Insertion of epitope tags in core abolishes infectivity. Schematics of epitope tags within core in the J6/JFH genome. Replication and infectious virus production from each genome at 48 h post-electroporation are indicated.

intracellular RNA at 48 h post-infection of naïve cells. With the exception of the slightly decreased stability of J6/JFH/C69-72A/A880P, the mutant core proteins did not appear to significantly affect virion integrity (Fig 4-16). These results indicated that the core protein mutations do not affect contacts that are critical for the stability of the particle. It is still possible, however, that these regions of core are required for structural component interactions early in assembly but that conformational changes during morphogenesis negate these associations in the mature particle.

Discussion

The advent of a tissue culture infectious system for HCV has allowed the role of the core protein in authentic virion production to be studied for the first time. Here, we have performed a comprehensive deletion and mutational analysis of core and identified numerous sequences essential for infectivity. Consistent with the ability of subgenomes lacking the structural proteins to replicate autonomously (21), we did not identify any core mutants with replication defects. Although core is not required for replication, mutations in conserved RNA structural elements within the core-coding region can affect replication in a full-length genome (134). We excluded from our analyses the coding regions of residues 1 to 56, which have been shown to contain functional RNA structural elements (134). The possible phenotypic contribution of RNA structure to mutants in the remainder of the core protein was not assessed.

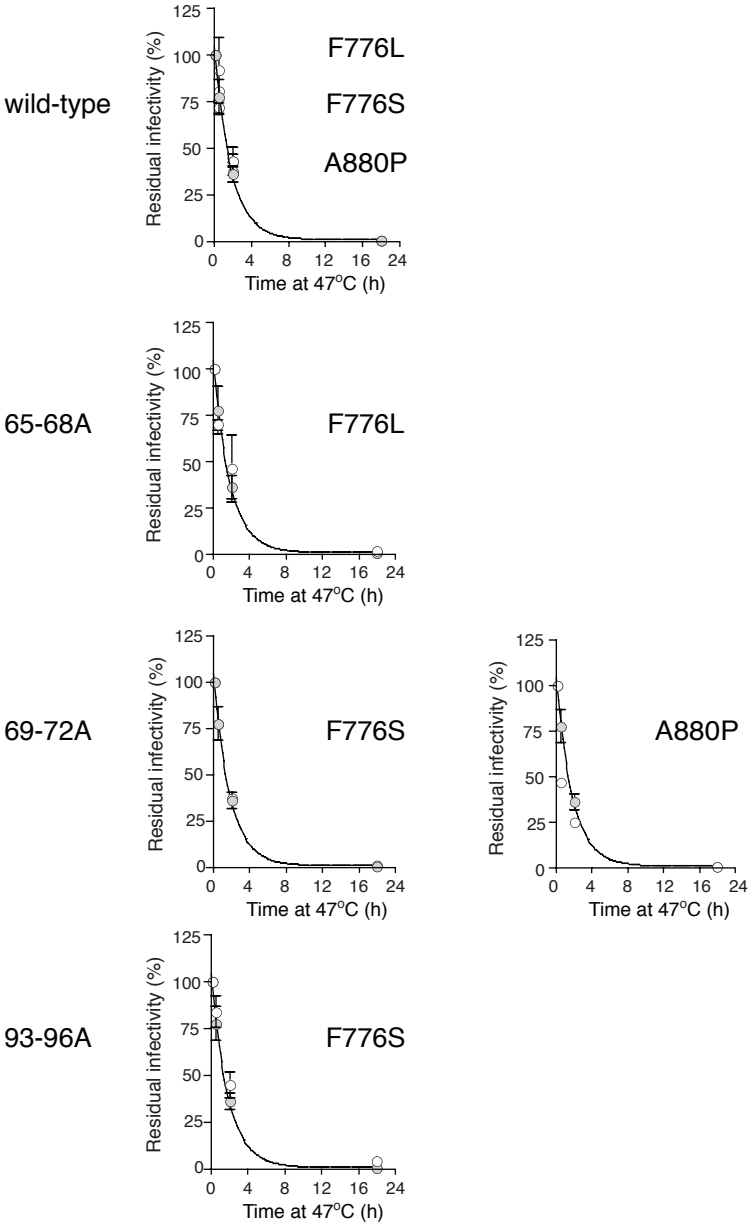

Fig 4-16. Core mutations do not affect virion stability. Virions containing mutant core proteins, rendered infectious by the presence of the indicated nonstructural protein changes, were incubated at 47°C for the indicated periods of time. Residual infectivity, as measured by qRT-PCR quantification of RNA replication in infected cells, is shown. Wild-type J6/JFH (—●—) and mutants (—○—).

Despite robust RNA replication, the majority of alanine-substitution mutants showed severely impaired virion production (summarized in Fig 4-17). Notably, mutation of the carboxy-terminal residues 181-190 did not significantly impact infectivity. These residues contribute to the E1 signal sequence, a known substrate of SPP (133). The tolerance of this region to mutation suggested that SPP cleavage might occur amino-terminal to these residues, or that the alanine substitutions in this region did not affect the efficiency of SPP processing. Previously, mutation of A180/S183/C184 to V/L/V has been suggested to abolish SPP processing of core (133, 3, 82). It is possible that substitution of these amino acids with alanine, rather than with the bulkier leucine or valine did not disrupt SPP cleavage. Consistent with this hypothesis, transmembrane regions containing helix-disrupting residues with small side chains have been shown to be optimal substrates for SPP (112), with the small side chain deemed sufficient in some reports (199). Alternately, residues 180-184 may not play a role in SPP processing in the HCVcc system. Interestingly, we found that mutation of residues 169-172 to alanine led to the production of very low levels of core that appeared to be incompletely processed. Notably, this sequence contains three conserved small or helix-disrupting residues (PGC) (30). It is also possible that SPP processing is disrupted by the carboxy-terminal alanine-substitutions, but that this cleavage is not required for infectious particle production. Although studies of related viruses and analysis of core from HCV-infected patient sera have strongly suggested an essential role for SPP cleavage (78, 199, 227), some

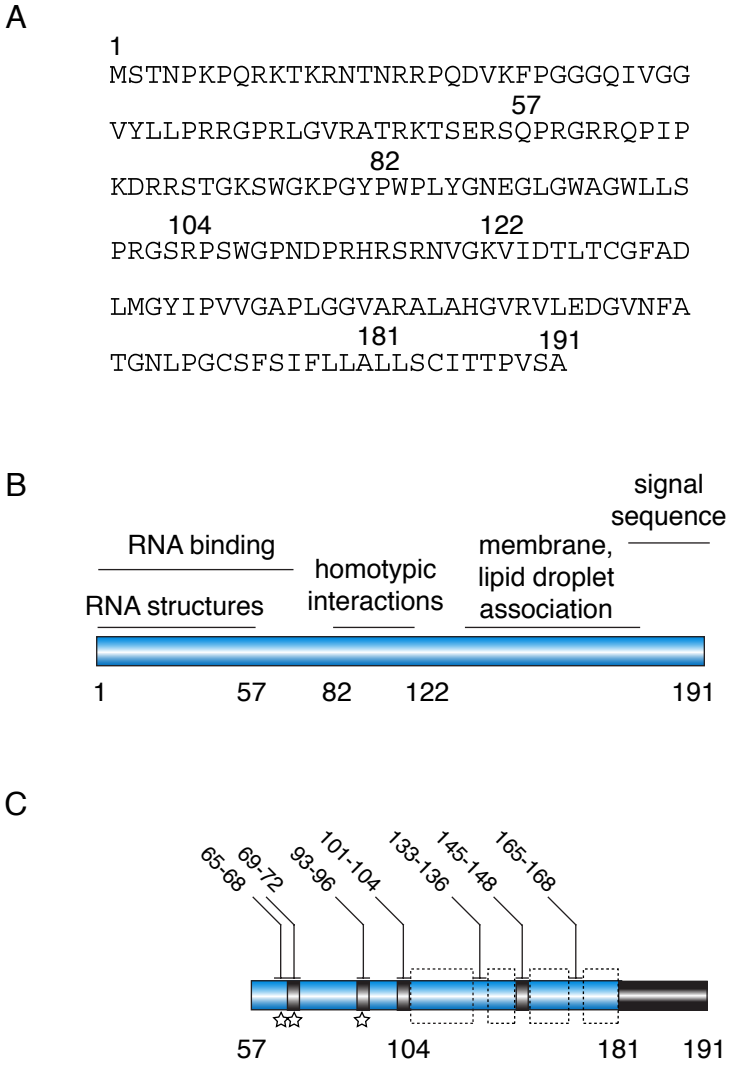

Fig 4-17. Summary of core alanine-scanning mutagenesis. (A) J6 core amino acid sequence. (B) Previously reported core functional regions (reviewed in reference 132). (C) Summary of results of alanine-scanning mutagenesis of residues 57-191. Infectious virus production indicated by shading: black, 50-100% J6/JFH(p7Rluc2A); grey, 0.3-1% wild-type. Residues highlighted by dashed box did not produce stable core protein. Isolation of compensatory mutations indicated by stars. Residues mutated to alanine are numbered above.

studies of NLP assembly have found SPP processing to be dispensable for budding (213, 128). Also unknown is whether the core signal sequence performs additional roles after its liberation by SPP. The insensitivity of this region to alanine-substitutions suggests it likely acts solely as a signal sequence, although it is possible that additional functions can accommodate these mutations.

A number of the alanine-substitution mutations severely affected the expression or stability of the core protein (Fig 4-17). These low or undetectable levels of core presumably led to the inability of these mutants to produce infectious virus. Several studies have reported that mutations, deletions, or truncations of the central hydrophobic domain of core lead to proteosome-mediated degradation of the protein (83, 196, 24, 133, 85). This instability has been suggested to result from impaired association of these mutants with membranes and lipid droplets (133). The amino-terminal domain of core, recognized as the first 117-120 amino acids (25, 132), is highly basic, flexible, and likely functions in binding and packaging the genomic RNA (25, 106, 105). Not surprisingly, the majority of mutations in this region did not lead to protein destabilization. Interestingly, the sensitivity of residues following amino acid 105 to mutation suggested that the highly flexible domain might be shorter than previously predicted.

Second-site mutations in nonstructural proteins p7, NS2, and NS3 were found to rescue the infectivity of several core alanine-substitution mutants by overcoming an early defect in virus morphogenesis, after the accumulation of

core at lipid droplets but before the assembly of an infectious particle (summarized in Fig 4-18). p7 is an integral membrane protein with two helical transmembrane domains and a short basic cytosolic loop (32). p7 has been shown to oligomerize, to form ion conductive channels *in vitro* (72), and to be essential for infectious virus production (179, 90). Here, mutations of p7 residue F776 to L or S was found to dramatically enhance infectivity of J6/JFH/C65-68A and J6/JFH/C69-72A, respectively, while an independently isolated F776S mutation had a much less significant ability to rescue infectivity of J6/JFH/C93-96A. These observations, along with the limited effects of F776 mutations on wild-type virus, suggested that F776 might be involved in a specific genetic interaction with core amino acids 65-72. This p7 residue is well conserved among HCV genotypes, with L, V or I also represented. Interestingly, a sequence encoding the F776S mutation has recently been isolated from a patient infected with a genotype 1a virus (33).

Structural modeling of p7 has suggested that F776 resides on the phenylalanine-rich face of transmembrane helix 1 (40, 32). Both hexameric and heptameric models of p7 oligomeric ion channels predict that F776 faces out of the pore, and possibly stabilizes interactions with transmembrane domain 2 (156, 40). This positioning of F776 could leave it accessible for interactions with other membrane-associated proteins, including core. Interaction of p7 with the structural proteins has recently been suggested by studies of intergenotypic chimeras in which homology of p7 and upstream sequences enhanced infectious

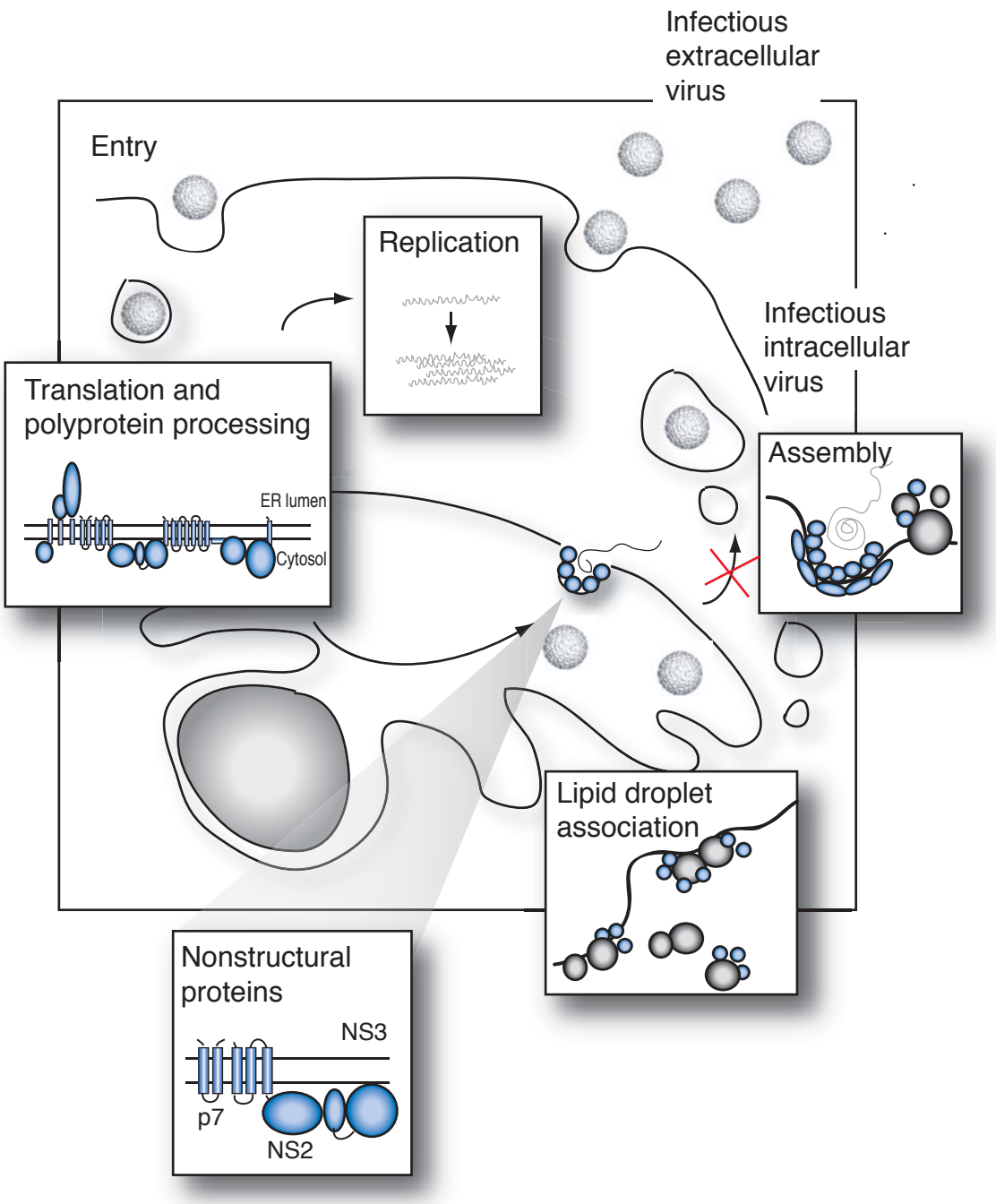

Fig 4-18. Core alanine-substitution mutants are blocked before infectious virus assemby. See text for details.

virus production (159). Our finding that incorporation of mutant core proteins did not disrupt interactions required for virion thermostability suggested that these sequences might interact with nonstructural, rather than structural, proteins. While a direct interaction of p7 and core might be envisioned for the hydrophobic amino acids 93-96, however, the basic nature of wild-type core amino acids 65-72 argues against their accessibility to p7 intramembrane sequences.

Alternately, compensatory mutations in p7 might act to increase interactions of core with any of the numerous factors involved in the production of an infectious particle. Determinants in transmembrane domain 1 have been shown to influence the delayed or incomplete processing of p7 from both E2 and NS2 (31). Putative disruption of transmembrane helix 1 or destablization of interactions between the transmembrane domains might be envisioned to increase processing of p7 intermediates, thereby increasing concentrations of E2 and NS2 available for assembly functions (31). A recent report of core binding to E1 has suggested that this interaction depends on core amino acids 72 to 91 (151), a region closely apposed to the alanine-substitution mutations in all three of the rescued genomes described here. The effects of the core mutations on E1 binding, and a possible role for p7 in modulation of these processes remain to be investigated.

An independent compensatory mutation in NS2 was isolated by passage of the J6/JFH/C69-72A genome. NS2 is a membrane-associated cysteine protease and immediately follows p7 in the viral polyprotein (67). Although the

exact topology of NS2 is disputed, the A880P mutation would be predicted to lie within the third transmembrane or membrane associated helix (226). Residue 880 is predominantly L, with V also represented and A prevalent in genotype 2 sequences. Proline in this position has not been reported, consistent with its predicted helical environment. Unlike the p7 changes, the A880P mutation significantly increased infectious virus production in the context of a wild-type genome. While this increase was much less dramatic than the corresponding enhancement of J6/JFH/C69-72A infectivity, it suggested that this adaptive mutation might act solely by overcoming a threshold of viral fitness, thereby suppressing the defective core phenotype. Alternately, the A880P mutation might mediate specific genetic interactions with core amino acids 69-72, in addition to a general enhancement of infectivity. Recent studies of intergenotypic chimeras have suggested that optimal infectivity requires NS2 transmembrane domain 1 and the structural proteins to be of the same genotype, as well as homology between the remainder of NS2 and the replicase proteins (159). While the normal RNA accumulation of J6/JFH/A880P suggested that interactions required for replication were not affected, association of NS2 with NS3 could be envisioned to affect infectious virus production, as found in the related *Pestiviruses* (2).

A compensatory mutation in NS3 was found to very slightly improve the infectivity of J6/JFH/C65-68A, likely through a weak, general increase in J6/JFH infectious virus production. This T1209A change resides between the protease

and helicase domains of NS3. Residue 1209 is predominantly M, with T prevalent in genotype 2A. Alanine can be found in other genotype 2 and genotype 3 sequences. A role for NS3 in HCV infectious virus production has recently been alluded to by the isolation of a Q1251L change that enhanced infectivity of an intergenotypic chimera (228). Involvement of NS3 in infectious virus production has also been documented in the related *Flaviviruses* and *Pestiviruses* (103, 2). Interestingly, recent microscopy studies have suggested that NS3 colocalizes with core on lipid droplets (176).

In conclusion, a comprehensive mutagenesis study of the HCV core protein has identified numerous residues critical for its role in virion production. The identification of compensatory mutations in p7 and NS2 that efficiently overcome several defects imposed by core protein mutation illustrates the central role of these nonstructural proteins in virion morphogenesis. The isolation of a weakly enhancing compensatory mutation in NS3 suggests that, as for other *Flaviviridae*, this multifunctional protein might also be involved in infectious virus production.

Chapter 5

Chapter 5: BVDV infectious virus production depends on nonstructural protein determinants

Introduction

BVDV nonstructural proteins NS2 and NS3 are multifunctional sequences with essential and not yet fully understood roles in many aspects of the viral life cycle (Fig 5-1). NS2 is a 54 kDa protein with a hydrophobic amino-terminus containing multiple transmembrane segments and a cytosolic carboxy-terminal protease domain (108). NS3 is a 76 kDa protein with an amino-terminal protease domain and a carboxy-terminal helicase/NTPase domain (217, 224, 197). It does not possess a transmembrane segment but is membrane associated, likely through interactions with NS4A (201).

Polyprotein processing

Along with N^{pro}, NS2 and NS3 constitute the viral proteases and are essential for the processing of the precursor polyprotein. NS2, an autoprotease, catalyzes a single cleavage of its own carboxy-terminus from NS3. Subsequent inhibition of its protease activity is predicted to result from irreversible binding of the processed carboxy-terminus to the active-site (109). The NS2 protease activity is dependent on a cellular cofactor, Jiv (J-domain protein interacting with viral protein, ref 171, 107). Jiv is an ER-associated, J-domain-containing chaperone protein related to Hsp40 (171). Little is known about its mechanisms of action or cellular interaction partners, although the human homologue has

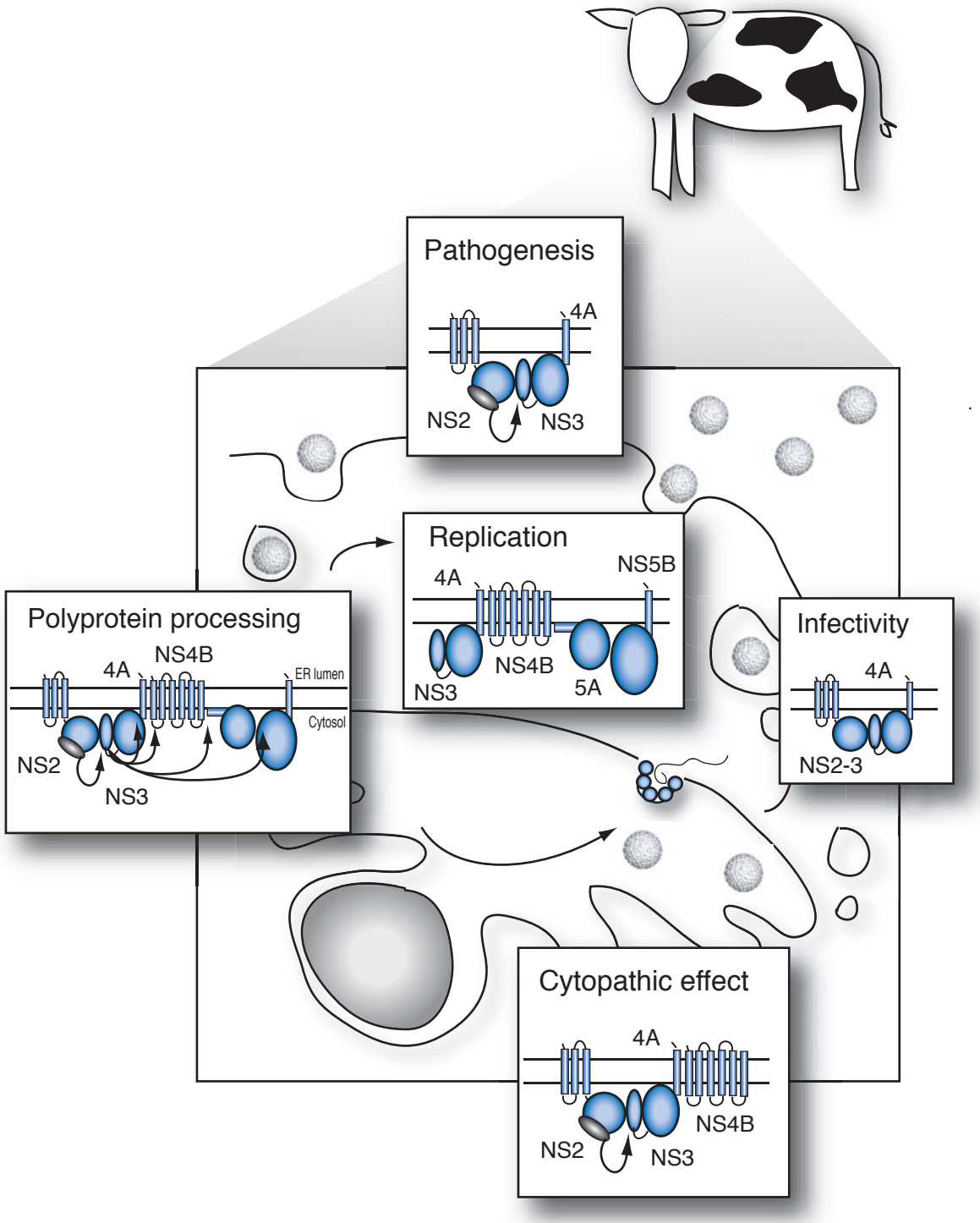

Fig 5-1. Functions of NS2 and NS3 in the BVDV life cycle. NS2 and NS3 are proteases required for polyprotein processing. Jiv, a cellular cofactor, grey. NS3 is required for RNA replication. NS2-3 cleavage, with NS4B modulates the cytopathic effect. Uncleaved NS2-3 is required for infectious virus production. NS2-3 cleavage correlates with fatal disease in infected animals.

been implicated in the transport of the dopamine receptor to the cell surface (18). Jiv interacts with NS2 in the vicinities of both the active-site and the scissile bond and is thought to appose these domains in a conformation that facilitates cleavage (109). Unlike a canonical chaperone activity, Jiv does not dissociate from NS2 after NS2-3 processing and therefore becomes unavailable for further activities as a cofactor (107). Since intracellular levels of Jiv expression are low, titration of this limiting cofactor leads to increasingly inefficient NS2-3 cleavage, and the accumulation of an uncleaved NS2-3 product during the course of infection (107).

The NS3 protease also has autocatalytic activity and processes its own carboxy-terminus from NS4A (224). Unlike NS2, however, NS3 is not subsequently inactivated and goes on to cleave at additional downstream sites, liberating the nonstructural proteins from the polyprotein (224, 225, 201**).** NS4A is a required cofactor for the NS3 protease activity, possibly because of its ability to tether NS3 to the ER membrane or by a conformational change-induced activation (224, 201, 44).

Replication

Naturally occurring BVDV genomes that have deletions of the first two nonstructural proteins (p7 and NS2), as well as the structural proteins, replicate autonomously and can be packaged into virions in the presence of a coinfecting helper virus, eliminating the possibility of an essential function for NS2 in RNA

replication (16). When NS2 is present in a genome, however, its autoproteolytic cleavage from NS3 is absolutely required for RNA replication (108).

Both the protease and helicase/NTPase activities of NS3 are essential for RNA replication (225, 69). The protease activity of NS3 is required for correct maturation of the replicase proteins, including the RNA-dependent RNA polymerase (NS5B), and the helicase/NTPase domain may be involved in unwinding RNA secondary structures. The inhibitory effect of a catalytically inactive NS2 protease on viral growth indicates that the NS3 is not active in the uncleaved NS2-3 form (108). The temporal decrease in NS2-3 cleavage as the Jiv cofactor is consumed is therefore a mechanism of regulating RNA replication (107).

Cytopathic effect

BVDV replication in tissue culture can lead to a dramatic cytopathic effect (CPE) beginning approximately 24 h post-infection. Not all BVDV sequences are able to induce this effect, with many instead establishing a persistent infection without inducing cell death. This observation has led to the division of BVDV strains into two biotypes, cytopathic (cp) and noncytopathic (ncp) (reviewed in 142). Interestingly, the efficiency of NS2-3 cleavage has been found to correlate with the ability of BVDV to kill cells in tissue culture. While both cp and ncp viruses express large amounts of uncleaved NS2-3, only cp BVDV produces discrete NS3 in significant quantities. Although ncp genomes were long thought

to be entirely deficient in NS2-3 cleavage, recent evidence has shown that ncp viruses do produce processed NS3, albeit at very low levels and only early in infection (108). This reconciles with the observation that NS3 can only act in replication after its liberation from the NS2-3 precursor (108). In keeping with this role for discrete NS3 in replication, cp genomes accumulate RNA to higher levels than ncp viruses. Interestingly, infectious virus titers do not differ significantly different between the biotypes, suggesting that RNA replication is not the limiting factor in virion production (108).

The mechanism by which cleaved NS3 leads to cytopathogenicity is not understood. Neither cleaved NS3 nor the high levels of RNA replication *per se* appear to be cytotoxic, since both phenotypes can be uncoupled from CPE by adaptive mutations in NS4B (163). It has also been suggested that these mutations in NS4B may block apoptotic pathways, thereby masking the deleterious effects of overwhelming viral replication (Paulson M. and CMR, unpublished data).

Pathogenesis

The cell culture cytopathic phenotype has significance to disease progression in infected animals. Whereas exposure of adult animals to BVDV often results in asymptomatic infection, calves infected *in utero* can become immunotolerant to and persistently infected with the virus (reviewed in 142). These calves may go on to develop fatal mucosal disease. While ncp BVDV

alone can be isolated from asymptomatic animals, both cp and ncp viruses can be found in animals suffering from mucosal disease. Since these viruses are antigenically related, and are nearly identical in sequence, cp BVDV is thought to develop from the ncp virus within the infected animal (142).

cp BVDV genomes can arise in a variety of ways, all of which affect processing at the NS2/NS3 junction. Cellular or viral insertions, deletions, and even point mutations have been found to give rise to NS3 expression and resulting cytopathogenicity (13, 16, 104, 136, 200). NADL (National Animal Disease Laboratories), the American prototype cp BVDV, contains a 270-nucleotide insertion in NS2 that potentiates the partial cleavage of NS2-3 (136). Sequencing of this insertion identified it as encoding a 90-amino acid portion of Jiv, the same J-domain chaperone required as an essential cofactor in NS2-3 cleavage (171). Removal of this insertion results in NADL Jiv 90^{-}, an ncp BVDV strain in which NS2-3 remains predominantly uncleaved (136). Portions of the Jiv coding sequence have subsequently been found in several other BVDV genomes isolated from diseased animals (148, 150). Insertions of Jiv, as well as other insertions and mutations that increase NS2-3 cleavage, have been proposed to overcome the limitations of the titratable cellular cofactor (107). The resulting insensitivity to the temporal down-regulation of replication, however, means that these viruses cannot establish persistent infections and ultimately kill their host (107).

Infectious virus production

Work in our laboratory has determined that NS2 and NS3, in the context of the uncleaved NS2-3 precursor, are essential for the production of infectious virus (2). This additional role for these proteins coincides well with the observed accumulation of uncleaved NS2-3 late in infection, when progeny virions are produced (108). Abrogation of uncleaved NS2-3 expression by insertion of either a Ubi monomer or an IRES between the two proteins led to complete processing of NS2-3 and prevented infectious virion formation without decreasing RNA replication (2). Reintroduction of uncleaved NS2-3 either within the bicistronic genome, or in *trans* restored uncleaved NS2-3 expression and infectious particle production. The mechanisms by which uncleaved NS2-3 functions in infectivity are not understood.

NS2 and NS3 have essential functions at almost every stage of the viral life cycle, from inter-host transmission to the molecular mechanisms of replication. The central importance of these proteins to *Pestivirus* replication and disease led us to dissect the determinants of one of their functions, that of infectious virus production.

Results

Development of a quantitative *trans*-complementation assay for NS2-3

To better understand the role of uncleaved NS2-3 in infectious virus production, we investigated the minimal requirements for its activity. As a

convenient assay for such determinants, a *trans*-complementation system was developed. Previous observations had suggested that an NS2-3-deficient genome could be rescued by ectopic expression of the uncleaved protein. We used this observation as the basis of a quantitative *trans*-complementation assay.

The uncleaved NS2-3-deficient genome constituted the full-length NADL Jiv90^{-} genome with an *encephalomyocarditis virus* (EMCV) IRES inserted between NS2 and NS3 (Fig 5-2A). The first cistron consists of the authentic BVDV IRES followed by N^{pro} and the structural proteins up to NS2; the second cistron is modified by the addition of a second copy of N^{pro} followed by the coding sequences for NS3 to NS5B. The autoproteolytic activity of N^{pro} allows the authentic NS3 amino-terminus to be created, which is essential for efficient replication (203). The second cistron is sufficient for autonomous replication and is similar to naturally occurring BVDV subgenomes (sg), which possess large deletions of the structural proteins. The uncleaved NS2-3-deficient genome was therefore termed N^{pro}-NS2/sg (Fig 5-2A).

Ectopic expression of NS2-3 was achieved using a second bicistronic genome. In this genome, N^{pro}-p7-NS2-NS3-NS4A is encoded in the first cistron under the control of the BVDV IRES (Fig 5-2A). N^{pro} is required for efficient translation and cleaves itself from the amino-terminus of p7 (149). The second cistron, driven by the EMCV IRES, is identical to that of N^{pro}-NS2/sg. This construct was termed p7-NS2-NS3-4A/sg (Fig 5-2A).

Fig 5-2. Development of a quantitative *trans*-complementation assay for NS2-3. (A) Schematics of mono and bicistronic genomes. Wild-type NADL and NADL Jiv90-, top. Uncleaved NS2-3 deficient genome, middle, and p7-NS2-3-4A expressing genome, bottom. (B) RNA replication of N^{pro}-NS2/sg and p7-NS2-3-4A/sg at 30 h post-transfection as measured by NS3 expression. Mean and SEM of duplicate experiments are shown. (C) Intracellular protein expression at 30 h post-electroporation. Western blot for NS3-containing species using polyclonal Ab G40, top panel, and for β-actin, lower panel. (D) Quantification of infectious virus production at 30 h post-electroporation by immunofluorescence, left, or flow cytometry, right, of infected cells. Staining uses mAb 184 directed against NS3.

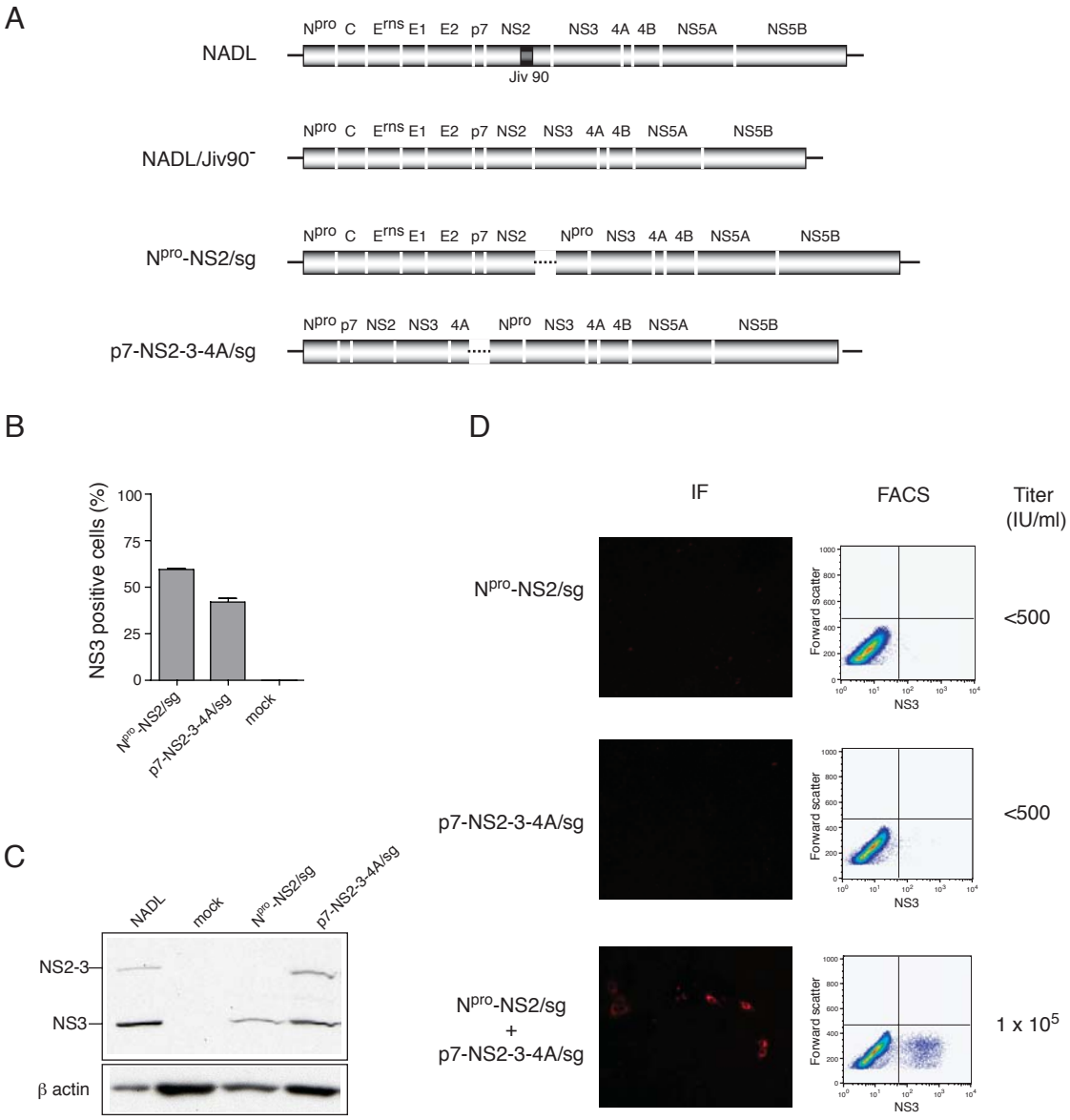
A
NADL
Npro C Erns E1 E2 p7 NS2 NS3 4A 4B NS5A NS5B
Jiv 90
NADL/Jiv90-
Npro C Erns E1 E2 p7 NS2 NS3 4A 4B NS5A NS5B
Npro-NS2/sg
Npro C Erns E1 E2 p7 NS2 Npro NS3 4A 4B NS5A NS5B
p7-NS2-3-4A/sg
Npro p7 NS2 NS3 4A Npro NS3 4A 4B NS5A NS5B
B
NS3 positive cells (%)
100
75
50
25
0
Npro-NS2/sg
p7-NS2-3-4A/sg
mock
C
NADL
mock
Npro-NS2/sg
p7-NS2-3-4A/sg
NS2-3
NS3
β actin
D
IF
FACS
Titer (IU/ml)
Npro-NS2/sg
<500
p7-NS2-3-4A/sg
<500
Npro-NS2/sg + p7-NS2-3-4A/sg
1 x 10^5
Forward scatter
NS3

In vitro generated RNA transcripts of each genome were electroporated into MDBK cells. The replication efficiency of each genome was determined at 30 h post-electroporation by immunostaining for NS3 and quantification of positive cells by flow cytometry (FACS). Both N^{pro}-NS2/sg and p7-NS2-NS3-4A/sg replicated to similar levels (Fig 5-2B). To verify that p7-NS2-NS3-4A/sg expressed the uncleaved NS2-3 protein, cell lysates harvested 24 h post-electroporation were analyzed by Western blot with an anti-NS3 polyclonal Ab (G40, ref 42, 41). NADL-transfected cell lysates were used as a marker for native NS2 and NS2-3. Uncleaved NS2-3 was expressed by p7-NS2-NS3-4A/sg, but not by N^{pro}-NS2/sg (Fig 5-2C). Consistent with the cytopathogenicity of NADL, and the slight CPE induced by N^{pro}-NS2/sg, the β-actin loading control was slightly reduced in these lanes (Fig 5-2C).

Infectious virus produced by the *trans*-complementation of NS2-3 is incapable of subsequent rounds of infection since only a single genome is packaged in the infectious particle. The standard plaque or focus forming assays for viral titer depend on the amplification of an infectious unit by spread to neighboring cells and could therefore not be used to quantify the pseudoinfectious virus released by the *trans*-complementing genomes. To overcome this, we developed a FACS-based assay for infectivity. Clarified cell culture supernatants were used to infect naïve MDBK cells. At 30 h post-infection, the cells were trypsinized, fixed, and stained for NS3 expression (mAb 184, ref 47). The proportion of cells expressing NS3, each assumed to represent

a single infectious event, was then determined by FACS (Fig 5-2D, right panel). NS3-positive cell quantification by FACS correlated well with visualization of immunofluorescently labelled cells (Fig 5-2D, left panel). Using this approach, the titer of pseudoinfectious virus released from N^{pro}-NS2/sg and p7-NS2-NS3-4A/sg co-electroporated cells was determined to be 1 x 10^5 infectious units/ml (IU/ml, Fig 5-2D). N^{pro}-NS2/sg or p7-NS2-NS3-4A/sg alone were not expected to produce infectious virus, as these genomes lack uncleaved NS2-3 and envelope proteins, respectively. Accordingly, infection of naïve cells with supernatants collected 48 h after electroporation with only N^{pro}-NS2/sg or p7-NS2-NS3-4A/sg revealed levels of virus below the limit of detection (500 IU/ml, Fig 5-2D).

To rule out the possibility that recombination between the co-electroporated genomes was responsible for the recovered virus, the supernatants were passaged on MDBK cells. Recombinant genomes would be expected to increase in titer during passaging. After the first passage, however, virus was undetectable, suggesting recombinants were not present (data not shown). These data suggested that an NS2-3 deficient genome could be rescued by expression of the p7-NS2-NS3-4A polyprotein fragment in *trans*, and that this infectivity could be quantified using a FACS-based assay.

p7 is not required in *cis* for NS2-3 function

p7 is a small hydrophobic protein that immediately precedes NS2 in the polyprotein and has also been shown to be essential for *Pestivirus* infectious

virion production (76); its mechanism of action in infectivity is not understood. To determine if p7 was required in *cis* with NS2-3 for the activity of the uncleaved protein in infectious virus production, we expressed the NS2-3-4A polyprotein fragment in MDBK cells. A bicistronic BVDV genome was created in which the first cistron, driven by the BVDV IRES, encoded 39 amino acids of N^{pro}, a Ubi monomer, and the NS2 to NS4A region of the NADL Jiv90^{-} genome. The fragment of N^{pro} was included to allow efficient translation from the BVDV IRES, and the Ubi monomer to direct correct processing at the amino-terminus of NS2 (149). The downstream cistron, expressed from the EMCV IRES, is identical to that of N^{pro}-NS2/sg. The resulting construct was termed Ubi-NS2-NS3-4A/sg (Fig 5-3A).

In vitro transcribed RNA of Ubi-NS2-NS3-4A/sg was electroporated into MDBK cells alone, or in combination with N^{pro}-NS2/sg. Replication efficiencies were determined at 30 h post-electroporation by FACS-based quantification of NS3 positive cells. Ubi-NS2-NS3-4A/sg replication was equivalent to that of N^{pro}-NS2/sg and p7-NS2-NS3-4A/sg (Fig 5-3B). Levels of NS2-3 protein expression were compared by Western blot analysis of cell lysates collected 24h post-electroporation. Similar to p7-NS2-NS3-4A/sg, Ubi-NS2-NS3-4A/sg produced NS2-3 and NS3 at levels comparable to NADL; N^{pro}-NS2/sg produced only cleaved NS3 (Fig 5-3C).

Infectious virus production at 48 h post-electroporation was assessed by FACS analysis of naïve cells inoculated with clarified cell culture supernatant.

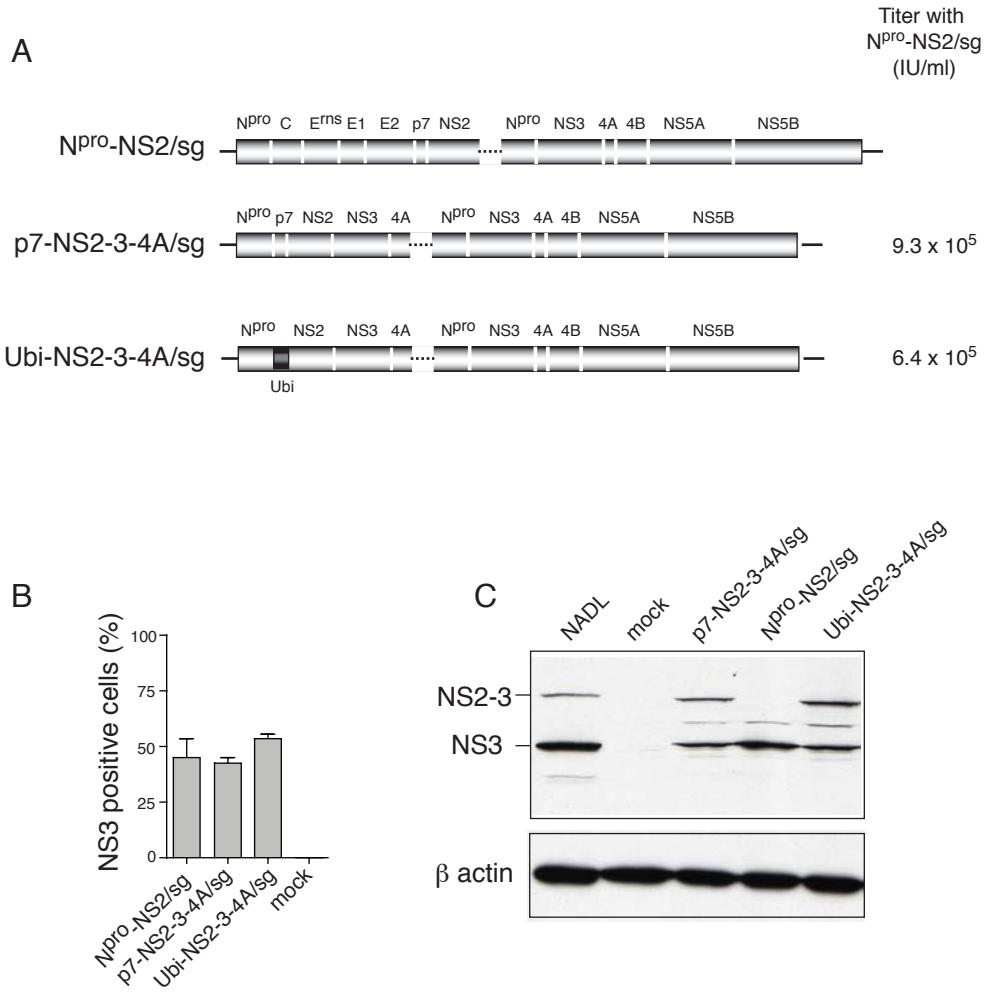

Fig 5-3. p7 is not required in *cis* for NS2-3 function. (A) Schematics of bicistronic genomes. NS2-3 deficient genome, top, p7-NS2-3-4A-expressing genome, middle, and NS2-3-4A-expressing genome, bottom. Ubi, black box, designates a ubiquitin monomer. Infectious titers produced by co-transfection of indicated genome with N^{pro}-NS2/sg are shown, right. Infectious units/ml (IU/ml) were calculated by flow cytometry analysis of infected cells for NS3 expression. (B) Replication of bicistronic genomes at 30 h post-electroporation, as calculated by flow cytometry for NS3 expression. Mean and SEM of quadruplicate experiments are shown. (C) Expression of NS3-containing protein products at 24 h post-electroporation.

Neither N^{pro}-NS2/sg, p7-NS2-NS3-4A/sg, nor Ubi-NS2-NS3-4A/sg alone were able to produce infectious virus (data not shown). p7-NS2-NS3-4A/sg or Ubi-NS2-NS3-4A/sg, however, each *trans*-complemented N^{pro}-NS2/sg with similar efficiencies, producing titers of 9.3×10^5 and 6.4×10^5 IU/ml, respectively (Fig 5-3A). These data suggested that p7 is not required in *cis* with NS2-3 for its function in infectious virus production.

NS4A is required in *cis* for optimal NS2-3 function

To further understand the minimal polyprotein region required for uncleaved NS2-3 function, we investigated whether NS4A was required in *cis* with NS2-3 for infectious virus production. Bicistronic genomes p7-NS2-3-4A(Δ9-64)/sg and p7-NS2-3/sg were created to express p7-NS2-NS3 in the absence of NS4A (Fig 5-4A). p7-NS2-3-4A(Δ9-64)/sg expressed N^{pro} followed by p7, NS2, NS3, and the amino-terminal eight amino acids of NS4A under the control of the BVDV IRES. p7-NS2-3/sg expressed N^{pro} followed by p7, NS2, NS3 and a stop codon, completely deleting NS4A. Both genomes contained a second cistron identical to that of N^{pro}-NS2/sg, the expression of which was directed by the EMCV IRES.

Replication of p7-NS2-3-4A(Δ9-64)/sg and p7-NS2-3/sg were assessed by FACS analysis of NS3 expression in cells at 30 h post-electroporation (Fig 5-4B). Although p7-NS2-3-4A(Δ9-64)/sg appeared to replicate slightly less efficiently than p7-NS2-3/sg, neither was significantly lower in NS3 accumulation than the

Fig 5-4. Determinants of NS2-3 function. (A) Schematics of bicistronic genomes. NS2-3 deficient genome, top, and genomes expressing the indicated regions of the NADL Jiv90- polyprotein. S1842A, black line, designates a lethal serine to alanine change in the NS3 protease active-site. Infectious titers produced by co-transfection of the indicated genome with N^{pro}-NS2/sg are shown, right. Infectious titers (IU/ml) were calculated by flow cytometry analysis of infected cells for NS3 expression. (B) Replication of bicistronic genomes at 30 h post-electroporation, as calculated by flow cytometry for NS3 expression. Mean and SEM of duplicate experiments are shown. (C) Expression of NS3-containing protein products at 24 h post-electroporation.

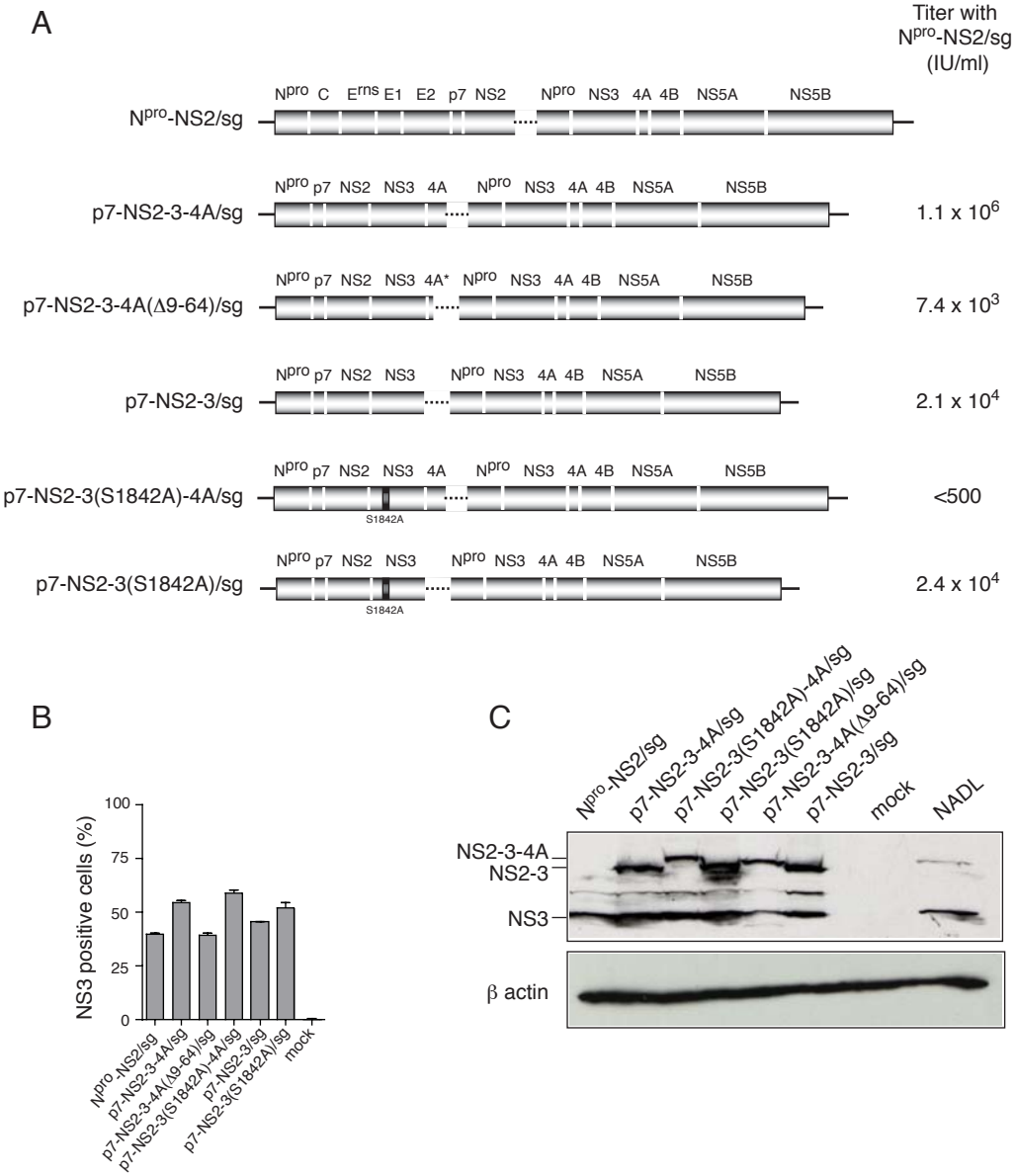
A
Titer with Npro-NS2/sg (IU/ml)
Npro-NS2/sg
p7-NS2-3-4A/sg
1.1 x 10^6
p7-NS2-3-4A(Δ9-64)/sg
7.4 x 10^3
p7-NS2-3/sg
2.1 x 10^4
p7-NS2-3(S1842A)-4A/sg
<500
p7-NS2-3(S1842A)/sg
2.4 x 10^4
S1842A
B
NS3 positive cells (%)
100
75
50
25
0
Npro-NS2/sg
p7-NS2-3-4A/sg
p7-NS2-3-4A(Δ9-64)/sg
p7-NS2-3(S1842A)-4A/sg
p7-NS2-3/sg
p7-NS2-3(S1842A)/sg
mock
C
Npro-NS2/sg
p7-NS2-3-4A/sg
p7-NS2-3(S1842A)-4A/sg
p7-NS2-3(S1842A)/sg
p7-NS2-3-4A(Δ9-64)/sg
p7-NS2-3/sg
mock
NADL
NS2-3-4A
NS2-3
NS3
β actin

parental construct, p7-NS2-3-4A/sg. Analysis of protein expression at 24 h post-electroporation indicated that both p7-NS2-3-4A(Δ9-64)/sg and p7-NS2-3/sg expressed uncleaved NS2-3 in addition to NS3 (Fig 5-4C). A slight difference in migration of NS2-3 was detected in the case of p7-NS2-3-4A(Δ9-64)/sg, suggesting that the residual eight amino acids of NS4A had not been cleaved by the NS3 protease.

Infectious virus production at 48 h post-electroporation was measured by FACS analysis of cells infected with clarified culture supernatants. In accordance with the absence of structural proteins, neither p7-NS2-3-4A(Δ9-64)/sg nor p7-NS2-3/sg alone produced infectious virus (data not shown). Both genomes, however, were able to rescue infectivity of N^{pro}-NS2/sg, with titers reaching 7.4 x 10^3 IU/ml (p7-NS2-3-4A(Δ9-64)/sg) and 2.1 x 10^4 IU/ml (p7-NS2-3/sg). *Trans*-complementation of N^{pro}-NS2/sg by p7-NS2-3/sg, although slightly more efficient than by p7-NS2-3-4A(Δ9-64)/sg, produced almost 100-fold less infectivity than when NS2-3 was expressed in the context of p7-NS2-3-4A/sg (Fig 5-4A). These results suggested that the presence of NS4A in *cis* is required for optimal function of NS2-3, and that an uncleavable fragment of NS4A may interfere with this function.

NS3 protease activity is not required for NS2-3 function

The serine protease activity of NS3 is required for polyprotein processing and RNA replication. To determine if this enzymatic activity was also required for

the function of NS2-3 in infectivity, we created p7-NS2-3(S1842A)-4A/sg. This genome is identical to p7-NS2-3-4A/sg but with a mutation of the NS3 active-site serine (1842) to alanine (Fig 5-4A, ref 201). Replication of p7-NS2-3(S1842A)-4A/sg at 30 h post-electroporation was similar to that of the parental genome, p7-NS2-3-4A/sg (Fig 5-4B). Western blot analysis of cell lysates harvested at 24 h post-electroporation indicated the expression of NS3 in addition to NS2-3-4A (Fig 5-4C). NS4A was not cleaved from NS2-3 as the NS3 protease activity is required for this processing event. Assay for infectious virus production at 48 h post-electroporation revealed that p7-NS2-3(S1842A)-4A/sg was not capable of *trans*-complementing N^{pro}-NS2/sg infectivity, leading to background levels of NS3 expression by both FACS analysis and direct visualization of immunofluorescent staining (Fig 5-4A and data not shown).

We hypothesized that the retention of NS4A on the carboxy-terminus of NS2-3 may be deleterious to its function. We therefore created p7-NS2-3(S1842A)/sg, which is identical to p7-NS2-3(S1842A)-4A/sg but with a complete deletion of NS4A (Fig 5-4A). Replication of p7-NS2-3(S1842A)/sg at 48 h post-electroporation was equivalent to that of p7-NS2-3-4A/sg (Fig 5-4B) and Western blot analysis of cell lysates at 24 h post-electroporation indicated that NS3 and NS2-3 were expressed (Fig 5-4C). Whereas no infectious virus was produced from MDBK cells harboring p7-NS2-3(S1842A)/sg alone (data not shown), coexpression with N^{pro}-NS2/sg resulted in a titer of 2.4×10^4 IU/ml (Fig 5-4A). This level of infectivity was similar to that produced by co-electroporation of p7-

NS2-3/sg with N^{pro}-NS2/sg, a genome identical to p7-NS2-3(S1842A)/sg except for the activity of the NS3 protease (Fig 5-4A). These results suggested that, apart from its role in cleaving NS2-3 from NS4A, the protease activity of NS3 is not absolutely required for NS2-3 function in morphogenesis.

Discussion

All positive-sense RNA viruses express their genomes as long polyproteins that must be cleaved to liberate the individual gene products. These cleavage events are often carefully regulated and processing intermediates can mediate functions unique from the final cleavage products (15, 193). In BVDV-infected cells, the NS2-3 uncleaved precursor accumulates to high levels. Work in our laboratory determined that this cleavage intermediate performs an essential function in infectious virus production, which could not be mediated by either of the individual proteins (2). This strict requirement for NS2-3 in the viral life cycle is supported by the observation that the uncleaved protein is maintained in all autonomous BVDV genomes, despite the increased processing at the NS2/NS3 junction in many cp BVDV strains. Preservation of the protein is achieved either by incomplete processing at this junction or by duplication of the uncleaved protein elsewhere in the genome. The selective pressure towards incomplete NS2-3 processing is illustrated by the Osloss strain of BVDV, a naturally occurring isolate that encodes a Ubi monomer inserted between NS2 and NS3 (138). Cleavage of Ubi by the cellular enzyme Ubi carboxy-terminal

hydrolase is not complete in this context, and is thought to be inhibited by two or more mutations in the cellular insertion (46, 137, 202). The importance of uncleaved NS2-3 encoded by genomic duplications is seen in the JaCp strain. This cp BVDV genome contains an insertion of a portion of light chain 3 of microtubule-associated proteins 1A and 1B (LC3*) upstream of NS3, causing the complete release of NS3 from the polyprotein (140). The genome also encodes a duplication of NS2 up to the amino-terminal part of NS4B; removal of the duplicated region resulted in a genome that did not express uncleaved NS2-3 and was not infectious (140).

Genomic duplications arising to compensate for complete processing of NS2-3 induced by cellular insertions offer information about the minimal sequences required for uncleaved NS2-3 activity. The results of our *trans*-complementation assays suggested that the expression of NS4A in *cis* was important for optimal NS2-3 function. Interestingly, duplications in cp genomes encompass not only NS2-3, but also the entire NS4A coding sequence (8, 13, 14, 140, 162, 161). This may indicate a requirement for the protease domain of NS3 to interact with its cofactor, NS4A, in order for NS2-3 to function optimally. Although NS4A is expressed from the second cistron in all the bicistronic constructs, this protein may be sequestered by NS3 encoded immediately upstream, and therefore be unavailable for interaction with NS2-3.

Although the NS3 protease cofactor, NS4A, was found to be important for NS2-3 function, the catalytic activity of the protease did not appear to be required

for virion production (summarized in Fig 5-5). It is possible that the NS3 protease is not active in the context of wild-type NS2-3, a hypothesis supported by the report that NS3 must be cleaved from NS2 in order to function in replication (108). This, however, is inconsistent with reports that NS3-4A processing occurs primarily in *cis*, a result supported by our finding that a mutation in the NS3 protease active-site prevented NS2-3 processing from NS4A despite the presence of an active NS3 protease in the downstream cistron. Uncoupling of the proteolysis and replication activities of NS3 has been reported, as truncations of NS3 that are lethal for replication can allow polyprotein processing to occur (201, 203). Cleavage at the NS3-4A junction was found to be the least sensitive to NS3 modification (201). Therefore, while the NS3 protease activity likely is active in the context of NS2-3, this activity is not required for the function of the uncleaved protein in infectivity.

In two constructs reported here NS4A sequences could not be cleaved from NS2-3, either due to inactivation of the protease (p7-NS2-3(S1842A)-4A/sg), or because of NS4A truncation (p7-NS2-3-4A(Δ9-64)/sg) (45). These genomes were severely impaired in their ability to *trans*-complement infectivity of N^{pro}-NS2/sg. One possibility for this phenotype is that a general conformational change or misfolding of NS3 might be induced by the carboxy-terminal extension. Alternately, the NS3-4A junction may be recognized by the protease but retained in the active-site in the absence of processing. Studies of the HCV NS3 protease have shown potent inhibition of catalytic activity by peptides mimicking its

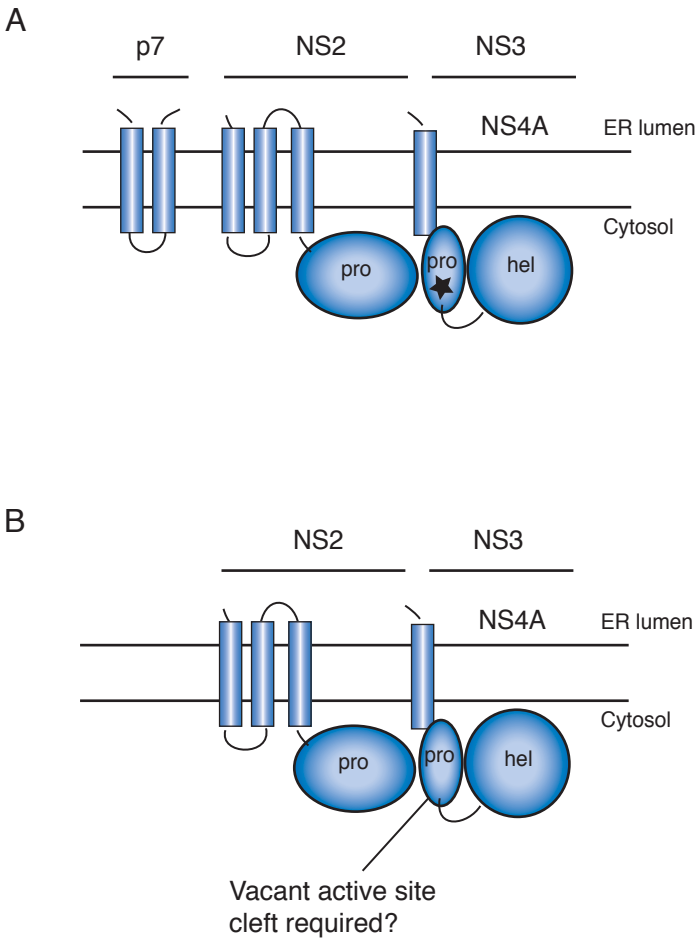

Fig 5-5. Summary of determinants of NS2-3 functions in infectious virus production. (A) Putative topology diagram of the p7 to NS4A region of the BVDV polyprotein. NS3 active-site S1842 is designated by a star. (B) Minimal regions of the polyprotein required for NS2-3 function.

substrates (189). The latter hypothesis would suggest that the NS3 active-site cleft, but not its catalytic activity, is required for NS2-3 function (Fig 5-5). These studies were conducted before the discovery of a second protease activity in NS2 (108). The contribution of NS2 enzymatic activity to NS2-3 function, therefore, is not known.

While NS4A was required in *cis* with NS2-3 for optimal infectivity, p7 was not (Fig 5-5). This result was surprising given the presumed role of p7 as a signal sequence for NS2 (76). Interestingly, the HCV NS2 protein, which is also essential for infectious virus production, was similarly functional in the absence of the p7-derived signal sequence (90). For HCV, although the carboxy-terminus of p7 has been shown to act as a signal sequence (32), NS2 is targeted to membranes in its absence (226). These results suggest that proteins encoded by both these viruses may have redundancies in their mechanisms of membrane targeting.

We have developed a quantitative *trans*-complementation system for NS2-3 and used it to investigate the determinants of uncleaved NS2-3 involved in infectious *Pestivirus* production. The optimal activity of NS2-3 in this role requires a close genetic association with the protease cofactor, NS4A, but does not require the catalytic activity of the protease. NS2-3 function does not require *cis*-expression of p7, or the signal sequence it provides. The indication of a role for BVDV NS2-3-4A proteins in infectious virus production adds to the

accumulating evidence that this region of the polyprotein performs essential functions in morphogenesis for all genera of the *Flaviviridae*.

Chapter 6

Chapter 6: Discussion

Production of an infectious virion represents the culmination of numerous processes initiated by expression of the viral genome within the host cell environment. Virus morphogenesis itself involves numerous interactions between viral, and often cellular, components, disruption of any one of which could lead to novel therapeutic agents. We have investigated the determinants of infectious virion production in the *Pestiviruses* and *Hepaciviruses*. As well as the importance of the structural building blocks of the virion, we have found numerous indications that nonstructural proteins are integral components of the assembly pathway.

Structural and nonstructural proteins in infectious virus production

Role of the capsid proteins

To investigate the mechanisms of *Flaviviridae* assembly, we studied an important virion structural component, the viral capsid proteins. Biochemical studies of BVDV capsid suggested that it is a nonspecific RNA condensing agent, a hypothesis that was supported by its functional replacement of such a protein *in vivo*. We hypothesize that the *Pestivirus* capsid does not form a discrete shell around the RNA genome, but rather complexes with it to condense, neutralize, and package the nucleic acid molecule into the budding particle. Consistent with

this hypothesis, *Flavivirus* particles have been reported to contain nucleoprotein complexes of undefined symmetry, rather than an icosahedral core; structures of *Pestivirus* and *Hepacivirus* particles have not been determined. In addition to a structured carboxy-terminal domain, HCV core possesses a basic amino-terminal region that is disordered in solution (106, 25). We propose this domain to be functionally equivalent to the BVDV capsid protein. Consistent with this hypothesis, studies of recombinant core proteins encompassing this flexible domain demonstrated RNA binding and aggregation behaviors similar to BVDV capsid (105, CLM and CMR, unpublished observations).

Alanine-scanning mutagenesis of HCV core provided an opportunity to examine the properties of the amino-terminal domain in the context of an infectious virus. Although a portion of the highly basic domain (residues 1-56) was omitted from our analysis, mutation of amino acids 57 through 104 did not disrupt the stability of the core protein, consistent with the predicted flexibility of this region. It was somewhat surprising, however, that these mutations were deleterious to infectious virus production, since our model would predict that significant changes could be tolerated as long as enough basic residues were retained. Since the efficiency of the HCVcc system is relatively low, it is possible that J6/JFH infectivity is not robust enough to tolerate even small perturbations in the RNA binding region. Alternately, residues prior to amino acid 57 may be the primary RNA condensing sequences, and those in the region of mutagenesis might be involved in additional interactions instead of, or in addition to, charge

neutralization within the particle. Our finding that incorporation of mutant core proteins did not compromise virion stability suggested that limited changes in this region did not affect efficient constraint of the RNA genome, consistent with the proposed flexibility of this function.

The presence of nonspecific RNA binding sequences in the capsid proteins may have additional relevance to the viral life cycle. Both *Pestiviruses* and *Hepaciviruses* are capable of establishing chronic infections. This ability to persist for months or years is dependent on an evasion of host defenses, including innate cellular responses against markers of viral infection such as double stranded RNA (dsRNA). HCV is thought to combat these innate defenses through several mechanisms, including NS3-mediated cleavage and inactivation of two dsRNA response factors, Cardiff and TRIF (reviewed in 62). Core itself has been reported to up-regulate an inhibitor of interferon signaling, SOCS-3 (22). The nonspecific RNA binding abilities of the capsid proteins might be envisioned to mask intracellular viral RNA as an additional mechanism of innate immune system evasion.

The *Flaviviridae* capsid proteins have the critical task of containing the genomic RNA within the particle and may play additional roles in managing replicating RNA within the cell. Our studies of BVDV capsid suggest that a flexible, basic sequence alone can accomplish this. HCV and *Flavivirus* capsid proteins consist of a similarly disordered arm coupled to a globular domain. The

requirement for this additional domain may relate to differing mechanisms of assembly or to further additional functions for the proteins (165).

Role of the nonstructural proteins

While the capsid proteins provide the structural components of the virion, such a complex macromolecular assembly likely requires orchestration by accessory factors. Converging evidence from each of the *Flaviviridae* genera implicates nonstructural proteins in infectious particle production. The NS2 and NS3 proteins of all these viruses appear to be architects of assembly. We report that for BVDV, uncleaved NS2-3 is essential for infectivity, and that the NS3 cofactor, but not the protease catalytic activity, is important for this function. The HCV NS2 protein is also essential in virion morphogenesis, functioning at an early step, prior to the accumulation of intracellular infectious virus (90). Consistent with this, we identified a compensatory mutation in NS2 that rescued a core mutant from a block early in infectious virus assembly. Although uncleaved NS2-3 is not required for HCV infectivity (90), rescue of a second core mutant by a weak compensatory mutation in NS3 suggested that the processed protein might nonetheless be involved in infectious virion production.

The viruses of the genus *Flavivirus* do not encode an autoprotease equivalent to NS2. Amino-terminal to NS3 are two hydrophobic proteins that span the membrane several times. One of these, NS2B, is the NS3 protease cofactor, the other, NS2A, is important for infectious virus production (103). The

NS2B-3 protease cleaves NS2A at a cryptic internal site, creating a truncated form of the protein termed NS2Aα (153). Mutational analysis of this cleavage site revealed that NS2Aα *per se* was not required for infectivity, but that the basic sequence in this region was essential for the formation or budding of nucleocapsids (103). Second-site mutations in the helicase domain of NS3 were found to suppress mutations in this motif and restore virus production, suggesting a required interaction between NS2A and NS3 in *Flavivirus* morphogenesis (103). Interactions between NS3, its protease cofactor, and an associated integral membrane protein may therefore be a common theme in nonstructural protein requirements for *Flaviviridae* infectious virion production.

The p7 protein of *Pestiviruses* and *Hepaciviruses* is another nonstructural protein essential for infectious virus production (76, 179, 90). This small hydrophobic protein is incompletely processed by signal peptidase, leading to an accumulation of uncleaved E2-p7 (114, 54). This association with an envelope protein suggested p7 might be incorporated into virions as a minor component. This precursor, however, is not essential for BVDV or HCV infectivity, and p7 has never been detected in *Pestivirus* particles (205); studies of HCV virions are ongoing. HCV p7 has been found to function early in infectious virion production, similar to NS2 (90). Optimal infectivity of HCV intergenotypic chimeras requires homology between regions of p7 and NS2, suggesting that these nonstructural factors may work in concert (159). Uncleaved p7-NS2 precursors also accumulate in BVDV and HCV infected cells (54, 114). The finding that this

precursor is not essential for HCV infectivity, however, as well as our observations that BVDV p7 is not required in *cis* with NS2-3 indicate that the putative association between these pathways is not a result of unprocessed forms. Like the other nonstructural proteins implicated in morphogenesis, we found that certain core mutations could be rescued by changes in p7.

Flaviviridae nonstructural proteins engineer the production of an infectious virion. While the NS2 and NS3 proteins of all *Flaviviridae* appear to be essential for infectivity, only the *Pestivirus* and *Hepacivirus* genera have a requirement for p7. The hypothesis that p7 and NS2 may function together early in particle morphogenesis coincides well with our finding that mutations in either of these proteins rescued core mutants after localization to putative sites of budding, but before the assembly of an infectious particle.

Mechanisms of nonstructural protein action

The mechanisms of nonstructural protein involvement in *Flaviviridae* infectious particle production are not understood. During the assembly of an intricate macromolecular complex such as an infectious virion, however, numerous roles for nonstructural cofactors can be envisioned (Fig 6-1).

Enzymatic activities

Several of the nonstructural proteins implicated in *Flaviviridae* morphogenesis have enzymatic activities. *Pestivirus* and *Hepacivirus* NS2

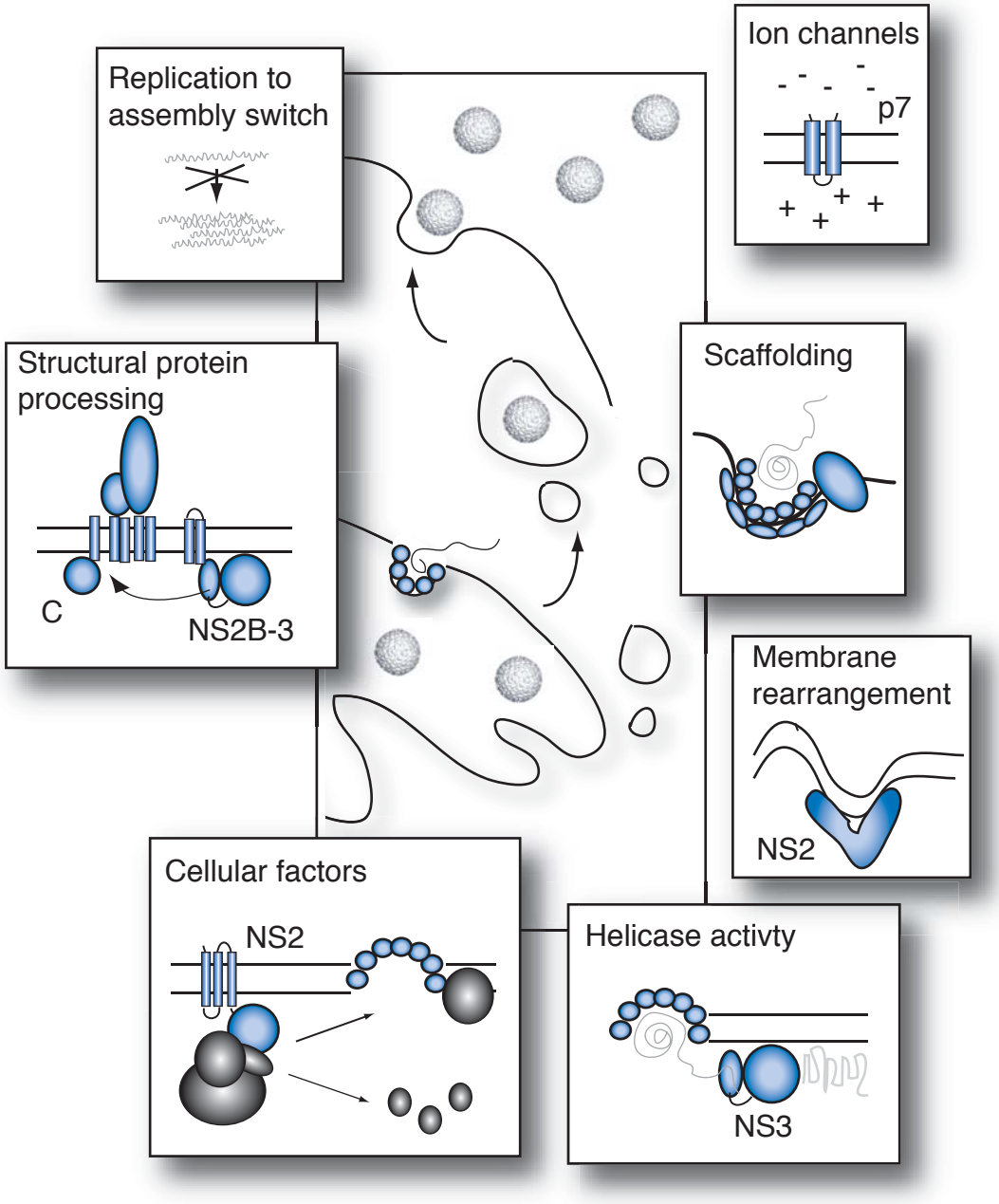

Fig 6-1. Nonstructural proteins and virion morphogenesis. Nonstructural proteins speculated to act by each mechanism are designated. Cellular factors are shown in grey. See text for details.

proteins are autoproteases, and the NS3 sequences of all *Flaviviridae* have protease, helicase, and NTPase activities. It is an intriguing possibility that these enzymatic activities may function in viral assembly as well as in nonstructural protein processing and replication.

The NS2 protease mediates a single cleavage at its own carboxy-terminus. The recent crystal structure of HCV NS2 revealed that this dedicated protease activity results from retention of the carboxy-terminal residue in the active-site after cleavage, thereby inactivating the enzyme (122). Consistent with this, the catalytic activity of NS2 is not essential for infectious virus production, although the protease domain itself is required (90). BVDV NS2 has been predicted to undergo similar product inhibition (109), although the role of the autoprotease activity in assembly has not been determined.

In *Flaviviruses*, the protease activity of NS3, with its cofactor NS2B, mediates cleavage of the capsid protein from its membrane anchor, and is thus essential for infectious virus production. Inspection of the capsid protein sequences from *Pestiviruses* and *Hepaciviruses* revealed the presence of NS3 protease recognition sites in the corresponding membrane anchors (180, 2). Subsequently it was found that a host enzyme, SPP, and not NS3, was responsible for processing this region of capsid. This finding was confirmed by mapping the carboxy-terminal amino acid of the virion associated *Pestivirus* capsid protein to alanine 90, three amino acids after the predicted NS3 cleavage site (78). In HCV, the carboxy-terminus of the mature capsid protein is not

known, leaving the formal possibility that NS3 may clip a few additional residues after SPP processing has occurred. Mutagenesis of the NS3-recognition sequence in the HCV core protein, however, did not support this hypothesis, since a mutation previously reported to abolish NS3 cleavage (100) did not impair infectivity.

Although the viral protease activities do not appear to influence infectivity, the helicase activity of NS3 might be envisioned to participate. In *Flaviviruses*, NS2A and the NS3 helicase are proposed to work in concert to mediate nucleocapsid incorporation into budding particles (103). Compensatory mutations in NS3 that partially rescued an HCV core mutant mapped to the linker between protease and helicase domains, and thus could be predicted to affect either activity. The NS3 helicase is important for unwinding RNA secondary structures during replication. This ability might also facilitate packaging of a genomic RNA substrate. In addition to secondary structure unwinding, an ability of RNA helicases to dissociate proteins from nucleic acid has been demonstrated (57). Removal of replication or translation machinery from the genomic RNA is likely to be an important prerequisite for assembly.

Regulation of replication and assembly

Although the catalytic activities of the nonstructural proteins may not be required for infectious particle production, these enzymes are essential for replication. This dichotomy suggests that nonstructural sequences might be

important in regulating the switch from active replication to virion production. This hypothesis is illustrated by the findings that BVDV NS3 alone is active in replicating the viral genome, whereas uncleaved NS2-3 is required for infectious virus production. The kinetics of *Pestivirus* NS3 and NS2-3 expression closely mirrors the switch from active replication to infectious particle production.

In *Flaviviruses*, only genomes capable of autonomous replication are substrates for the packaging machinery, suggesting replication and assembly are coupled processes (95). It has been hypothesized that this linkage may arise from a physical connection between membranous replication and assembly sites (95, 126). NS2A colocalizes with replication complexes (125) and is essential for infectious virus production (103), suggesting it may mediate a switch between the two processes. The ability of NS2A to bind RNA has led to the hypothesis that this integral membrane protein might channel genomic substrates out of membrane bound replication complexes and to the sites of packaging (125). Since NS3 binds RNA, and NS2 is an integral membrane protein, a similar mechanism might be proposed of the functions of these proteins in *Pestivirus* and *Hepacivirus* virion morphogenesis.

Ion channels

Viroporins are a group of small, hydrophobic, virally encoded proteins that increase membrane permeability. While some of these proteins, such as influenza virus M2, are structural, most are not major components of the virion;

all, however, are involved in enhancing infectious particle production (reviewed in 66). As well as *influenza virus* M2, viroporins include HCV and BVDV p7, HIV Vpu, *Alphavirus* 6K, and *poliovirus* 2B. Oligomerization and ion channel activities of these proteins have been observed by insertion of these sequences into planar lipid membranes, liposomes, and *Xenopus* oocytes (66). With the exception of M2, the relevance of the *in vitro* ion channel activity to a role in infectious particle production is not known. The M2 protein has dual functions in the *influenza virus* life cycle. It protects the glycoproteins from low-pH mediated inactivation during their transit though the *trans*-Golgi network, and it increases the permeability of the virion to ions, facilitating dissociation of the particle during entry. HCV and BVDV particles also transit the low-pH compartments of the secretory pathway, suggesting that the p7 proteins of these viruses may be important in protecting the exposed glycoproteins from undergoing premature acid-induced fusion. In conflict with this hypothesis are the findings that both HCV and BVDV are acid resistant until they are triggered by unknown factors during entry, suggesting protection from low pH may not be necessary (209). In addition, recent studies have indicated that HCV p7 is essential for early assembly events, indicating that a putative role as an ion channel in egress cannot be its only function (90).

Membrane rearrangements

In cellular vesicle budding systems, such as endocytosis or intracellular vesicular transport, an array of specialized proteins are required to induce

membrane curvature and vesicle fission (reviewed in 135). In addition to possibly recruiting such cellular proteins to assist in virus budding, structural or nonstructural proteins themselves might be envisioned to induce membrane rearrangements. As well as possible roles for ion channel activities in entry and egress, modifications of membrane potential have been suggested to induce instabilities in the bilayer, which might facilitate budding (26, 184). A role for p7 in membrane adjustments would reconcile with data that it functions early in HCV assembly (90). The HCV NS2 protease domain, which is also essential for early morphogenesis, forms a crescent shaped dimer (122). Interestingly, this kinked conformation, and attached amino-terminal membrane-associated helices, resembles the membrane curvature-inducing structure of the bin/amphiphysin/rvs-homology (BAR) domain (158). A function for NS2 in creating membrane curvature would be consistent with our finding that an alanine to proline mutation in one of the predicted amino-terminal helices rescued the infectivity of a core mutant. In this model, the proline would kink the putative helix, increasing force on the membrane and augmenting budding efficiency.

Binding to cellular factors

With the exception of the host proteases, signal peptidase and SPP, cellular factors required for *Pestivirus* or HCV assembly and release have not yet been identified. In other viral systems the host cell environment is an integral cofactor in infectious particle production. The involvement of the secretory

pathway and the requirement for cellular membrane rearrangements for *Flaviviridae* morphogenesis suggests the involvement of many host factors, any number of which could be targets of recruitment, inhibition, or regulation by viral proteins. During HIV infection of certain cell lines, the nonstructural protein Vpu is known to increase infectious virus production by interactions with at least two cellular factors. Vpu is a small, integral membrane protein that has been classified as a viroporin. Vpu does not localize to sites of assembly, does not interact with the structural proteins, and does not incorporate into virions (152). The enhancement of infectivity mediated by Vpu is a result of modulation of cellular protein functions. The first mechanism of Vpu action is to down-regulate expression of the HIV receptor, CD4, on the cell surface by interacting with the receptor in the ER and targeting it for degradation. This prevents secreted particles from re-entering the infected cell and allows dissemination of the infection (26). In an independent role, Vpu ensures release of mature viral particles from the plasma membrane by counteracting an inhibitory cellular factor that promotes tethering (152). This cellular factor, the identity of which is not known, has been hypothesized to be a membrane protein that becomes incorporated into virions and adheres to the plasma membrane (152).

Scaffolding

Many double stranded DNA (dsDNA) viruses require scaffolding proteins to assist in assembly (reviewed in 49). These nonstructural proteins associate

transiently with the forming viral particle but are not present in the mature infectious virion. Scaffolding proteins catalyze assembly through a variety of mechanisms. A *Herpesvirus* scaffolding protein associates with assembly intermediates and transports them to the sites of particle construction, thereby promoting nucleation events. Several phage scaffolding proteins mediate associations between structural components, often bringing subunits into close proximity allowing conformational switches to occur, which then stabilize the interactions. Many capsid subunit proteins have intrinsically flexible regions that provide the conformational variability necessary in building a virion shell; some scaffolding proteins act as chaperones, managing this intrinsic disorder until the appropriate interactions can be made. Several scaffolding proteins of the dsDNA phages form internal or external bracing structures, ensuring a virion shell of the correct size and shape is formed. Internal scaffolding proteins usually exit the shell as the genomic DNA is packaged.

Our finding of genetic interactions between HCV core and p7, NS2, and NS3 might indicate the importance of transient physical interactions. In addition to the proposed interaction with core, NS2 has also been reported to interact with E2 (183). Such interactions might point to a role for *Flaviviridae* nonstructural proteins in scaffolding structural protein associations or in transport of virion building blocks to the sites of assembly. In addition to direct frameworking functions, the ability of BVDV NS2 to bind a cellular chaperone protein might indicate a function in recruiting host cell scaffolding machinery (171).

Conclusions

We have investigated *Flaviviridae* infectious virus production from two convergent perspectives. The virion building blocks, the capsid proteins, have been found to consist of RNA condensing regions and structured domains of various relative proportions. Nonstructural protein domains required for infectious particle production have been identified, and the importance of these proteins at early events in morphogenesis has been highlighted. Investigations of *Pestivirus*, and especially *Hepacivirus*, infectivity have long been hampered by low yields of virus in tissue culture. With the advent of a new era of HCV research, these complementary elements of infectious particle assembly can begin to be understood.

References

1. **Acosta-Rivero, N., J. C. Aguilar, A. Musacchio, V. Falcon, A. Vina, M. C. de la Rosa, and J. Morales.** 2001. Characterization of the HCV core virus-like particles produced in the methylotrophic yeast Pichia pastoris. Biochem Biophys Res Commun **287:**122-5.

2. **Agapov, E. V., C. L. Murray, I. Frolov, L. Qu, T. M. Myers, and C. M. Rice.** 2004. Uncleaved NS2-3 is required for production of infectious bovine viral diarrhea virus. J Virol **78:**2414-25.

3. **Ait-Goughoulte, M., C. Hourioux, R. Patient, S. Trassard, D. Brand, and P. Roingeard.** 2006. Core protein cleavage by signal peptide peptidase is required for hepatitis C virus-like particle assembly. J Gen Virol **87:**855-60.

4. **Allison, S. L., J. Schalich, K. Stiasny, C. W. Mandl, and F. X. Heinz.** 2001. Mutational evidence for an internal fusion peptide in flavivirus envelope protein E. J Virol **75:**4268-75.

5. **Allison, S. L., K. Stadler, C. W. Mandl, C. Kunz, and F. X. Heinz.** 1995. Synthesis and secretion of recombinant tick-borne encephalitis virus protein E in soluble and particulate form. J Virol **69:**5816-20.

6. **Amberg, S. M., and C. M. Rice.** 1999. Mutagenesis of the NS2B-NS3-mediated cleavage site in the flavivirus capsid protein demonstrates a requirement for coordinated processing. J Virol **73:**8083-94.

7. **Barba, G., F. Harper, T. Harada, M. Kohara, S. Goulinet, Y. Matsuura, G. Eder, Z. Schaff, M. J. Chapman, T. Miyamura, and C. Bréchot.** 1997. Hepatitis C virus core protein shows a cytoplasmic localization and associates to cellular lipid storage droplets. Proc. Natl. Acad. Sci. USA **94:**1200-1205.

8. **Baroth, M., M. Orlich, H. J. Thiel, and P. Becher.** 2000. Insertion of cellular NEDD8 coding sequences in a pestivirus. Virology **278:**456-66.

9. **Bartenschlager, R.** 2006. Hepatitis C virus molecular clones: from cDNA to infectious virus particles in cell culture. Curr Opin Microbiol **9:**416-22.

10. **Bartenschlager, R., L. Ahlborn-Laake, J. Mous, and H. Jacobsen.** 1993. Nonstructural protein 3 of the hepatitis C virus encodes a serine-type proteinase required for cleavage at the NS3/4 and NS4/5 junctions. J. Virol. **67:**3835-3844.

11. **Bartosch, B., J. Dubuisson, and F. L. Cosset.** 2003. Infectious hepatitis C virus pseudo-particles containing functional E1-E2 envelope protein complexes. J Exp Med **197:**633-642.

12. **Baumert, T. F., S. Ito, D. T. Wong, and T. J. Liang.** 1998. Hepatitis C virus structural proteins assemble into viruslike particles in insect cells. J Virol **72:**3827-3836.

13. **Becher, P., M. Orlich, and H. J. Thiel.** 2001. RNA recombination between persisting pestivirus and a vaccine strain: generation of cytopathogenic virus and induction of lethal disease. J Virol **75:**6256-64.

14. **Becher, P., H. J. Thiel, M. Collins, J. Brownlie, and M. Orlich.** 2002. Cellular sequences in pestivirus genomes encoding gamma-aminobutyric acid (A) receptor-associated protein and Golgi-associated ATPase enhancer of 16 kilodaltons. J Virol **76:**13069-76.

15. **Bedard, K. M., and B. L. Semler.** 2004. Regulation of picornavirus gene expression. Microbes Infect **6:**702-13.

16. **Behrens, S.-E., C. W. Grassmann, H.-J. Thiel, G. Meyers, and N. Tautz.** 1998. Characterization of an autonomous subgenomic pestivirus RNA replicon. J. Virol. **72:**2364-2372.

17. **Behrens, S. E., L. Tomei, and R. De Francesco.** 1996. Identification and properties of the RNA-dependent RNA polymerase of hepatitis C virus. Embo J **15:**12-22.

18. **Bermak, J. C., M. Li, C. Bullock, and Q. Y. Zhou.** 2001. Regulation of transport of the dopamine D1 receptor by a new membrane-associated ER protein. Nat Cell Biol **3:**492-8.

19. **Bick, M. J., G. Gao, S. P. Goff, C. M. Rice, and M. R. MacDonald.** 2003. Expression of the zinc-finger antiviral protein inhibits alphavirus replication. J Virol **77:**11555-62.

20. **Blanchard, E., D. Brand, S. Trassard, A. Goudeau, and P. Roingeard.** 2002. Hepatitis C virus-like particle morphogenesis. J Virol **76:**4073-9.

21. **Blight, K. J., A. A. Kolykhalov, and C. M. Rice.** 2000. Efficient initiation of HCV RNA replication in cell culture. Science **290:**1972-1974.

22. **Bode, J. G., S. Ludwig, C. Ehrhardt, U. Albrecht, A. Erhardt, F. Schaper, P. C. Heinrich, and D. Haussinger.** 2003. IFN-alpha antagonistic activity of HCV core protein involves induction of suppressor of cytokine signaling-3. Faseb J **17:**488-90.

23. **Boulant, S., M. Becchi, F. Penin, and J. P. Lavergne.** 2003. Unusual multiple recoding events leading to alternative forms of hepatitis C virus core protein from genotype 1b. J Biol Chem **278:**45785-92.

24. **Boulant, S., R. Montserret, R. G. Hope, M. Ratinier, P. Targett-Adams, J. P. Lavergne, F. Penin, and J. McLauchlan.** 2006. Structural determinants that target the hepatitis C virus core protein to lipid droplets. J Biol Chem **281:**22236-47.

25. **Boulant, S., C. Vanbelle, C. Ebel, F. Penin, and J. P. Lavergne.** 2005. Hepatitis C virus core protein is a dimeric alpha-helical protein exhibiting membrane protein features. J Virol **79:**11353-65.

26. **Bour, S., and K. Strebel.** 2003. The HIV-1 Vpu protein: a multifunctional enhancer of viral particle release. Microbes Infect **5:**1029-39.

27. **Branza-Nichita, N., D. Durantel, S. Carrouee-Durantel, R. A. Dwek, and N. Zitzmann.** 2001. Antiviral effect of N-butyldeoxynojirimycin against bovine viral diarrhea virus correlates with misfolding of E2 envelope proteins and impairment of their association into E1-E2 heterodimers. J Virol **75:**3527-36.

28. **Bruschke, C. J., M. M. Hulst, R. J. Moormann, P. A. van Rijn, and J. T. van Oirschot.** 1997. Glycoprotein E^{rns} of pestiviruses induces apoptosis in lymphocytes of several species. J. Virol. **71:**6692-6696.

29. **Bukh, J., T. Pietschmann, V. Lohmann, N. Krieger, K. Faulk, R. E. Engle, S. Govindarajan, M. Shapiro, M. St. Claire, and R. Bartenschlager.** 2002. Mutations that permit efficient replication of hepatitis C virus RNA in Huh-7 cells prevent productive replication in chimpanzees. Proc Natl Acad Sci U S A **99:**14416-21.

30. **Bukh, J., R. H. Purcell, and R. H. Miller.** 1994. Sequence analysis of the core gene of 14 hepatitis C virus genotypes. Proc. Natl. Acad. Sci. USA **91:**8239-43.

31. **Carrere-Kremer, S., C. Montpellier, L. Lorenzo, B. Brulin, L. Cocquerel, S. Belouzard, F. Penin, and J. Dubuisson.** 2004. Regulation of hepatitis C virus polyprotein processing by signal peptidase involves structural determinants at the p7 sequence junctions. J Biol Chem **279:**41384-92.

32. **Carrere-Kremer, S., C. Montpellier-Pala, L. Cocquerel, C. Wychowski, F. Penin, and J. Dubuisson.** 2002. Subcellular Localization and Topology of the p7 Polypeptide of Hepatitis C Virus. J Virol **76:**3720-30.

33. **Castelain, S., D. Bonte, F. Penin, C. Francois, D. Capron, S. Dedeurwaerder, P. Zawadzki, V. Morel, C. Wychowski, and G. Duverlie.** 2007. Hepatitis C Virus p7 membrane protein quasispecies variability in chronically infected patients treated with interferon and ribavirin, with or without amantadine. J Med Virol **79:**144-54.

34. **Chambers, T. J., R. C. Weir, A. Grakoui, D. W. McCourt, J. F. Bazan, R. J. Fletterick, and C. M. Rice.** 1990. Evidence that the N-terminal domain of nonstructural protein NS3 from yellow fever virus is a serine protease responsible for site-specific cleavages in the viral polyprotein. Proc. Natl. Acad. Sci. USA **87:**8898-8902.

35. **Cheng, R. H., R. J. Kuhn, N. H. Olson, M. G. Rossmann, H. K. Choi, T. J. Smith, and T. S. Baker.** 1995. Nucleocapsid and glycoprotein organization in an enveloped virus. Cell **80:**621-630.

36. **Choi, H.-K., L. Tong, W. Minor, P. Dumas, U. Boege, M. G. Rossman, and G. Wengler.** 1991. Structure of Sindbis virus core protein reveals a chymotrypsin-like serine proteinase and the organization of the virion. Nature **354:**37-43.

37. **Choi, H. K., G. Lu, S. Lee, G. Wengler, and M. G. Rossmann.** 1997. Structure of Semliki Forest virus core protein. Proteins **27:**345-59.

38. **Choo, Q.-L., G. Kuo, A. J. Weiner, L. R. Overby, D. W. Bradley, and M. Houghton.** 1989. Isolation of a cDNA clone derived from a blood-borne non-A, non-B viral hepatitis genome. Science **244:**359-362.

39. **Chu, J. J., and M. L. Ng.** 2004. Infectious entry of West Nile virus occurs through a clathrin-mediated endocytic pathway. J Virol **78:**10543-55.

40. **Clarke, D., S. Griffin, L. Beales, C. S. Gelais, S. Burgess, M. Harris, and D. Rowlands.** 2006. Evidence for the formation of a heptameric ion channel complex by the hepatitis C virus p7 protein in vitro. J Biol Chem **281:**37057-68.

41. **Collett, M. S., R. Larson, S. K. Belzer, and E. Retzel.** 1988. Proteins encoded by bovine viral diarrhea virus: the genomic organization of a pestivirus. Virology **165:**200-208.

42. **Collett, M. S., R. Larson, C. Gold, D. Strick, D. K. Anderson, and A. F. Purchio.** 1988. Molecular cloning and nucleotide sequence of the pestivirus bovine viral diarrhea virus. Virology **165:**191-199.

43. **Cristofari, G., R. Ivanyi-Nagy, C. Gabus, S. Boulant, J. P. Lavergne, F. Penin, and J. L. Darlix.** 2004. The hepatitis C virus Core protein is a

potent nucleic acid chaperone that directs dimerization of the viral (+) strand RNA in vitro. Nucleic Acids Res **32:**2623-31.

44. **De Francesco, R., A. Pessi, and C. Steinkuhler.** 1999. Mechanisms of hepatitis C virus NS3 proteinase inhibitors. J Viral Hepat **6 Suppl 1:**23-30.

45. **De Francesco, R., A. Pessi, and C. Steinkuhler.** 1998. The hepatitis C virus NS3 proteinase: structure and function of a zinc- containing serine proteinase. Antivir Ther **3:**99-109.

46. **De Moerlooze, L., C. Lecomte, S. Brown-Shimmer, D. Schmetz, C. Guiot, D. Vandenbergh, D. Allaer, M. Rossius, G. Chappuis, D. Dina, and et al.** 1993. Nucleotide sequence of the bovine viral diarrhoea virus Osloss strain: comparison with related viruses and identification of specific DNA probes in the 5' untranslated region. J Gen Virol **74 (Pt 7):**1433-8.

47. **Deregt, D., S. A. Masri, H. J. Cho, and H. Bielefeldt Ohmann.** 1990. Monoclonal antibodies to the p80/125 gp53 proteins of bovine viral diarrhea virus: their potential use as diagnostic reagents. Can J Vet Res **54:**343-8.

48. **Doan, D. N., and T. Dokland.** 2003. Structure of the nucleocapsid protein of porcine reproductive and respiratory syndrome virus. Structure **11:**1445-51.

49. **Dokland, T.** 1999. Scaffolding proteins and their role in viral assembly. Cell Mol Life Sci **56:**580-603.

50. **Dokland, T., M. Walsh, J. M. Mackenzie, A. A. Khromykh, K. H. Ee, and S. Wang.** 2004. West Nile virus core protein; tetramer structure and ribbon formation. Structure **12:**1157-63.

51. **Dubuisson, J., S. Duvet, J. C. Meunier, A. Op De Beeck, R. Cacan, C. Wychowski, and L. Cocquerel.** 2000. Glycosylation of the hepatitis C virus envelope protein E1 is dependent on the presence of a downstream sequence on the the viral polyprotein. J Biol Chem **275:**30605-30609.

52. **Dubuisson, J., and C. M. Rice.** 1996. Hepatitis C virus glycoprotein folding: Disulfide bond formation and association with calnexin. J. Virol. **70:**778-786.

53. **Dunker, A. K., C. J. Brown, J. D. Lawson, L. M. Iakoucheva, and Z. Obradovic.** 2002. Intrinsic disorder and protein function. Biochemistry **41:**6573-82.

54. **Elbers, K., N. Tautz, P. Becher, D. Stoll, T. Rumenapf, and H.-J. Thiel.** 1996. Processing in the pestivirus E2-NS2 region: identification of proteins p7 and E2p7. J Virol **70:**4131-5.

55. **Evans, M. J., C. M. Rice, and S. P. Goff.** 2004. Phosphorylation of hepatitis C virus nonstructural protein 5A modulates its protein interactions and viral RNA replication. Proc Natl Acad Sci U S A **101:**13038-43.

56. **Failla, C., L. Tomei, and R. De Francesco.** 1994. Both NS3 and NS4A are required for proteolytic processing of hepatitis C virus nonstructural proteins. J Virol **68:**3753-60.

57. **Fairman, M. E., P. A. Maroney, W. Wang, H. A. Bowers, P. Gollnick, T. W. Nilsen, and E. Jankowsky.** 2004. Protein displacement by DExH/D "RNA helicases" without duplex unwinding. Science **304:**730-4.

58. **Ferlenghi, I., M. Clarke, T. Ruttan, S. L. Allison, J. Schalich, F. X. Heinz, S. C. Harrison, F. A. Rey, and S. D. Fuller.** 2001. Molecular organization of a recombinant subviral particle from tick-borne encephalitis virus. Mol Cell **7:**593-602.

59. **Fetzer, C., B. A. Tews, and G. Meyers.** 2005. The carboxy-terminal sequence of the pestivirus glycoprotein E(rns) represents an unusual type of membrane anchor. J Virol **79:**11901-13.

60. **Forsell, K., M. Suomalainen, and H. Garoff.** 1995. Structure-function relation of the NH2-terminal domain of the Semliki Forest virus capsid protein. J Virol **69:**1556-63.

61. **Frolov, I., and S. Schlesinger.** 1994. Translation of Sindbis virus mRNA: effects of sequences downstream of the initiating codon. J. Virol. **68:**8111-8117.

62. **Gale, M., Jr., and E. M. Foy.** 2005. Evasion of intracellular host defence by hepatitis C virus. Nature **436:**939-45.

63. **Garoff, H., M. Sjoberg, and R. H. Cheng.** 2004. Budding of alphaviruses. Virus Res **106:**103-16.

64. **Geigenmuller-Gnirke, U., H. Nitschko, and S. Schlesinger.** 1993. Deletion analysis of the capsid protein of Sindbis virus: identification of the RNA binding region. J. Virol. **67:**1620-6.

65. **Giannini, C., and C. Brechot.** 2003. Hepatitis C virus biology. Cell Death Differ **10 Suppl 1:**S27-38.

66. **Gonzalez, M. E., and L. Carrasco.** 2003. Viroporins. FEBS Lett **552:**28-34.

67. **Grakoui, A., D. W. McCourt, C. Wychowski, S. M. Feinstone, and C. M. Rice.** 1993. A second hepatitis C virus-encoded proteinase. Proc. Natl. Acad. Sci. USA **90:**10583-10587.

68. **Grakoui, A., C. Wychowski, C. Lin, S. M. Feinstone, and C. M. Rice.** 1993. Expression and identification of hepatitis C virus polyprotein cleavage products. J. Virol. **67:**1385-1395.

69. **Grassmann, C. W., O. Isken, and S. E. Behrens.** 1999. Assignment of the multifunctional NS3 protein of bovine viral diarrhea virus during RNA replication: an in vivo and in vitro study. J Virol **73:**9196-205.

70. **Gray, E. W., and P. F. Nettleton.** 1987. The ultrastructure of cell cultures infected with border disease and bovine virus diarrhoea viruses. J. Gen. Virol. **68:**2339-2346.

71. **Greiser-Wilke, I., K. E. Dittmar, B. Liess, and V. Moennig.** 1991. Immunofluorescence studies of biotype-specific expression of bovine viral diarrhoea virus epitopes in infected cells. J. Gen. Virol. **72:**2015-2019.

72. **Griffin, S. D., L. P. Beales, D. S. Clarke, O. Worsfold, S. D. Evans, J. Jaeger, M. P. Harris, and D. J. Rowlands.** 2003. The p7 protein of hepatitis C virus forms an ion channel that is blocked by the antiviral drug, Amantadine. FEBS Lett **535:**34-8.

73. **Griffin, S. D., R. Harvey, D. S. Clarke, W. S. Barclay, M. Harris, and D. J. Rowlands.** 2004. A conserved basic loop in hepatitis C virus p7 protein is required for amantadine-sensitive ion channel activity in mammalian cells but is dispensable for localization to mitochondria. J Gen Virol **85:**451-61.

74. **Gritsun, T. S., V. A. Lashkevich, and E. A. Gould.** 2003. Tick-borne encephalitis. Antiviral Res **57:**129-46.

75. **Grummer, B., M. Beer, E. Liebler-Tenorio, and I. Greiser-Wilke.** 2001. Localization of viral proteins in cells infected with bovine viral diarrhoea virus. J Gen Virol **82:**2597-605.

76. **Harada, T., N. Tautz, and H. J. Thiel.** 2000. E2-p7 region of the bovine viral diarrhea virus polyprotein: processing and functional studies. J. Virol. **74:**9498-506.

77. **Hedstrom, L.** 2002. Serine protease mechanism and specificity. Chem Rev **102:**4501-24.

78. **Heimann, M., G. Roman-Sosa, B. Martoglio, H. J. Thiel, and T. Rumenapf.** 2006. Core protein of pestiviruses is processed at the C terminus by signal peptide peptidase. J Virol **80:**1915-21.

79. **Heinz, F. X., K. Stiasny, G. Puschner-Auer, H. Holzmann, S. L. Allison, C. W. Mandl, and C. Kunz.** 1994. Structural changes and functional control of the tick-borne encephalitis virus glycoprotein E by the heterodimeric association with protein prM. Virology **198:**109-17.

80. **Hirsch, A. J., G. R. Medigeshi, H. L. Meyers, V. DeFilippis, K. Fruh, T. Briese, W. I. Lipkin, and J. A. Nelson.** 2005. The Src family kinase c-Yes is required for maturation of West Nile virus particles. J Virol **79:**11943-51.

81. **Hong, E. M., R. Perera, and R. J. Kuhn.** 2006. Alphavirus capsid protein helix I controls a checkpoint in nucleocapsid core assembly. J Virol **80:**8848-55.

82. **Hope, R. G., M. J. McElwee, and J. McLauchlan.** 2006. Efficient cleavage by signal peptide peptidase requires residues within the signal peptide between the core and E1 proteins of hepatitis C virus strain J1. J Gen Virol **87:**623-7.

83. **Hope, R. G., and J. McLauchlan.** 2000. Sequence motifs required for lipid droplet association and protein stability are unique to the hepatitis C virus core protein. J Gen Virol **81:**1913-25.

84. **Hope, R. G., D. J. Murphy, and J. McLauchlan.** 2002. The domains required to direct core proteins of hepatitis C virus and GB virus-B to lipid droplets share common features with plant oleosin proteins. J Biol Chem **277:**4261-70.

85. **Hourioux, C., M. Ait-Goughoulte, R. Patient, D. Fouquenet, F. Arcanger-Doudet, D. Brand, A. Martin, and P. Roingeard.** 2006. Core protein domains involved in hepatitis C virus-like particle assembly and budding at the endoplasmic reticulum membrane. Cell Microbiol.

86. **Jayaram, H., H. Fan, B. R. Bowman, A. Ooi, J. Jayaram, E. W. Collisson, J. Lescar, and B. V. Prasad.** 2006. X-ray structures of the N- and C-terminal domains of a coronavirus nucleocapsid protein: implications for nucleocapsid formation. J Virol **80:**6612-20.

87. **Jensen, K. B., K. Musunuru, H. A. Lewis, S. K. Burley, and R. B. Darnell.** 2000. The tetranucleotide UCAY directs the specific recognition of RNA by the Nova K-homology 3 domain. Proc Natl Acad Sci U S A **97:**5740-5.

88. **Johnson, J. E.** 1996. Functional implications of protein-protein interactions in icosahedral viruses. Proc Natl Acad Sci U S A **93:**27-33.

89. **Jones, C. T., L. Ma, J. W. Burgner, T. D. Groesch, C. B. Post, and R. J. Kuhn.** 2003. Flavivirus capsid is a dimeric alpha-helical protein. J Virol **77:**7143-9.

90. **Jones, C. T., Murray C.L., Eastman D., Tassello J., and Rice C.M.** 2007. submitted.

91. **Kanai, R., K. Kar, K. Anthony, L. H. Gould, M. Ledizet, E. Fikrig, W. A. Marasco, R. A. Koski, and Y. Modis.** 2006. Crystal structure of west nile virus envelope glycoprotein reveals viral surface epitopes. J Virol **80:**11000-8.

92. **Kato, T., T. Date, M. Miyamoto, A. Furusaka, K. Tokushige, M. Mizokami, and T. Wakita.** 2003. Efficient replication of the genotype 2a hepatitis C virus subgenomic replicon. Gastroenterology **125:**1808-17.

93. **Kato, T., M. Miyamoto, A. Furusaka, T. Date, K. Yasui, J. Kato, S. Matsushima, T. Komatsu, and T. Wakita.** 2003. Processing of hepatitis C virus core protein is regulated by its C-terminal sequence. J Med Virol **69:**357-66.

94. **Kelly, S. M., T. J. Jess, and N. C. Price.** 2005. How to study proteins by circular dichroism. Biochim Biophys Acta **1751:**119-39.

95. **Khromykh, A. A., A. N. Varnavski, P. L. Sedlak, and E. G. Westaway.** 2001. Coupling between replication and packaging of flavivirus RNA: evidence derived from the use of DNA-based full-length cDNA clones of Kunjin virus. J Virol **75:**4633-40.

96. **Khromykh, A. A., and E. G. Westaway.** 1996. RNA binding properties of core protein of the flavivirus Kunjin. Arch Virol **141:**685-99.

97. **Kiermayr, S., R. M. Kofler, C. W. Mandl, P. Messner, and F. X. Heinz.** 2004. Isolation of capsid protein dimers from the tick-borne encephalitis flavivirus and in vitro assembly of capsid-like particles. J Virol **78:**8078-84.

98. **Kim, D. W., R. Suzuki, T. Harada, I. Saito, and T. Miyamura.** 1994. *Trans*-suppression of gene expression by hepatitis C viral core protein. Jpn. J. Med. Sci. Biol. **47:**211-220.

99. **Klein, K. C., S. J. Polyak, and J. R. Lingappa.** 2004. Unique features of hepatitis C virus capsid formation revealed by de novo cell-free assembly. J Virol **78:**9257-69.

100. **Kolykhalov, A. A., E. V. Agapov, and C. M. Rice.** 1994. Specificity of the hepatitis C virus serine proteinase: Effects of substitutions at the 3/4A, 4A/4B, 4B/5A, and 5A/5B cleavage sites on polyprotein processing. J. Virol. **68:**7525-7533.

101. **Kuhn, R. J., W. Zhang, M. G. Rossmann, S. V. Pletnev, J. Corver, E. Lenches, C. T. Jones, S. Mukhopadhyay, P. R. Chipman, E. G. Strauss, T. S. Baker, and J. H. Strauss.** 2002. Structure of dengue virus: implications for flavivirus organization, maturation, and fusion. Cell **108:**717-25.

102. **Kuiken, C., K. Yusim, L. Boykin, and R. Richardson.** 2005. The Los Alamos hepatitis C sequence database. Bioinformatics **21:**379-84.

103. **Kümmerer, B., and C. M. Rice.** 2002. Mutations in the yellow fever virus nonstructural protein NS2A selectively block production of infectious virus. J. Virol. **76:**4773-84.

104. **Kümmerer, B. M., D. Stoll, and G. Meyers.** 1998. Bovine viral diarrhea virus strain Oregon: a novel mechanism for processing of NS2-3 based on point mutations. J. Virol. **72:**4127-4138.

105. **Kunkel, M., M. Lorinczi, R. Rijnbrand, S. M. Lemon, and S. J. Watowich.** 2001. Self-assembly of nucleocapsid-like particles from recombinant hepatitis C virus core protein. J Virol **75:**2119-29.

106. **Kunkel, M., and S. J. Watowich.** 2004. Biophysical characterization of hepatitis C virus core protein: implications for interactions within the virus and host. FEBS Lett **557:**174-80.

107. **Lackner, T., A. Muller, M. Konig, H. J. Thiel, and N. Tautz.** 2005. Persistence of bovine viral diarrhea virus is determined by a cellular cofactor of a viral autoprotease. J Virol **79:**9746-55.

108. **Lackner, T., A. Muller, A. Pankraz, P. Becher, H. J. Thiel, A. E. Gorbalenya, and N. Tautz.** 2004. Temporal modulation of an autoprotease is crucial for replication and pathogenicity of an RNA virus. J Virol **78:**10765-75.

109. **Lackner, T., H. J. Thiel, and N. Tautz.** 2006. Dissection of a viral autoprotease elucidates a function of a cellular chaperone in proteolysis. Proc Natl Acad Sci U S A **103:**1510-5.

110. **Langedijk, J. P.** 2002. Translocation activity of C-terminal domain of pestivirus Erns and ribotoxin L3 loop. J Biol Chem **277:**5308-14.

111. **Lecot, S., S. Belouzard, J. Dubuisson, and Y. Rouille.** 2005. Bovine viral diarrhea virus entry is dependent on clathrin-mediated endocytosis. J Virol **79:**10826-9.

112. **Lemberg, M. K., and B. Martoglio.** 2002. Requirements for signal peptide peptidase-catalyzed intramembrane proteolysis. Mol Cell **10:**735-44.

113. **Li, X., P. Romero, M. Rani, A. K. Dunker, and Z. Obradovic.** 1999. Predicting Protein Disorder for N-, C-, and Internal Regions. Genome Inform Ser Workshop Genome Inform **10:**30-40.

114. **Lin, C., B. D. Lindenbach, B. Prágai, D. W. McCourt, and C. M. Rice.** 1994. Processing of the hepatitis C virus E2-NS2 region: Identification of p7 and two distinct E2-specific products with different C termini. J. Virol. **68:**5063-5073.

115. **Lindenbach, B. D., M. J. Evans, A. J. Syder, B. Wolk, T. L. Tellinghuisen, C. C. Liu, T. Maruyama, R. O. Hynes, D. R. Burton, J. A. McKeating, and C. M. Rice.** 2005. Complete replication of hepatitis C virus in cell culture. Science **309:**623-6.

116. **Lindenbach, B. D., H. Thiel, and C. M. Rice.** 2007. *Flaviviridae*: The viruses and their replication, p. 991-1041. *In* D. M. Knipe and P. M. Howley (ed.), Fields Virology, Fourth ed, vol. 1. Lippincott-Raven Publishers, Philadelphia.

117. **Linger, B. R., L. Kunovska, R. J. Kuhn, and B. L. Golden.** 2004. Sindbis virus nucleocapsid assembly: RNA folding promotes capsid protein dimerization. RNA **10:**128-38.

118. **Lo, S.-Y., M. J. Selby, and J.-H. Ou.** 1996. Interaction between hepatitis C virus core protein and E1 envelope protein. J. Virol. **70:**5177-5182.

119. **Lobigs, M.** 1993. Flavivirus premembrane protein cleavage and spike heterodimer secretion requires the function of the viral proteinase NS3. Proc. Natl. Acad. Sci. USA **90:**6218-6222.

120. **Lohmann, V., F. Korner, J. O. Koch, U. Herian, L. Theilmann, and R. Bartenschlager.** 1999. Replication of subgenomic hepatitis C virus RNAs in a hepatoma cell line. Science **285:**110-113.

121. **Lorenz, I. C., S. L. Allison, F. X. Heinz, and A. Helenius.** 2002. Folding and dimerization of tick-borne encephalitis virus envelope proteins prM and E in the endoplasmic reticulum. J Virol **76:**5480-91.

122. **Lorenz, I. C., J. Marcotrigiano, T. G. Dentzer, and C. M. Rice.** 2006. Structure of the catalytic domain of the hepatitis C virus NS2-3 protease. Nature **442:**831-5.

123. **Lu, W., and J. H. Ou.** 2002. Phosphorylation of hepatitis C virus core protein by protein kinase A and protein kinase C. Virology **300:**20-30.

124. **Ma, L., C. T. Jones, T. D. Groesch, R. J. Kuhn, and C. B. Post.** 2004. Solution structure of dengue virus capsid protein reveals another fold. Proc Natl Acad Sci U S A **101:**3414-9.

125. **Mackenzie, J. M., A. A. Khromykh, M. K. Jones, and E. G. Westaway.** 1998. Subcellular localization and some biochemical properties of the flavivirus Kunjin nonstructural proteins NS2A and NS4A. Virology **245:**203-15.

126. **Mackenzie, J. M., and E. G. Westaway.** 2001. Assembly and maturation of the flavivirus Kunjin virus appear to occur in the rough endoplasmic reticulum and along the secretory pathway, respectively. J Virol **75:**10787-99.

127. **Mackenzie, J. S., D. J. Gubler, and L. R. Petersen.** 2004. Emerging flaviviruses: the spread and resurgence of Japanese encephalitis, West Nile and dengue viruses. Nat Med **10:**S98-109.

128. **Majeau, N., V. Gagne, M. Bolduc, and D. Leclerc.** 2005. Signal peptide peptidase promotes the formation of hepatitis C virus non-enveloped particles and is captured on the viral membrane during assembly. J Gen Virol **86:**3055-64.

129. **Markoff, L.** 1989. In vitro processing of dengue virus structural proteins: Cleavage of the pre-membrane protein. J. Virol. **63:**3345-3352.

130. **Matsumoto, M., S. B. Hwang, K.-S. Jeng, N. Zhu, and M. M. C. Lai.** 1996. Homotypic interaction and multimerization of hepatitis C virus core protein. Virology **218:**43-51.

131. **Matusan, A. E., M. J. Pryor, A. D. Davidson, and P. J. Wright.** 2001. Mutagenesis of the Dengue virus type 2 NS3 protein within and outside helicase motifs: effects on enzyme activity and virus replication. J Virol **75:**9633-43.

132. **McLauchlan, J.** 2000. Properties of the hepatitis C virus core protein: a structural protein that modulates cellular processes. J Viral Hepat **7:**2-14.

133. **McLauchlan, J., M. K. Lemberg, G. Hope, and B. Martoglio.** 2002. Intramembrane proteolysis promotes trafficking of hepatitis C virus core protein to lipid droplets. EMBO Journal **21:**3980-8.

134. **McMullan, L. K., A. Grakoui, M. J. Evans, K. Mihalik, M. Puig, A. D. Branch, S. M. Feinstone, and C. M. Rice.** 2007. Evidence for a functional RNA element in the hepatitis C virus core gene. Proc Natl Acad Sci U S A **104:**2879-84.

135. **McNiven, M. A., and H. M. Thompson.** 2006. Vesicle formation at the plasma membrane and trans-Golgi network: the same but different. Science **313:**1591-4.

136. **Mendez, E., N. Ruggli, M. S. Collett, and C. M. Rice.** 1998. Infectious bovine viral diarrhea virus (Strain NADL) RNA from stable cDNA clones: a cellular insert determines NS3 production and viral cytopathogenicity. J. Virol. **72:**4737-4745.

137. **Meyers, G., T. Rümenapf, and H.-J. Thiel.** 1989. Molecular cloning and nucleotide sequence of the genome of hog cholera virus. Virology **171:**555-567.

138. **Meyers, G., T. Rümenapf, and H.-J. Thiel.** 1989. Ubiquitin in a togavirus [letter]. Nature **341:**491.

139. **Meyers, G., A. Saalmuller, and M. Buttner.** 1999. Mutations abrogating the RNase activity in glycoprotein E(rns) of the pestivirus classical swine fever virus lead to virus attenuation. J Virol **73:**10224-35.

140. **Meyers, G., D. Stoll, and M. Gunn.** 1998. Insertion of a sequence encoding light chain 3 of microtubule-associated proteins 1A and 1B in a pestivirus genome: connection with virus cytopathogenicity and induction of lethal disease in cattle. J. Virol. **72:**4139-4148.

141. **Modis, Y., S. Ogata, D. Clements, and S. C. Harrison.** 2004. Structure of the dengue virus envelope protein after membrane fusion. Nature **427:**313-9.

142. **Moennig, V., and P. G. Plagemann.** 1992. The pestiviruses. Adv Virus Res **41:**53-98.

143. **Moennig, V. a. P., P. G. W.** 1992. The Pestiviruses. Advances in Virus Research **41:**53-98.

144. **Moradpour, D., R. Gosert, D. Egger, F. Penin, H. E. Blum, and K. Bienz.** 2003. Membrane association of hepatitis C virus nonstructural proteins and identification of the membrane alteration that harbors the viral replication complex. Antiviral Res **60:**103-9.

145. **Mukhopadhyay, S., B. S. Kim, P. R. Chipman, M. G. Rossmann, and R. J. Kuhn.** 2003. Structure of West Nile virus. Science **302:**248.

146. **Mukhopadhyay, S., R. J. Kuhn, and M. G. Rossmann.** 2005. A structural perspective of the flavivirus life cycle. Nat Rev Microbiol **3:**13-22.

147. **Mukhopadhyay, S., W. Zhang, S. Gabler, P. R. Chipman, E. G. Strauss, J. H. Strauss, T. S. Baker, R. J. Kuhn, and M. G. Rossmann.** 2006. Mapping the structure and function of the E1 and E2 glycoproteins in alphaviruses. Structure **14:**63-73.

148. **Muller, A., G. Rinck, H. J. Thiel, and N. Tautz.** 2003. Cell-derived sequences in the N-terminal region of the polyprotein of a cytopathogenic pestivirus. J Virol **77:**10663-9.

149. **Myers, T. M., V. G. Kolupaeva, E. Mendez, S. G. Baginski, I. Frolov, C. U. Hellen, and C. M. Rice.** 2001. Efficient translation initiation is required for replication of bovine viral diarrhea virus subgenomic replicons. J Virol **75:**4226-38.

150. **Nagai, M., Y. Sakoda, M. Mori, M. Hayashi, H. Kida, and H. Akashi.** 2003. Insertion of cellular sequence and RNA recombination in the structural protein coding region of cytopathogenic bovine viral diarrhoea virus. J Gen Virol **84:**447-52.

151. **Nakai, K., T. Okamoto, T. Kimura-Someya, K. Ishii, C. K. Lim, H. Tani, E. Matsuo, T. Abe, Y. Mori, T. Suzuki, T. Miyamura, J. H. Nunberg, K. Moriishi, and Y. Matsuura.** 2006. Oligomerization of hepatitis C virus core protein is crucial for interaction with the cytoplasmic domain of E1 envelope protein. J Virol **80:**11265-73.

152. **Neil, S. J., S. W. Eastman, N. Jouvenet, and P. D. Bieniasz.** 2006. HIV-1 Vpu promotes release and prevents endocytosis of nascent retrovirus particles from the plasma membrane. PLoS Pathog **2:**e39.

153. **Nestorowicz, A., T. J. Chambers, and C. M. Rice.** 1994. Mutagenesis of the yellow fever virus NS2A/2B cleavage site: Effects on proteolytic processing, viral replication and evidence for alternative processing of the NS2A protein. Virology **199:**114-123.

154. **Nolandt, O., V. Kern, H. Muller, E. Pfaff, L. Theilmann, R. Welker, and H. G. Krausslich.** 1997. Analysis of hepatitis C virus core protein interaction domains. J Gen Virol **78:**1331-1340.

155. **Owen, K. E., and R. J. Kuhn.** 1996. Identification of a region in the Sindbis virus nucleocapsid protein that is involved in specificity of RNA encapsidation. J Virol **70:**2757-63.

156. **Patargias, G., N. Zitzmann, R. Dwek, and W. B. Fischer.** 2006. Protein-protein interactions: modeling the hepatitis C virus ion channel p7. J Med Chem **49:**648-55.

157. **Perera, R., K. E. Owen, T. L. Tellinghuisen, A. E. Gorbalenya, and R. J. Kuhn.** 2001. Alphavirus nucleocapsid protein contains a putative coiled coil alpha-helix important for core assembly. J Virol **75:**1-10.

158. **Peter, B. J., H. M. Kent, I. G. Mills, Y. Vallis, P. J. Butler, P. R. Evans, and H. T. McMahon.** 2004. BAR domains as sensors of membrane curvature: the amphiphysin BAR structure. Science **303:**495-9.

159. **Pietschmann, T., A. Kaul, G. Koutsoudakis, A. Shavinskaya, S. Kallis, E. Steinmann, K. Abid, F. Negro, M. Dreux, F. L. Cosset, and R. Bartenschlager.** 2006. Construction and characterization of infectious intragenotypic and intergenotypic hepatitis C virus chimeras. Proc Natl Acad Sci U S A **103:**7408-13.

160. **Pileri, P., Y. Uematsu, S. Compagnoli, G. Galli, F. Falugi, R. Petracca, A. J. Weiner, M. Houghton, D. Rosa, G. Grandi, and S. Abrignani.** 1998. Binding of hepatitis C virus to CD81. Science **282:**938-941.

161. **Qi, F., J. F. Ridpath, and E. S. Berry.** 1998. Insertion of a bovine SMT3B gene in NS4B and duplication of NS3 in a bovine viral diarrhea virus genome correlate with the cytopathogenicity of the virus. Virus Res **57:**1-9.

162. **Qi, F., J. F. Ridpath, T. Lewis, S. R. Bolin, and E. S. Berry.** 1992. Analysis of the bovine viral diarrhea virus genome for possible cellular insertions. Virology **189:**285-292.

163. **Qu, L., L. K. McMullan, and C. M. Rice.** 2001. Isolation and characterization of noncytopathic pestivirus mutants reveals a role for nonstructural protein NS4B in cytopathogenicity. J. Virol. **75:**10651-10662.

164. **Ray, R. B., L. M. Lagging, K. Meyer, R. Steele, and R. Ray.** 1995. Transcriptional regulation of cellular and viral promoters by the hepatitis C virus core protein. Virus Res. **37:**209-220.

165. **Ray, R. B., and R. Ray.** 2001. Hepatitis C virus core protein: intriguing properties and functional relevance. FEMS Microbiol Lett **202:**149-56.

166. **Ray, R. B., R. Steele, K. Meyer, and R. Ray.** 1997. Transcriptional repression of p53 promoter by hepatitis C virus core protein. J. Biol. Chem. **272:**10983-10986.

167. **Rey, F., F. X. Heinz, C. Mandl, H. Holzmann, C. Kunz, B. Harris, and S. C. Harrison.** 1994. Crystal structure of the envelope glycoprotein E from tick borne encephalitis virus.in preparation.

168. **Rice, C. M., J. R. Bell, M. W. Hunkapiller, E. G. Strauss, and J. H. Strauss.** 1982. Isolation and characterization of the hydrophobic COOH-terminal domains of the sindbis virion glycoproteins. J Mol Biol **154:**355-78.

169. **Rice, C. M., and J. H. Strauss.** 1982. Association of Sindbis virion glycoproteins and their precursors. J. Mol. Biol. **154:**325-348.

170. **Rijnbrand, R., T. van der Straaten, P. A. van Rijn, W. J. Spaan, and P. J. Bredenbeek.** 1997. Internal entry of ribosomes is directed by the 5' noncoding region of classical swine fever virus and is dependent on the presence of an RNA pseudoknot upstream of the initiation codon. J. Virol. **71:**451-457.

171. **Rinck, G., C. Birghan, T. Harada, G. Meyers, H. J. Thiel, and N. Tautz.** 2001. A cellular J-domain protein modulates polyprotein processing and cytopathogenicity of a pestivirus. J Virol **75:**9470-82.

172. **Risco, C., I. M. Anton, L. Enjuanes, and J. L. Carrascosa.** 1996. The transmissible gastroenteritis coronavirus contains a spherical core shell consisting of M and N proteins. J Virol **70:**4773-7.

173. **Romero, Obradovic, and K. Dunker.** 1997. Sequence Data Analysis for Long Disordered Regions Prediction in the Calcineurin Family. Genome Inform Ser Workshop Genome Inform **8:**110-124.

174. **Romero, P., Z. Obradovic, X. Li, E. C. Garner, C. J. Brown, and A. K. Dunker.** 2001. Sequence complexity of disordered protein. Proteins **42:**38-48.

175. **Rost, B., and C. Sander.** 1993. Prediction of protein secondary structure at better than 70% accuracy. J Mol Biol **232:**584-99.

176. **Rouille, Y., F. Helle, D. Delgrange, P. Roingeard, C. Voisset, E. Blanchard, S. Belouzard, J. McKeating, A. H. Patel, G. Maertens, T. Wakita, C. Wychowski, and J. Dubuisson.** 2006. Subcellular localization of hepatitis C virus structural proteins in a cell culture system that efficiently replicates the virus. J Virol **80:**2832-41.

177. **Rumenapf, T., R. Stark, M. Heimann, and H. J. Thiel.** 1998. N-terminal protease of pestiviruses: identification of putative catalytic residues by site-directed mutagenesis. J Virol **72:**2544-7.

178. **Rümenapf, T., G. Unger, J. H. Strauss, and H.-J. Thiel.** 1993. Processing of the envelope glycoproteins of pestiviruses. J. Virol. **67:**3288-3294.

179. **Sakai, A., M. S. Claire, K. Faulk, S. Govindarajan, S. U. Emerson, R. H. Purcell, and J. Bukh.** 2003. The p7 polypeptide of hepatitis C virus is critical for infectivity and contains functionally important genotype-specific sequences. Proc Natl Acad Sci U S A **100:**11646-51.

180. **Santolini, E., G. Migliaccio, and N. La Monica.** 1994. Biosynthesis and biochemical properties of the hepatitis C virus core protein. J. Virol. **68:**3631-3641.

181. **Schneider, R., G. Unger, R. Stark, E. Schneider-Scherzer, and H. J. Thiel.** 1993. Identification of a structural glycoprotein of an RNA virus as a ribonuclease. Science **261:**1169-71.

182. **Schwer, B., S. Ren, T. Pietschmann, J. Kartenbeck, K. Kaehlcke, R. Bartenschlager, T. S. Yen, and M. Ott.** 2004. Targeting of hepatitis C virus core protein to mitochondria through a novel C-terminal localization motif. J Virol **78:**7958-68.

183. **Selby, M. J., E. Glazer, F. Masiarz, and M. Houghton.** 1994. Complex processing and protein:protein interactions in the E2:NS2 region of HCV. Virology **204:**114-122.

184. **Sens, P., and H. Isambert.** 2002. Undulation instability of lipid membranes under an electric field. Phys Rev Lett **88:**128102.

185. **Shih, C.-M., C.-M. Chen, S.-Y. Chen, and Y.-H. W. Lee.** 1995. Modulation of the *trans*-suppression activity of hepatitis C virus core protein by phosphorylation. J. Virol. **69:**1160-1171.

186. **Shih, C. M., S. J. Lo, T. Miyamura, S. Y. Chen, and Y. H. Lee.** 1993. Suppression of hepatitis B virus expression and replication by hepatitis C virus core protein in HuH-7 cells. J. Virol. **67:**5823-5832.

187. **Shimoike, T., S. Mimori, H. Tani, Y. Matsuura, and T. Miyamura.** 1999. Interaction of hepatitis C virus core protein with viral sense RNA and suppression of its translation. J Virol **73:**9718-25.

188. **Stadler, K., S. L. Allison, J. Schalich, and F. X. Heinz.** 1997. Proteolytic activation of tick-borne encephalitis virus by furin. J. Virol. **71:**8475-8481.

189. **Steinkuhler, C., G. Biasiol, M. Brunetti, A. Urbani, U. Koch, R. Cortese, A. Pessi, and R. De Francesco.** 1998. Product inhibition of the hepatitis C virus NS3 protease. Biochemistry **37:**8899-905.

190. **Sterling, R. K., and S. Bralow.** 2006. Extrahepatic manifestations of hepatitis C virus. Curr Gastroenterol Rep **8:**53-9.

191. **Stocks, C. E., and M. Lobigs.** 1995. Posttranslational signal peptidase cleavage at the flavivirus C-prM junction in vitro. J. Virol. **69:**8123-6.

192. **Stocks, C. E., and M. Lobigs.** 1998. Signal peptidase cleavage at the flavivirus C-prM junction: dependence on the viral NS2B-3 protease for efficient processing requires determinants in C, the signal peptide, and prM. J Virol **72:**2141-9.

193. **Strauss, J. H., and E. G. Strauss.** 1994. The alphaviruses: gene expression, replication, evolution. Microbiol. Rev. **58:**491-562.

194. **Suzich, J. A., J. K. Tamura, F. Palmer-Hill, P. Warrener, A. Grakoui, C. M. Rice, S. M. Feinstone, and M. S. Collett.** 1993. Hepatitis C virus NS3 protein polynucleotide-stimulated nucleoside triphosphatase and comparison with the related pestivirus and flavivirus enzymes. J. Virol. **67:**6152-6158.

195. **Suzuki, R., S. Sakamoto, T. Tsutsumi, A. Rikimaru, K. Tanaka, T. Shimoike, K. Moriishi, T. Iwasaki, K. Mizumoto, Y. Matsuura, T. Miyamura, and T. Suzuki.** 2005. Molecular determinants for subcellular localization of hepatitis C virus core protein. J Virol **79:**1271-81.

196. **Suzuki, R., K. Tamura, J. Li, K. Ishii, Y. Matsuura, T. Miyamura, and T. Suzuki.** 2001. Ubiquitin-mediated degradation of hepatitis C virus core protein is regulated by processing at its carboxyl terminus. Virology **280:**301-9.

197. **Tamura, J. K., P. Warrener, and M. S. Collett.** 1993. RNA-stimulated NTPase activity associated with the p80 protein of the pestivirus bovine viral diarrhea virus. Virology **193:**1-10.

198. **Tan, B.-T., J. Fu, R. J. Sugrue, E.-H. Yap, Y.-C. Chan, and Y. H. Tan.** 1996. Recombinant dengue type 1 virus NS5 protein expressed in *Escherichia coli* exhibits RNA-dependent RNA polymerase activity. Virology **216:**317-325.

199. **Targett-Adams, P., T. Schaller, G. Hope, R. E. Lanford, S. M. Lemon, A. Martin, and J. McLauchlan.** 2006. Signal peptide peptidase cleavage of GB virus B core protein is required for productive infection in vivo. J Biol Chem **281:**29221-7.

200. **Tautz, N., T. Harada, A. Kaiser, G. Rinck, S. Behrens, and H. J. Thiel.** 1999. Establishment and characterization of cytopathogenic and noncytopathogenic pestivirus replicons. J Virol **73:**9422-32.

201. **Tautz, N., A. Kaiser, and H. J. Thiel.** 2000. NS3 serine protease of bovine viral diarrhea virus: characterization of active site residues, NS4A cofactor domain, and protease-cofactor interactions. Virology **273:**351-63.

202. **Tautz, N., G. Meyers, and H.-J. Thiel.** 1993. Processing of poly-ubiquitin in the polyprotein of an RNA virus. Virology **197:**74-85.

203. **Tautz, N., and H. J. Thiel.** 2003. Cytopathogenicity of pestiviruses: cleavage of bovine viral diarrhea virus NS2-3 has to occur at a defined position to allow viral replication. Arch Virol **148:**1405-12.

204. **Tellinghuisen, T. L., and R. J. Kuhn.** 2000. Nucleic acid-dependent cross-linking of the nucleocapsid protein of Sindbis virus. J Virol **74:**4302-9.

205. **Thiel, H.-J., R. Stark, E. Weiland, T. Rümenapf, and G. Meyers.** 1991. Hog cholera virus: molecular composition of virions from a pestivirus. J. Virol. **65:**4705-4712.

206. **Thiel, H. J., R. Stark, E. Weiland, T. Rumenapf, and G. Meyers.** 1991. Hog cholera virus: molecular composition of virions from a pestivirus. J Virol **65:**4705-12.

207. **Tomori, O.** 2004. Yellow fever: the recurring plague. Crit Rev Clin Lab Sci **41:**391-427.

208. **Tompa, P.** 2005. The interplay between structure and function in intrinsically unstructured proteins. FEBS Lett **579:**3346-54.

209. **Tscherne, D. M., C. T. Jones, M. J. Evans, B. D. Lindenbach, J. A. McKeating, and C. M. Rice.** 2006. Time- and temperature-dependent activation of hepatitis C virus for low-pH-triggered entry. J Virol **80:**1734-41.

210. **Tsukiyama-Kohara, K., N. Iizuka, M. Kohara, and A. Nomoto.** 1992. Internal ribosome entry site within hepatitis C virus RNA. J. Virol. **66:**1476-1483.

211. **Tuplin, A., J. Wood, D. J. Evans, A. H. Patel, and P. Simmonds.** 2002. Thermodynamic and phylogenetic prediction of RNA secondary structures in the coding region of hepatitis C virus. RNA **8:**824-41.

212. **Uversky, V. N.** 2002. What does it mean to be natively unfolded? Eur J Biochem **269:**2-12.

213. **Vauloup-Fellous, C., V. Pene, J. Garaud-Aunis, F. Harper, S. Bardin, Y. Suire, E. Pichard, A. Schmitt, P. Sogni, G. Pierron, P. Briand, and A. R. Rosenberg.** 2006. Signal peptide peptidase-catalyzed cleavage of hepatitis C virus core protein is dispensable for virus budding but destabilizes the viral capsid. J Biol Chem **281:**27679-92.

214. **Verna, E. C., and R. S. Brown, Jr.** 2006. Hepatitis C virus and liver transplantation. Clin Liver Dis **10:**919-40.

215. **Wakita, T., T. Pietschmann, T. Kato, T. Date, M. Miyamoto, Z. Zhao, K. Murthy, A. Habermann, H. G. Krausslich, M. Mizokami, R. Bartenschlager, and T. J. Liang.** 2005. Production of infectious hepatitis C virus in tissue culture from a cloned viral genome. Nat Med **11:**791-6.

216. **Walewski, J. L., T. R. Keller, D. D. Stump, and A. D. Branch.** 2001. Evidence for a new hepatitis C virus antigen encoded in an overlapping reading frame. RNA **7:**710-21.

217. **Warrener, P., and M. S. Collett.** 1995. Pestivirus NS3 (p80) protein possesses RNA helicase activity. J. Virol. **69:**1720-1726.

218. **Warrener, P., J. K. Tamura, and M. S. Collett.** 1993. An RNA-stimulated NTPase activity associated with yellow fever virus NS3 protein expressed in bacteria. J. Virol. **67:**989-996.

219. **Weiland, F., E. Weiland, G. Unger, A. Saalmuller, and H. J. Thiel.** 1999. Localization of pestiviral envelope proteins E(rns) and E2 at the cell surface and on isolated particles. J Gen Virol **80:**1157-65.

220. **Weiss, B., U. Geigenmuller-Gnirke, and S. Schlesinger.** 1994. Interactions between Sindbis virus RNAs and a 68 amino acid derivative of the viral capsid protein further defines the capsid binding site. Nucleic Acids Res. **22:**780-6.

221. **Wengler, G., and G. Wengler.** 1991. The carboxy-terminal part of the NS3 protein of the West Nile flavivirus can be isolated as a soluble protein after proteolytic cleavage and represents an RNA-stimulated NTPase. Virology **184:**707-715.

222. **WHO.** 1997. Hepatitis C: global prevalence. Wkly Epidemiol. Rec. **72:**341-344.

223. **Wiskerchen, M., S. K. Belzer, and M. S. Collett.** 1991. Pestivirus gene expression: The first protein product of the bovine viral diarrhea virus large open reading frame, p20, possesses proteolytic activity. J. Virol. **65:**4508-4514.

224. **Wiskerchen, M., and M. S. Collett.** 1991. Pestivirus gene expression: protein p80 of bovine viral diarrhea virus is a proteinase involved in polyprotein processing. Virology **184:**341-350.

225. **Xu, J., E. Mendez, P. R. Caron, C. Lin, M. A. Murcko, M. S. Collett, and C. M. Rice.** 1997. Bovine viral diarrhea virus NS3 serine proteinase: polyprotein cleavage sites, cofactor requirements, and molecular model of an enzyme essential for pestivirus replication. J. Virol. **71:**5312-5322.

226. **Yamaga, A. K., and J. H. Ou.** 2002. Membrane topology of the hepatitis C virus NS2 protein. J Biol Chem **277:**33228-34.

227. **Yasui, K., T. Wakita, K. Tsukiyama-Kohara, S. I. Funahashi, M. Ichikawa, T. Kajita, D. Moradpour, J. R. Wands, and M. Kohara.** 1998. The native form and maturation process of hepatitis C virus core protein. J Virol **72:**6048-6055.

228. **Yi, M., Y. Ma, J. Yates, and S. M. Lemon.** 2007. Compensatory mutations in E1, p7, NS2, and NS3 enhance yields of cell culture-infectious intergenotypic chimeric hepatitis C virus. J Virol **81:**629-38.

229. **Yu, I. M., M. L. Oldham, J. Zhang, and J. Chen.** 2006. Crystal structure of the severe acute respiratory syndrome (SARS) coronavirus nucleocapsid protein dimerization domain reveals evolutionary linkage between corona- and arteriviridae. J Biol Chem **281:**17134-9.

230. **Zhang, W., P. R. Chipman, J. Corver, P. R. Johnson, Y. Zhang, S. Mukhopadhyay, T. S. Baker, J. H. Strauss, M. G. Rossmann, and R. J.**

Kuhn. 2003. Visualization of membrane protein domains by cryo-electron microscopy of dengue virus. Nat Struct Biol **10:**907-12.

231. **Zhang, W., S. Mukhopadhyay, S. V. Pletnev, T. S. Baker, R. J. Kuhn, and M. G. Rossmann.** 2002. Placement of the structural proteins in Sindbis virus. J Virol **76:**11645-58.

232. **Zhang, Y., J. Corver, P. R. Chipman, W. Zhang, S. V. Pletnev, D. Sedlak, T. S. Baker, J. H. Strauss, R. J. Kuhn, and M. G. Rossmann.** 2003. Structures of immature flavivirus particles. Embo J **22:**2604-13.

233. **Zhang, Y., V. A. Kostyuchenko, and M. G. Rossmann.** 2007. Structural analysis of viral nucleocapsids by subtraction of partial projections. J Struct Biol **157:**356-64.

234. **Zhang, Y., W. Zhang, S. Ogata, D. Clements, J. H. Strauss, T. S. Baker, R. J. Kuhn, and M. G. Rossmann.** 2004. Conformational changes of the flavivirus E glycoprotein. Structure **12:**1607-18.

235. **Zhong, J., P. Gastaminza, G. Cheng, S. Kapadia, T. Kato, D. R. Burton, S. F. Wieland, S. L. Uprichard, T. Wakita, and F. V. Chisari.** 2005. Robust hepatitis C virus infection in vitro. Proc Natl Acad Sci U S A **102:**9294-9.

236. **Zhong, W., L. L. Gutshall, and A. M. Del Vecchio.** 1998. Identification and characterization of an RNA-dependent RNA polymerase activity within the nonstructural protein 5B region of bovine viral diarrhea virus. J Virol **72:**9365-9.